POWER SYSTEM STABILITY ENHANCEMENT THROUGH WIDE AREA MEASUREMENTS

BY
IRFAN AHMED KHAN

A Thesis Presented to the
DEANSHIP OF GRADUATE STUDIES

KING FAHD UNIVERSITY OF PETROLEUM & MINERALS

DHAHRAN, SAUDI ARABIA

In Partial Fulfillment of the
Requirements for the Degree of

MASTER OF SCIENCE

In

ELECTRICAL ENGINEERING

DECEMBER 2012

KING FAHD UNIVERSITY OF PETROLEUM & MINERALS
DHAHRAN- 31261, SAUDI ARABIA
DEANSHIP OF GRADUATE STUDIES

This thesis, written by **IRFAN AHMED KHAN** under the direction of his thesis advisor and approved by his thesis committee, has been presented and accepted by the Dean of Graduate Studies, in partial fulfillment of the requirements for the degree of **MASTER OF SCIENCE IN ELECTRICAL ENGINEERING.**

Thesis Committee

Dr. Ali A. Al-Shaikhi
Department Chairman

Dr. M. A. Abido
(Advisor)

Dr. Salam A. Zummo
Dean of Graduate Studies

Dr. Ibrahim M. El Amin
(Member)

7/1/13
Date

Dr. Ali T. Al-Awami
(Member)

POWER SYSTEM STABILITY ENHANCEMENT THROUGH WIDE AREA MEASUREMENTS

Irfan Ahmed Khan

Electrical Engineering Department

December 2012

KING FAHD UNIVERSITY OF PETROLEUM & MINERALS
DHAHRAN- 31261, SAUDI ARABIA
DEANSHIP OF GRADUATE STUDIES

This thesis, written by **IRFAN AHMED KHAN** under the direction of his thesis advisor and approved by his thesis committee, has been presented and accepted by the Dean of Graduate Studies, in partial fulfillment of the requirements for the degree of **MASTER OF SCIENCE IN ELECTRICAL ENGINEERING.**

Thesis Committee

_____
Dr. Ali A. Al-Shaikhi
Department Chairman

_____
Dr. M. A. Abido
(Advisor)

_____
Dr. Salam A. Zummo
Dean of Graduate Studies

_____
Dr. Ibrahim M. El Amin
(Member)

_____
Date

_____
Dr. Ali T. Al-Awami
(Member)

Dedication

This Thesis is dedicated to my beloved Parents

ACKNOWLEDGMENTS

All praise and glory to Allah SWT (الله سبحانه و تعالىٰ) who has given me the strength and courage to complete this thesis as without His help I cannot even imagine that this would have been possible.

Firstly, I would like to thank KFUPM for providing the excellent research facilities at the university and encouraging students to take part in active research. Especially the Power and Energy Research Group for providing wonderful fully equipped RTDS laboratory. I would like to acknowledge my thesis adviser Dr. M. A. Abido for his constant guidance during this thesis. He is an extra ordinary talented instructor that I found in all over my life, I wish him a very successful future. I am also deeply thankful to my committee members, Dr. Ibrahim Al-Amin and Dr. Ali T. Al-Awami for their involvement in this thesis.

I am also sincerely grateful to my family and my friends at KFUPM for their moral support and guidance.

TABLE OF CONTENTS

ACKNOWLEDGMENTS ..... **V**

TABLE OF CONTENTS ..... **VI**

LIST OF FIGURES ..... **X**

LIST OF TABLES ..... **XVIII**

ABSTRACT ..... **XIX**

ABSTRACT (ARABIC) ..... **XX**

NOMENCLATURE ..... **XXI**

CHAPTER 1 INTRODUCTION **1**

1.1 Overview **1**

1.2 Motivation **2**

1.3 Thesis Objectives **5**

1.4 Thesis Contribution **5**

1.5 Thesis Organization **7**

CHAPTER 2 LITRATURE REVIEW 8

2.1 Phasor Measurement Units 9

2.2 Inter Area Oscillations 14

2.3 Power System Stabilizer Design 19

2.4 Backup Damping Control 21

CHAPTER 3 POWER SYSTEM MODEL 23

3.1 Single Machine Infinite Bus System 23

3.2 Multimachine Power System 25

3.3 Excitation system 27

3.4 Power System Stabilizers 28

CHAPTER 4 PROPOSED APPROACH 31

4.1 Optimal Location for Power System Stabilizer 32

4.2 Power System Stabilizers Structure 33

4.3 Power System Stabilizer Tuning 35

4.4 Optimization Technique 35

4.5 Eigenvalue Analysis and non-linear Time Domain Simulations 37

4.6 Backup Protection for Transient Stabilities 38

CHAPTER 5 EXPERIMENTAL SETUP 39

5.1 Real time Digital Simulator 39

5.2 Phasor Measurement Unit (PMU) 40

5.3 Power System Stabilizers Model 40

5.4 Transmission Line Model 41

5.5 Generator Model 41

5.6 IEE2ST PSS Integrated with PMU 42

CHAPTER 6 RESULTS AND TESTING 44

6.1 Test Case 1: 3-Machine 9-Bus system 44

6.1.1 Optimal placement of PSS 45

6.1.2 Stabilizer Design 46

6.1.3 Eigenvalue Analysis 46

6.1.4 Simulation Results for Test Case 1 47

6.1.5 RTDS Results for Test Case 1 53

6.1.6 Comparison of Simulated and RTDS results for test case 1 62

6.2 Test Case 2: 5-Machine 14-Bus system 63

6.2.1 Optimal placement of PSS 63

6.2.2 Stabilizer Design 64

6.2.3 Eigenvalue Analysis 65

6.2.4 Simulation Results for Test Case 2 66

6.2.5 RTDS Results for Test Case 2 74

6.2.6 Comparison of Simulated and RTDS results for test case 2 88

6.3 Development of Backup Damping Controller 88

CHAPTER 7 CONCLUSION AND FUTURE WORK..... 92

7.1 Conclusion..... 92

7.2 Future Work 94

APPENDICES..... 95

REFERENCES 119

VITAE..... 130

LIST OF FIGURES

Figure 2.1: Representation of common reference signal at remote locations possible due to GPS synchronization 9
Figure 2.2: Major elements of the modern PMU [34]..... 12
Figure 2.3: Hierarchy of the phasor measurement systems, and levels of phasor data concentrators [34]. 12
Figure 3.1: Philips-Heffron linearized model..... 24
Figure 3.2: Single machine infinite bus system with local load..... 24
Figure 3.3: Linearized model of the ith machine in multi-machine power system..... 26
Figure 3.4: IEEE type-ST1 excitation system with lead-lag PSS 28
Figure 3.5: General PSS block diagram 29
Figure 3.6: IEE2ST type PSS..... 29
Figure 3.7: PSS2A type PSS 30
Figure 4.1: Proposed IEE2ST type PSS..... 33
Figure 4.2: Flowchart of DE optimization method 37
Figure 5.1: Representation of PMU Block in RTDS..... 40
Figure 5.2: IEEEST and IEE2ST Power system stabilizers..... 41
Figure 5.3: Transmission line model..... 41
Figure 5.4: Synchronous generator model with governor, exciter and PSS..... 42
Figure 5.5: Generator model with IEE2ST PSS integrated with PMU for damping inter-area oscillations..... 43
Figure 6.1: Bus diagram of three-machine nine-bus system..... 45
Figure 6.2: Simulated response of rotor speed at generator-1 under three-phase six-cycle fault at t=0.5sec (a) Without PSS (b)With IEEEST type single input PSS

and (c) With IEE2ST type multi-input PSS 49
Figure 6.3: Simulated response of rotor speed at generator-2 under three-phase six-cycle fault at t=0.5sec (a) Without PSS (b)With IEEEST type single input PSS and (c) With IEE2ST type multi-input PSS 49
Figure 6.4: Simulated response of rotor speed at generator-3 under three-phase six-cycle fault at t=0.5sec (a) Without PSS (b)With IEEEST type single input PSS and (c) With IEE2ST type multi-input PSS 50
Figure 6.5: Simulated response of rotor angle at generator-2 under three-phase six-cycle fault at t=0.5sec (a) Without PSS (b)With IEEEST type single input PSS and (c) With IEE2ST type multi-input PSS 50
Figure 6.6: Simulated response of rotor angle at generator-3 under three-phase six-cycle fault at t=0.5sec (a) Without PSS (b)With IEEEST type single input PSS and (c) With IEE2ST type multi-input PSS 51
Figure 6.7: Simulated response of real power at generator-1 under three-phase six-cycle fault at t=0.5sec (a) Without PSS (b)With IEEEST type single input PSS and (c) With IEE2ST type multi-input PSS 51
Figure 6.8: Simulated response of real power at generator-2 under three-phase six-cycle fault at t=0.5sec (a) Without PSS (b)With IEEEST type single input PSS and (c) With IEE2ST type multi-input PSS 52
Figure 6.9: Simulated response of real power at generator-3 under three-phase six-cycle fault at t=0.5sec (a) Without PSS (b)With IEEEST type single input PSS and (c) With IEE2ST type multi-input PSS 52
Figure 6.10: RTDS model of three-machine nine-bus system 54
Figure 6.11: RTDS response of three-phase six-cycle fault on three-machine nine-bus system 56
Figure 6.12: RTDS response of rotor speed at generator-1 under three-phase six-cycle

fault at t=0sec (a) Without PSS (b)With IEEEST type single input PSS and (c) With IEE2ST type multi-input PSS..... 56

Figure 6.13: RTDS response of rotor speed at generator-2 under three-phase six-cycle fault at t=0sec (a) Without PSS (b)With IEEEST type single input PSS and (c) With IEE2ST type multi-input PSS..... 57

Figure 6.14: RTDS response of rotor speed at generator-3 under three-phase six-cycle fault at t=0sec (a) Without PSS (b)With IEEEST type single input PSS and (c) With IEE2ST type multi-input PSS..... 57

Figure 6.15: RTDS response of rotor angle at generator-1 under three-phase six-cycle fault at t=0sec (a) Without PSS (b)With IEEEST type single input PSS and (c) With IEE2ST type multi-input PSS..... 58

Figure 6.16: RTDS response of rotor angle at generator-2 under three-phase six-cycle fault at t=0sec (a) Without PSS (b)With IEEEST type single input PSS and (c) With IEE2ST type multi-input PSS..... 58

Figure 6.17: RTDS response of rotor angle at generator-3 under three-phase six-cycle fault at t=0sec (a) Without PSS (b)With IEEEST type single input PSS and (c) With IEE2ST type multi-input PSS..... 59

Figure 6.18: RTDS response of real power at generator-1 under three-phase six-cycle fault at t=0sec (a) Without PSS (b)With IEEEST type single input PSS and (c) With IEE2ST type multi-input PSS..... 59

Figure 6.19: RTDS response of real power at generator-2 under three-phase six-cycle fault at t=0sec (a) Without PSS (b)With IEEEST type single input PSS and (c) With IEE2ST type multi-input PSS..... 60

Figure 6.20: RTDS response of real power at generator-3 under three-phase six-cycle fault at t=0sec (a) Without PSS (b)With IEEEST type single input PSS and (c) With IEE2ST type multi-input PSS..... 60

Figure 6.21: RTDS response of terminal voltage at generator-1 under three-phase six-cycle fault at t=0sec (a) Without PSS (b)With IEEEST type single input PSS and (c) With IEE2ST type multi-input PSS 61
Figure 6.22: RTDS response of terminal voltage at generator-2 under three-phase six-cycle fault at t=0sec (a) Without PSS (b)With IEEEST type single input PSS and (c) With IEE2ST type multi-input PSS 61
Figure 6.23: RTDS response of terminal voltage at generator-3 under three-phase six-cycle fault at t=0sec (a) Without PSS (b)With IEEEST type single input PSS and (c) With IEE2ST type multi-input PSS 62
Figure 6.24: A detailed 5-Machine 14-Bus test system 63
Figure 6.25: Simulated response of rotor speed at generator-1 under three-phase six-cycle fault at t=0.5sec (a) Without PSS (b)With IEEEST type single input PSS and (c) With IEE2ST type multi-input PSS 67
Figure 6.26: Simulated response of rotor speed at generator-2 under three-phase six-cycle fault at t=0.5sec (a) Without PSS (b)With IEEEST type single input PSS and (c) With IEE2ST type multi-input PSS 68
Figure 6.27: Simulated response of rotor speed at generator-3 under three-phase six-cycle fault at t=0.5sec (a) Without PSS (b)With IEEEST type single input PSS and (c) With IEE2ST type multi-input PSS 68
Figure 6.28: Simulated response of rotor speed at generator-4 under three-phase six-cycle fault at t=0.5sec (a) Without PSS (b)With IEEEST type single input PSS and (c) With IEE2ST type multi-input PSS 69
Figure 6.29: Simulated response of rotor speed at generator-5 under three-phase six-cycle fault at t=0.5sec (a) Without PSS (b)With IEEEST type single input PSS and (c) With IEE2ST type multi-input PSS 69
Figure 6.30: Simulated response of rotor angle at generator-2 under three-phase six-cycle

fault at t=0.5sec (a) Without PSS (b)With IEEEST type single input PSS and (c) With IEE2ST type multi-input PSS 70
Figure 6.31: Simulated response of rotor angle at generator-3 under three-phase six-cycle fault at t=0.5sec (a) Without PSS (b)With IEEEST type single input PSS and (c) With IEE2ST type multi-input PSS 70
Figure 6.32: Simulated response of rotor angle at generator-4 under three-phase six-cycle fault at t=0.5sec (a) Without PSS (b)With IEEEST type single input PSS and (c) With IEE2ST type multi-input PSS 71
Figure 6.33: Simulated response of rotor angle at generator-5 under three-phase six-cycle fault at t=0.5sec (a) Without PSS (b)With IEEEST type single input PSS and (c) With IEE2ST type multi-input PSS 71
Figure 6.34: Simulated response of real power at generator-1 under three-phase six-cycle fault at t=0.5sec (a) Without PSS (b)With IEEEST type single input PSS and (c) With IEE2ST type multi-input PSS 72
Figure 6.35: Simulated response of real power at generator-2 under three-phase six-cycle fault at t=0.5sec (a) Without PSS (b)With IEEEST type single input PSS and (c) With IEE2ST type multi-input PSS 72
Figure 6.36: Simulated response of real power at generator-3 under three-phase six-cycle fault at t=0.5sec (a) Without PSS (b)With IEEEST type single input PSS and (c) With IEE2ST type multi-input PSS 73
Figure 6.37: Simulated response of real power at generator-4 under three-phase six-cycle fault at t=0.5sec (a) Without PSS (b)With IEEEST type single input PSS and (c) With IEE2ST type multi-input PSS 73
Figure 6.38: Simulated response of real power at generator-5 under three-phase six-cycle fault at t=0.5sec (a) Without PSS (b)With IEEEST type single input PSS and (c) With IEE2ST type multi-input PSS 74

Figure 6.39: RTDS Model for 5-Machine 14-Bus system 75
Figure 6.40: RTDS response of three-phase six-cycle fault on five-machine fourteen-bus system 76
Figure 6.41: RTDS response of rotor speed at generator-1 under three-phase six-cycle fault at t=0sec (a) Without PSS (b)With IEEEST type single input PSS and (c) With IEE2ST type multi-input PSS..... 78
Figure 6.42: RTDS response of rotor speed at generator-2 under three-phase six-cycle fault at t=0sec (a) Without PSS (b)With IEEEST type single input PSS and (c) With IEE2ST type multi-input PSS..... 78
Figure 6.43: RTDS response of rotor speed at generator-3 under three-phase six-cycle fault at t=0sec (a) Without PSS (b)With IEEEST type single input PSS and (c) With IEE2ST type multi-input PSS..... 79
Figure 6.44: RTDS response of rotor speed at generator-4 under three-phase six-cycle fault at t=0sec (a) Without PSS (b)With IEEEST type single input PSS and (c) With IEE2ST type multi-input PSS..... 79
Figure 6.45: RTDS response of rotor speed at generator-5 under three-phase six-cycle fault at t=0sec (a) Without PSS (b)With IEEEST type single input PSS and (c) With IEE2ST type multi-input PSS..... 80
Figure 6.46: RTDS response of rotor angle at generator-1 under three-phase six-cycle fault at t=0sec (a) Without PSS (b)With IEEEST type single input PSS and (c) With IEE2ST type multi-input PSS..... 80
Figure 6.47: RTDS response of rotor angle at generator-2 under three-phase six-cycle fault at t=0sec (a) Without PSS (b)With IEEEST type single input PSS and (c) With IEE2ST type multi-input PSS..... 81
Figure 6.48: RTDS response of rotor angle at generator-3 under three-phase six-cycle fault at t=0sec (a) Without PSS (b)With IEEEST type single input PSS and

(c) With IEE2ST type multi-input PSS..... 81
Figure 6.49: RTDS response of rotor angle at generator-4 under three-phase six-cycle fault at t=0sec (a) Without PSS (b)With IEEEST type single input PSS and (c) With IEE2ST type multi-input PSS..... 82
Figure 6.50: RTDS response of rotor angle at generator-5 under three-phase six-cycle fault at t=0sec (a) Without PSS (b)With IEEEST type single input PSS and (c) With IEE2ST type multi-input PSS..... 82
Figure 6.51: RTDS response of real power at generator-1 under three-phase six-cycle fault at t=0sec (a) Without PSS (b)With IEEEST type single input PSS and (c) With IEE2ST type multi-input PSS..... 83
Figure 6.52: RTDS response of real power at generator-2 under three-phase six-cycle fault at t=0sec (a) Without PSS (b)With IEEEST type single input PSS and (c) With IEE2ST type multi-input PSS..... 83
Figure 6.53: RTDS response of real power at generator-3 under three-phase six-cycle fault at t=0sec (a) Without PSS (b)With IEEEST type single input PSS and (c) With IEE2ST type multi-input PSS..... 84
Figure 6.54: RTDS response of real power at generator-4 under three-phase six-cycle fault at t=0sec (a) Without PSS (b)With IEEEST type single input PSS and (c) With IEE2ST type multi-input PSS..... 84
Figure 6.55: RTDS response of real power at generator-5 under three-phase six-cycle fault at t=0sec (a) Without PSS (b)With IEEEST type single input PSS and (c) With IEE2ST type multi-input PSS..... 85
Figure 6.56: RTDS response of terminal voltage at generator-1 under three-phase six-cycle fault at t=0sec (a) Without PSS (b)With IEEEST type single input PSS and (c) With IEE2ST type multi-input PSS 85
Figure 6.57: RTDS response of terminal voltage at generator-2 under three-phase six-

cycle fault at t=0sec (a) Without PSS (b)With IEEEST type single input PSS and (c) With IEE2ST type multi-input PSS 86

Figure 6.58: RTDS response of terminal voltage at generator-3 under three-phase six-cycle fault at t=0sec (a) Without PSS (b)With IEEEST type single input PSS and (c) With IEE2ST type multi-input PSS 86

Figure 6.59: RTDS response of terminal voltage at generator-4 under three-phase six-cycle fault at t=0sec (a) Without PSS (b)With IEEEST type single input PSS and (c) With IEE2ST type multi-input PSS 87

Figure 6.60: RTDS response of terminal voltage at generator-5 under three-phase six-cycle fault at t=0sec (a) Without PSS (b)With IEEEST type single input PSS and (c) With IEE2ST type multi-input PSS 87

Figure 6.61: Rotor speed response of 3-Machine 9-Bus system for three-phase 30-cycle fault at t=0sec without supervisory control (a) Generator 1 (b) Generator 2 and (c) Generator 3 90

Figure 6.62: Rotor speed response of 3-Machine 9-Bus system for three-phase 30-cycle fault at t=0sec with supervisory control (a) Generator 1 (b) Generator 2 and (c) Generator 3 90

Figure 6.63: Braking resistor control response of 3-Machine 9-Bus system for three-phase 30-cycle fault at t=0sec with supervisory control..... 91

LIST OF TABLES

Table 2.1: Comparison between SCADA and PHASOR technologies..... 11

Table 2.2: System collapse and blackouts due to Inter-area Oscillations 14

Table 6.1: Optimal Location Identification for PSS Installation (Test Case-1)..... 45

Table 6.2: Optimal PSS Controller Gains for 3-Machine 9-Bus system..... 46

Table 6.3: Three-machine nine-bus system eigenvalues for without PSS, IEEEST PSS and IEE2ST PSS..... 47

Table 6.4: Optimal Location Identification for PSS Installation..... 64

Table 6.5: Optimal PSS Controller Gains for 5-Machine 14-Bus system..... 64

Table 6.6: 5-machine 14-bus system eigenvalues for without PSS, IEEEST PSS and IEE2ST PSS 65

ABSTRACT

Full Name : Irfan Ahmed Khan

Thesis Title : Power System Stability Enhancement Through Wide Area Measurements

Major Field : Electrical Engineering

Date of Degree : Dec, 2012

Low frequency inter-area oscillations in power systems is one of the main concerns for system operation and control. Since it imposes a limit in power transfer capability, therefore, adequate damping of inter-area oscillations is necessary to ensure, secure system operations and system reliability. Conventionally, power system stabilizers (PSSs) are used to enhance the system stability that is efficient for local modes. However, to enhance system damping of local as well as inter-area modes, remote signals needed to be measured and feedback to the power system stabilizers. In this context phasor measurement units are used as an important source of real-time data. For this purpose modern dual-input IEE2ST type PSSs are optimally placed in conjunction with Phasor Measurement Unit (PMU), for wide area damping control. In this thesis, enhancing the system damping of the inter-area modes using wide area measurements is addressed. Supervisory damping controller with braking resistor as a backup protection is also considered. The PMU-based wide-area power system stabilizer is designed, tested and validated on real-time digital simulator (RTDS).

KING FAHD UNIVERSITY OF PETROLEUM AND MINERALS,
DHAHRAN
DEC, 2012

ABSTRACT (ARABIC)

ملخص الرسالة

الاسم الكامل: عرفان أحمد خان

عنوان الرسالة: تعزيز اتزان نظم القوى الكهربائية باستخدام وحدات قياس المتجهات

التخصص: الهندسة الكهربائية

تاريخ الدرجة العلمية: ديسمبر 2012

تعتبر التذبذبات البينية ذات الترددات المنخفضة في مجال أنظمة القوى الكهربائية هي واحدة من الاهتمامات الرئيسية لتشغيل النظام والتحكم فيه. وحيث أن هناك حد في إمكانية نقل القوى الكهربائية نتيجة لهذه التذبذبات، فانه يجب توفيرالاخماد المناسب لهذة التذبذبات البينية وذلك لضمان آمان وموثوقية النظام. ويتم تقليديا استخدام مثبتات نظام القوى الكهربائية (Power System Stabilizers) لتعزيز استقرار النظام وتتسم هذة الطريقة بالكفاءة خصوصا فى اخماد الترددات المحلية. وعلى الرغم من ذلك، فانه من أجل تعزيز نظام الاخماد للترددات المحلية وكذلك التذبذبات البينية يتم قياس إشارات عن بعد وتغذيتها مرة أخرى لمثبتات نظام القوى الكهربائية. في هذا السياق يتم استخدام وحدات قياس المتجهات كمصدر مهم للبيانات في الوقت الحقيقي. لهذا الغرض يتم وضع المدخلات الحديثة المزدوجة (Power System Stabilizers) من النوع (IEE2ST) على النحو الأمثل بالتعاون مع وحدة قياس المتجهات (Phasor Measurement Units)، للتحكم فى منطقة واسعة الأخماد.

وفي هذه الرسالة يتم دراسة تعزيز نظام الأخماد للترددات البينية الواسعة باستخدام القياسات ومعالجتها. وكذلك أيضا يتم دراسة استخدام التحكم الإشرافي مع المقاومة الكبحية كحماية احتياطية. ولقد تم تصميم نظام استقرار القوى الكهربائية بمساعدة وحدة قياس المتجهات وتم التحقق من صحته واختباره باستخدام جهاز المحاكاة الرقمية في الوقت الحقيقي (Real Time Digital Simulation).

جامعة الملك فهد للبترول والمعادن

الظهران

ديسمبر 2012

NOMENCLATURE

Abbreviations

SMIB	Single-machine infinite bus
AVR	Automatic Voltage Regulator
DE	Differential Evolution
FACTS	Flexible AC transmission system
GPS	Global positioning system
LFIOs	Low-frequency inter-area oscillations
pu	Per unit
PSS	Power system stabilizer
PMU	Phasor measurement units
PDC	Phasor data concentrator
RTDS	Real time digital Simulator
SVC	Static Var Compensator
SCADA	Supervisory control and data acquisition
WAMAC	Wide area monitoring and control
WAMS	Wide area measurement system
WACS	Wide area control system
WADC	Wide area damping control

Symbols

P_m, P, P_e	Mechanical input power and electrical output power of the generator
D	Machine damping coefficient
M, H	Machine inertia coefficient and inertia constant
v_d, v_q	d- and q-axis terminal voltage
i_d, i_q	d- and q-axis armature current
x_d, x_d'	d-axis reactance and d-axis transient reactances
T_{do}'	Open-circuit field time constant
x_q	Generator q-axis reactance
E_q', E_{fd}	Generator internal and field voltages
V *or* v	Generator terminal voltage
V_{ref}	Reference voltage
U_{PSS}	PSS control signal
K_A, T_A	Gain and time constant of the excitation system

Y_L	Load impedance
Z, X, R	Transmission line impedance, reactance, and resistance
G, B	Load Inductance and susceptance
δ	Rotor angle
ω	Rotor speed
ω_b	Synchronous speed
ζ	Damping ratio
σ	Damping factor

CHAPTER 1

INTRODUCTION

1.1 Overview

Vast changes appeared during the last decades in the electricity markets led to an increased utilization and a higher loading of the electric transmission grids worldwide. These changes are mainly due to deregulation of the electrical energy markets and the extensions of large interconnected power systems. With the increase in high power flow transmission systems are nowadays operated on the edge of their technical limits and thus became more vulnerable to instabilities and more cascading failures occur than before [1–4].

The expansion of the transmission grids, on the other hand, is limited due to environmental and cost restrictions. The result is that the available transmission and generation facilities are highly utilized with large amounts of power interchanges taking place through tie-lines and geographical regions [5]. The tie lines operate near their

maximum capacity, especially those connected to the heavy load areas. As a result, the system operator can find itself close to or outside the secure operating limits under severe contingencies. Stressed operating conditions can increase the possibility of inter-area oscillations between different control areas and even collapse of the whole system.

Reliability and good performance are necessary in power system operation to ensure a safe and continuous energy supply [6,7]. However, weakly damped low frequency electromechanical oscillations (also called inter-area oscillations ranges 0.2 - 1 Hz) inherent to large interconnected power systems during transient conditions, are not only dangerous for the reliability and performance of such systems but also for the quality of the supplied energy [8]. The power flows over certain network branches resulting from generator oscillations can take peak values that are dangerous from the point of view of secure system operation and lead to limitations in network control.

1.2 Motivation

With the heavier power transfers ahead, the damping of inter-area oscillations is very difficult unless new lines are built or other heavy and expensive high-voltage equipment such as series-compensation is added to the grid's substations [9]. The construction of new lines, however, is restricted by environmental and cost factors. Therefore, achievement of maximum available transfer capability has become a major concern. This concern requires the need for a better system control, leading to damping improvement [10].

The increased number of annual power outages worldwide shows that the need of better monitoring concepts and tools fitted to the actual and future situation of power systems became urgent [11]. Such systems will support the system operators by the online assessment of the system current situations and control the power system by providing extra stability with fore sighting of overall system. In this context, the use of synchronized phasor measurements is becoming an important tendency for the surveillance of the power systems[12,13]. They are provided by phasor measurements units (PMUs), considered to be one of the most important measuring devices in the future of power systems. That's why PMUs are turned to useful sources of real-time data. They provide the required information needed by the grid operator on the actual system state and are combined with relevant data of the given system with the aim to early detect the instability. The monitoring method proposed, describes an efficient alternative for the online surveillance of the power system stability using PMUs data.

One of the most common applications of phasor measurement units (PMUs) is power system monitoring, especially for monitoring wide-area disturbances and low frequency electromechanical oscillations [14,15]. PMUs are a solution to increase observability in traditional monitoring systems and provide additional insight of power system dynamics. In recent years, the introduction of synchrophasor measurement technology has significantly improved observability of power system dynamics and is expected to play a more important role in the enhancement of power system controllability. With the development of wide-area measurement technology, real-time-feedback-control based on PMU becomes increasingly feasible than ever [16], which

is a promising solution for dynamics performance improvement, such as inter-area oscillations damping, in a large scale interconnected power system. Due to a lack of global observability, traditional damping controllers like power system stabilizers (PSSs), cannot always deal with inter-area oscillations effectively. Continuous wide-area controls offer observability and controllability benefits where conventional local continuous controls cannot.

The PSS provides supplementary control action through the excitation system of generators and thus aids in damping the oscillations of synchronous machine rotors via modulation of the generator excitation. To provide damping, the stabilizer must produce a component of electrical torque in phase with the rotor speed deviations [17]. The PSS usually rely on local information (such as generator rotor speed or electric power) and are effective in damping local modes [18]. The performance requirements of PSS for closed-loop applications are discussed in [19].Carefully tuned PSSs may also be able to damp some inter-area oscillations; those which can be observed in the monitored input signals. By appropriately tuning available PSSs, together with wide-area measurements obtained from PMUs, it is expected that inter-area damping can be effectively improved. The basic function of a PSS is to add damping to the generator rotor oscillations by controlling its excitation using auxiliary stabilizing signal(s).

With more experience accumulated from interconnected electric power system operation, power system engineers are now convinced that the low-frequency oscillations are due to the lack of damping of the mechanical mode of the

interconnected system, and the desired additional damping can be provided by supplementary excitation control. It is expected that real-time monitoring and control using synchrophasor measurements could help enhancing system stability and security, particularly by enhancing inter-area damping control [20].

1.3 Thesis Objectives

In summary, the objectives of the proposed work are:

- Developing a wide area monitoring and control system that aims to mitigate the inter-area oscillations.
- Designing of PSS integrated to PMUs' to damp out the oscillations more efficiently.
- Development of a backup damping controller on a standard test systems.
- Building a test system integrated with a number of PMU's on the modern powerful tool, Real time Digital Simulator, RTDS.

1.4 Thesis Contribution

Low frequency inter-area oscillations in power systems is one of the main concerns for system operation and control. Therefore, adequate damping of inter-area oscillations is necessary for secure system operation and ensure system reliability. However, to enhance the damping of inter-area modes remote signal is needed to be measured and feedback to the power system stabilizers. It is found that if remote signals from one or more distant locations of the power system are applied to the controller design, the system dynamic performance can be enhanced for the inter-area oscillations [21]. The remote signals are

often referred to as global signals to illustrate the fact that they contain information about overall network dynamics as opposed to local control signals which lack adequate observability of some of the significant inter-area modes. In this thesis enhancing the damping of the inter-area modes using wide area measurements has been addressed. Where dynamic performance is enhanced by wide area measurements through phasor measurement units (PMU's). Dual input PSSs integrated with PMUs to damp inter-area oscillations are tested and validated on real-time digital simulator (RTDS). The proposed work involves the following steps.

i) *Development of Dual Input PSS controller integrated with PMU's:* Power system stabilizers are essential for the providing the stability under fault conditions and also for damping of low frequency oscillations [22,23]. However these PSSs control the local generator, to a limited extent. For local modes, the largest observability is associated with a local signal, e.g., generator rotor speed signal for PSS. But for inter-area modes, the local signals may not be the ones with maximum observability [20]. In order to damp local as well as inter-area modes, local signal integrated with remote signal is needed to be measured in synchronism with GPS clock to enhance the damping of PSSs for low frequency inter-area oscillations. This is the first time that dual input IEE2ST type PSS is integrated with PMU for damping these oscillations.

ii) *Development of Backup Damping Controller:* Under fault conditions it is noticeable that PSS provides damping to some extent. But what will happen if the system becomes unstable due to a severe fault, then there should be some backup loop. Here the backup is based on frequency sensitivity of the system provided by PMUs, which triggers

the braking resistor to maintain system stability. It keeps the system within the operating limits avoiding system collapse. Based on frequency sensitivity, this control will be activated before tripping of generators, by maintaining secure and reliable continuous power flow over the network.

1.5 Thesis Organization

The subsequent chapters of this thesis are organized as follows:

Chapter 2 gives a brief introduction of inter-area oscillations damping control based on recent practical applications. Chapter 3 presents the modeling and analysis of large power system dynamics. The proposed approach to solve the problem is formulated in chapter 4, which gives a description of the optimal location of PSSs integrated with PMUs, its optimization and supervisory backup control as a second level protection. Experimental setup is presented in Chapter 5. Chapter 6 presents the promising results of the proposed approach developed in chapter 4. The thesis is finalized in chapter 7 by drawing some conclusions and outlining the work to be carried out in the future.

CHAPTER 2

LITRATURE REVIEW

Power system oscillation damping remains as one of the major concerns for secure and reliable operation of large power systems, and is of great current interest to both industry and academia [24]. The principal reason for this is that the inception of poorly-damped low-frequency inter-area oscillations (LFIOs) when power systems are operating under stringent conditions may lead to system-wide breakups or considerably reduce the power transfers over critical corridors. With the availability of high-sampling rate phasor measurement units (PMUs), there is an increasing interest for effectively utilizing conventional damping control devices, such as power system stabilizers (PSSs), by using these measurements as control input signals. In this chapter, we provide a comprehensive overview of distinct elements (or "building blocks") necessary for wide-area power system damping using phasor measurement units and PSSs. This chapter presents the latest developments in the implementation of synchrophasor measurements in WAMS and WACS as well as their prospective for WADC applications.

2.1 Phasor Measurement Units

It is considered to be one of the most important measurement technologies in the future of power systems due to its unique ability to sample analog voltage and current waveform data in synchronism with a GPS-clock [25] and compute the corresponding 60 Hz phasor component (i.e. complex numbers representing the magnitude and phase angle of a 60 Hz sinusoidal waveform) from widely dispersed locations. Fig. 2.1 represents the synchronized sampling process of the different waveforms and provide a common reference for the phasor calculations at all the different locations [26]. Just as in DC circuits, power flows from high voltages to low voltages, in an AC power system, real power flows from a higher voltage phase angle to a lower voltage phase angle [26] – the larger the phase angle difference between the source and the sink, the greater the power flow between those points implying larger the static stress being exerted across that interface and closer the proximity to instability.

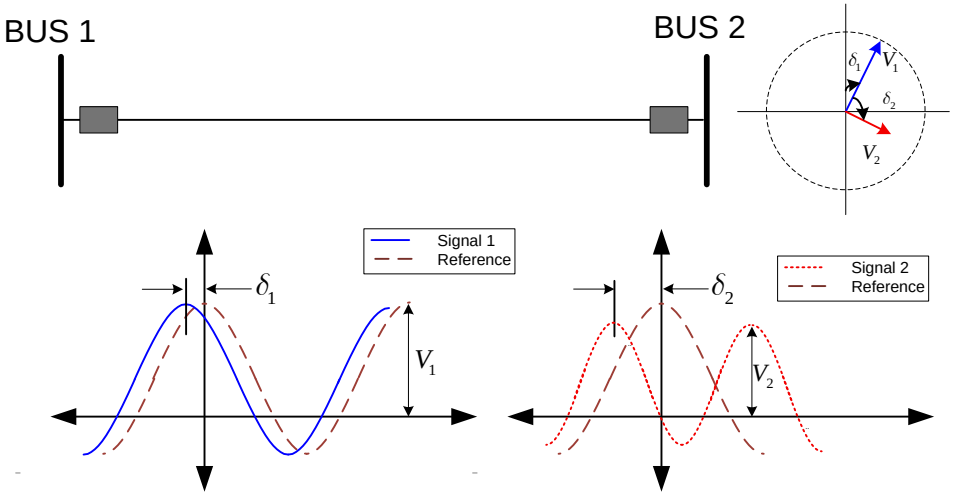

Figure 2.1: Representation of common reference signal at remote locations possible due to GPS synchronization

Voltage phasor angles of power network buses have always been of special interest to power system engineers. It is well known that active (real) power flow in a power line is very nearly proportional to the angle difference between voltages at the two terminals of the line. The flow of real power and angle differences across transmission has been of concern for many years. The earliest modern application involving direct measurement of phase angle differences was reported in early 1980s [27–29]. These systems used LORAN-C, GEOs satellite transmissions, and the HBG radio transmissions (in Europe) in order to obtain synchronization of reference time at different locations in a power system.

Operation of the power system is based on SCADA and EMS systems that have evolved over the last 50 years. Phasor measurement is the next generation of measurement technology that is needed for the real-time wide area monitoring of the power system. Phasor address the problems that have surfaced in most of the major blackouts that have occurred around the world, notably August 2003 Eastern Interconnection Blackout in the U.S. [30], August 1996 Western Interconnection Blackout in the U.S.[31], Summer 2003 and 2004 blackouts in Europe and elsewhere [32]. All these blackout investigations reached some combination of the following conclusions:

- Lack of wide area visibility
- Lack of time-synchronized data
- Lack of ability to monitor system dynamics behavior in real-time.

However, phasor technology addresses these shortcomings because, phasor is considered as the MRI (Magnetic Resonance Imaging) of the power system providing

high resolution, time-synchronized data for system-wide grid dynamics visibility, compared to the "x-ray quality" visibility of the traditional SCADA-based systems. SCADA was designed for local area control, monitoring and management. Development of power system interconnections and regional markets have shifted the focus for grid monitoring and control to a much larger geographic footprints and adapting SCADA to meet this emerging need is cost prohibitive. Phasor technology overcomes the limitations of SCADA for wide area, time-synchronized, dynamic, real-time grid monitoring and control. Table 2.1 compares phasor capabilities with SCADA [33].

Table 2.1: Comparison between SCADA and PHASOR technologies

ATTRIBUTE	SCADA	PHASOR
Measurement	Analog	Digital
Resolution	2-4 samples per sec	Up to 60 samples per sec
Observability	Steady State	Dynamic/Transient
Monitoring	Local	Wide-Area
Phase Angle Measurement	No	Yes
Measured Quantity	Magnitude – (RMS) – MW, MVAR	Magnitude (RMS) and phase offset from common reference – MW, MVAR, and Angle Difference

The Block diagram of PMU is illustrated in Fig. 2.2, where the analog inputs are currents and voltages, obtained from the secondary windings of the current and voltage transformers. All three-phase currents and voltages are used so that positive-sequence measurement can be carried out. The current and voltage signals are converted into digital form by analog-to-digital converters. The sampling clock is phase-locked with the GPS clock. Sampling rates start with a rate of 12 samples per cycle to as high as 96 or 128 samples per cycle in more modern devices [34].

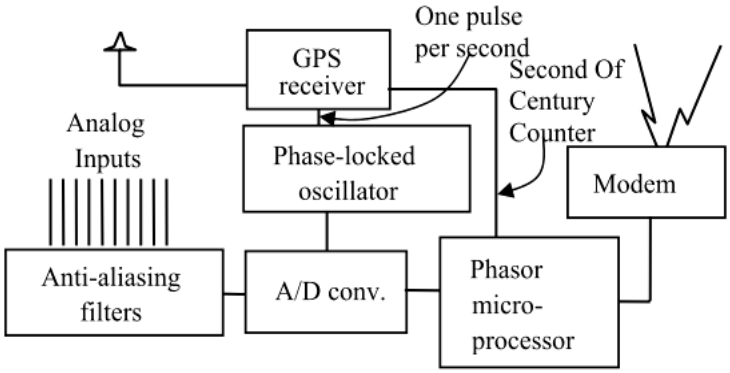

Figure 2.2: Major elements of the modern PMU [34].

The PMUs are installed in power system substations. The selection of substations where these installations take place depends upon the use to be made of the measurements they provide. In most applications, the phasor data is used at locations remote from the PMUs. Thus an architecture involving PMUs, communication links, and data concentrators must exist in order to realize the full benefit of the PMU measurement system. A generally accepted architecture of such a system is shown in Fig. 2.3.

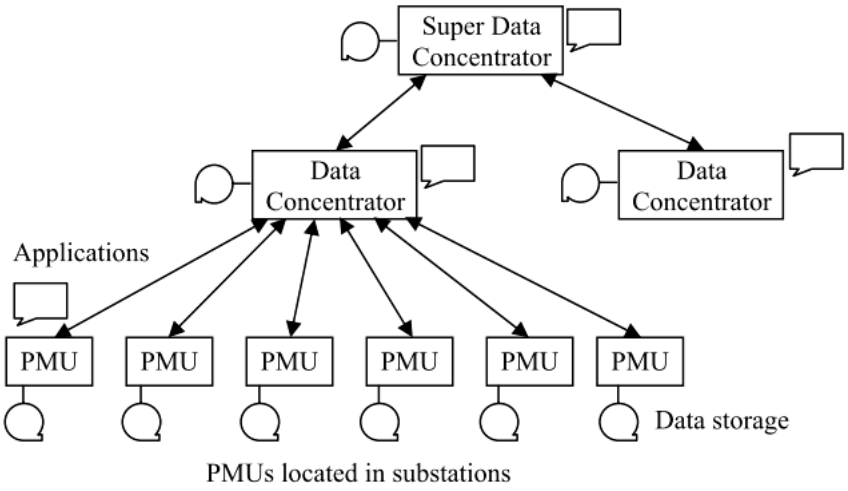

Figure 2.3: Hierarchy of the phasor measurement systems, and levels of phasor data concentrators [34].

In Fig. 2.3 the PMUs are situated in power system substations, and provide measurements of time-stamped positive-sequence voltages and currents of all monitored

buses and feeders (as well as frequency and rate of change of frequency). The measurements are stored in local data storage devices, which can be accessed from remote locations for post-mortem or diagnostic purposes. The local storage capacity is necessarily limited, and the stored data belonging to an interesting power system event must be flagged for permanent storage so that it is not overwritten when the local storage capacity is exhausted. The phasor data is also available for real-time applications in a steady stream as soon as the measurements are made. There may well be some local application tasks which require PMU data, in which case it can be made available locally for such tasks. However, the main use of the real-time data is at a higher level where data from several PMUs is available.

The devices at next level of the hierarchy are commonly known as "phasor data concentrators" (PDCs). Typical function of the PDCs is to gather data from several PMUs, reject bad data, align the time–stamps, and create a coherent record of simultaneously recorded data from a wider part of the power system. There are local storage facilities in the PDCs, as well as application functions which need the PMU data available at the PDC. This can be made available by the PDCs to the local applications in real-time. One may view the first hierarchical level of PDCs as being regional in their data-gathering capability. On a system wide scale, one must consider another level of the hierarchy (Super Data Concentrator in Fig. 2.3). The functions at this level are similar to those at the PDC levels – that is, there is facility for data storage of data aligned with time-tags as well as a steady stream of near real-time data for applications which require data over the entire system. Fig. 2.3 shows the communication links to be bidirectional. Indeed, most of the data flow is upward in the hierarchy, although there are some tasks which require communication capability in the reverse direction [34].

2.2 Inter Area Oscillations

Even today, when voltage problems are by far, more important for network operators than damping control, large disturbances tend to induce wide-area low frequency oscillations in major grids throughout the world: at 0.6 Hz in the Hydro-Quebec system [35,36], 0.2 Hz in the western North-American interconnection [37,38], 0.15-0.25 Hz in Brazil [39] and 0.19-0.36 Hz in the UCTE/CENTREL interconnection in Europe [40]. The recent 2003 blackout in eastern Canada and US was equally accompanied by severe 0.4 Hz oscillations in several post-contingency stages [41]. The two famous WECC cases in the summers of 1996 and 2000 were both associated with poorly damped inter-area oscillations under conditions of high power transfer on long paths [38]. A brief history of major system collapse and blackouts in all over the world due to low frequency inter-area oscillations are shown in Table 2.2.

Table 2.2: System collapse and blackouts due to Inter-area Oscillations

Year	Locations
2003	Eastern Canada and USA
2006	UCTE/CENTREL interconnection in Europe
2003	Western North-American interconnection
1964, 1996, 2000	Western Electric Coordinating Council (WECC)
1960s, 1985	Hydro-Quebec system
1960	Finland-Sweden-Norway-Denmark
1971, 1974	Italy-Yugoslavia-Austria
197 1,1972	Mid-continent area power pool (MAPP)
1966	Saskatchewan-Manitoba Hydro-Western Ontario
1975	South East Australia (1975)
1978	Scotland-England
1982 , 1983	Western Australia
1985	Taiwan

Inter-area oscillations are a part of the nature of interconnected power systems. Large power systems being connected by weak ties transmitting heavy power flows tend to exhibit such modes. These oscillations are a result of the swing between groups of machines in one area against groups of machines in another area, interacting via the transmission system. They may be caused by small disturbances such as changes in loads or may occur as an aftermath of large disturbances. This type of instability (small-signal rotor-angle instability) in interconnected power systems is mostly dominated by low frequency inter-area oscillations (LFIO). LFIOs may be result in small disturbances, if this is the case, their effects might not be instantaneously noticed. However, over a period of time, they may grow in amplitude and cause the system to collapse [42]. Incidents of inter-area oscillations have been reported form many decades.

Characteristics of inter-area oscillations are analyzed in [43] using modal analysis of network variables such as voltage magnitude and angle; these are quantities that can be measured directly by PMUs. The study gives a deeper understanding of how inter-area oscillations propagate in the power system network and proposes an alternative for system oscillatory mode analysis and mode tracing by focusing on network variables.

Power system oscillation damping has always been a major concern for the reliable operation of power systems. To increase damping, several approaches have been proposed; the most common ones being excitation control through power system stabilizers (PSS), SVCs and other FACTS devices [44,45]. In this thesis, the main focus is on PSS excitation control using control input signals derived from PMU data.

Over the past decades, the concept of wide area measurement and control systems has been widely discussed. The concept is particularly based on data collection and control of large interconnected power systems by means of time synchronized phasor measurements [46]. Due to economical constraints, electric utilities are being forced to optimally operate power system network, under very stringent conditions. In addition, deregulation has forced more power transfers over a limited transmission infrastructure.

As a consequence, power systems are being driven closer to their capacity limits which may lead to system breakdowns. For this reason, it is necessary for power systems to have high power transfer capacity while maintaining high reliability. One of the main problems of current Energy Management System (EMS) is insufficient view of system dynamics from Supervisory Control and Data Acquisition (SCADA) and uncoordinated local actions. Wide-Area Measurement Systems (WAMS) and Wide-Area Control Systems (WACS) based on synchronized phasor measurement propose a solution to these issues. Consequently, the importance of WAMS and WACS has significantly increased and more attention has been paid towards their increased development [47].

In the recent years, PMU based WAMS devices has received ever increasing attention from the academia as well as from the industry. Power utilities have been designing and implementing WAMS to provide more intelligent monitoring, control, and protection of the power grid, in order to achieve real-time operations in the modern power systems [48]. WAMS basic purpose is for the wide-area security assessment to provide early warnings of deteriorating system conditions to the control center [49].

The WAMS project was founded in 1995 by the U.S. Department of Energy to encourage the development of advanced tools for wide-area measurement, control and operation in the Western North American power system (WECC) [50]. U.S. Eastern Interconnection [51], Canada [52] , Russia [53], China [54,55], Brazil [56], Italy[57], Europe [58], Mexico [59], Nordic countries [60] and others have installed WAMS [61]. The measurement devices used in WAMS are GPS-time synchronized PMUs which provides high sample rate of voltage and current phasor measurements. It is noted that the most commonly used applications of WAMS are phase angle and oscillation monitoring with limited use for voltage stability monitoring. Its application is to improve the knowledge of system dynamics. For efficient system dynamics and economics, studies shows that optimal placement of PMU is necessary for large interconnected power systems [62–64].

WACS serves as a base for emergency control systems using measurements obtained from WAMS [65]. The objectives of this control system are blackout prevention, power system stability improvement, and transmission capacity enhancement. WACS uses PMUs as an advanced measurement technology, fiber optics communication, and real-time control computers. The communication infrastructure causes some delays. However, preliminary investigation of the problem of inter-area oscillation damping using remote measurements revealed that a small amount of delay (up to 200ms) did not significantly reduce the performance of the response of the system under small-signal or transient conditions during time-domain simulations [66]. The communication infrastructure of time delays of PMU are discussed in [67–69].

Some salient features of WACS described are improvement of observability and controllability, outage control, and high reliability and flexibility. The remaining challenges are to shift from monitoring to control (WAMS to WACS) and to fully utilize the benefit of synchrophasor measurement technology.

The objectives for control in today's large interconnected power systems are to improve dynamic performance and to enhance transfer capacity in weak tie-lines. Several studies suggest that due to the lack of observability in local measurements of certain inter-area modes, damping control using global signals may be more effective than local control [52,70–73]. One promising application of WACS using global measurements is wide-area damping control (WADC). The concept is to design the controller that use wide-area measurements to improve power system oscillation damping. WADC implementations, such as control of PSSs using synchronized phasor measurements are discussed in [74,75].

A wide-area measurement project was started by Fingrid, the Finnish transmission system, back in 2006. Nowadays the system deploys 12 phasor measurement units (PMU) and a phasor data concentrator (PDC) with applications. PMU are also installed to wide-area measurement systems in Norway and Denmark [76]. WADC with SVCs are installed in the Nordic power system are presented in [77]. Present and past applications of WAMS and WACS at Hydro-Québec are discussed in [52], where recent studies have been focused on damping stability control. The WAMS implementation at Hydro-Québec shows that wide-area stabilizing PSS controllers using PMU information can improve the

dynamic performance of the system. Simulation results on China's Northern grid have demonstrated that the proposed design was successful at achieving its design specifications [78].

Recently, a successful implementation of WADC on China's Southern Power Grid was reported in [79]. PMUs integrated with SVCs are installed on six 500kV HVDC link substations in China Southern Power Grid. Closed-loop field tests show a promising future for WADC. The field test results show that the commission of WADC system can increase the damping ratio of the dominant modes more than 10%. The only PMU based continuous feedback control, in the real bulk power grid is developed in China [79]. Which is still in testing phase and based on SVC's to provide reactive power to the substations. It lacks the controlling of excitation system such as dual input PSS to damp inter-area oscillations.

2.3 Power System Stabilizer Design

Power System Stabilizers are supplementary control devices which are installed in generator excitation systems. Their main function is to improve stability by adding an additional stabilizing signal to compensate for undamped oscillations [80]. The action of a PSS is to extend the angular stability limits of a power system by providing supplemental damping to the oscillation of synchronous machine rotors through the generator excitation. This damping is provided by an electric torque applied to the rotor that is in phase with the speed varies.

It has been suggested in several studies that the information obtained from PMUs is valuable for damping control, and with properly tuned controllers, global control may yield better performance than local control. This research mainly focuses on the problem of improving the performance of conventional PSS, for a better damping of inter-area oscillations, by using instantaneous measurements from remote locations of the grid as its supplementary inputs. The optimal placement of power system stabilizer (PSS) on remote generators for damping electromechanical oscillation of power system is discussed in [81,82].

Generator speed, terminal-bus frequency, and active power are the most commonly used control input signals. The most common input signal for local control is generator speed deviations [83]. Controllers based on speed deviation would ideally use a differential-type of regulation and a high gain. Since this is impractical in reality, the previously mentioned lead-lag structure is commonly used. However, one of the limitations of the speed-input PSS is that it may excite torsional oscillatory modes [83,84]. A power/speed (ΔPe-ω) PSS design was proposed as a solution to the torsional interaction problem suffered by the speed-input PSS [85]. The power signal used is the generator electrical power, which has high torsional attenuation. Due to this, the gain of the PSS may be increased without the resultant loss of stability, which leads to greater oscillation damping [83].

Recently, wide-area or global signals obtained from PMUs have gradually gained popularity as promising alternatives to local signals. In [86], it is shown that if $\Delta\omega$ signals

are used, they must be synchronized. For PSSs using PMU control input signals, this important aspect has not been addressed in the literature. However, this is a topic currently being investigated at KTH and interesting results will be available soon [86].

Current research has focused on rotor speed as a control variable [3,87–89]. It has been found that frequency is highly sensitive to the strength of the transmission system, that is, more sensitive when the system is weaker, which may offset the controller action on the electrical torque of the machine. The signal with maximum observability for a particular mode can be from a remote location or combined information from several locations. Therefore, in combination with local control, a remote signal provides more stability to the wide area power system. For that reason, PMU carries out an important task to provide the real-time synchronized remote signal, to the input of PSS, which would damp the low frequency oscillations in the wide area system to a wide extent. The disadvantages of local signals are lack of global observability and lack of mutual coordination. Several approaches for the selection of PSS control input signals for damping of inter-area oscillations are described in [3,87–91]. The results show that the wide-area signal yield better performance than that of the conventional approach. Therefore, dual input PSS integrated with PMUs are considered to damp out local as well as inter-area modes.

2.4 Backup Damping Control

Many serious accidents are due to malfunction of relay, breakers, and other switching devices. The backup protection is used to clear the fault when main protection of

electrical equipment or the corresponding circuit breaker refused to work with equipment fault protection. For this purpose dynamic braking resistor is used for backup damping controller. The dynamic braking resistor has been known to be a useful tool in stabilizing power systems following large disturbances in the system. The braking resistor can be viewed as fast load injection to absorb the excess transient energy of an area caused by a disturbance. It has generally been studied as a shunt resistor load connected at a generator site and its energy absorbing capacity is limited by the maximum temperature rise of the braking resistor material. Dynamic braking resistors are in use in the USA, Japan and the USSR [92].

Normally, switching of the resistors in these installations is done on the basis of open-loop, predetermined strategies. A number of theoretical and computer studies on braking resistor switching strategies are reported in the literature [93,94]. The strategy is based on the switching of a braking resistor and shunt reactor alternately depending on speed deviations. The resistor absorbs the excess energy when the machine accelerates. The strategy that the brake will be switched in and out several times to absorb the excessive power and settles downs the transient instabilities. A backup damping control is provided by using braking resistor in addition to the PSS, before generators isolation from the system.

CHAPTER 3

POWER SYSTEM MODEL

3.1 Single Machine Infinite Bus System

The 4^{th} order non-linear model of SMIB is given as,

$$\dot{\delta} = \omega_0 \Delta\omega \tag{3.1}$$

$$\dot{\omega} = \frac{1}{2H}\left[P_m - P_e - P_D\right] \tag{3.2}$$

$$\dot{e}'_q = \frac{1}{T'_{do}}\left[E_{fd} - e'_q - (x_d - x'_d)i_d\right] \tag{3.3}$$

$$\dot{E}_{fd} = \frac{1}{T_A}\left[K_A(V_{ref} - V_t) - E_{fd}\right] \tag{3.4}$$

Here, the states [δ ω e'_q E_{fd}] are generator rotor angle, speed, field voltage, and d-q components of the internal voltages respectively.

A complete system model for Low-frequency oscillation studies can be derived from the block diagram as shown in Fig. 3.1 [95,96].

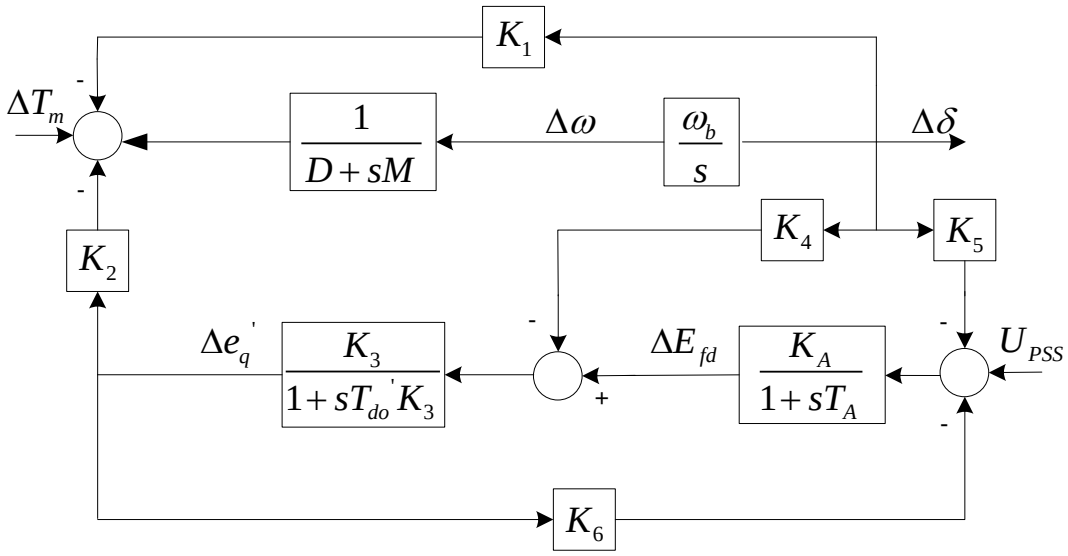

Figure 3.1: Philips-Heffron linearized model

For controller design purposes, it is usually more convenient to work with a linear model. The first step to develop the linearized model of the power system for low frequency oscillation studies is to calculate the initial conditions such as initial currents, initial voltages, initial rotor angles …etc. Linearized equations are obtained from the Fig. 3.1 while Fig. 3.2 represents the SMIB system for calculating the initial conditions. Initial condition calculation, linearization constants K_1, K_2, ..., K_6 and the state space model of SMIB is shown in appendix A.

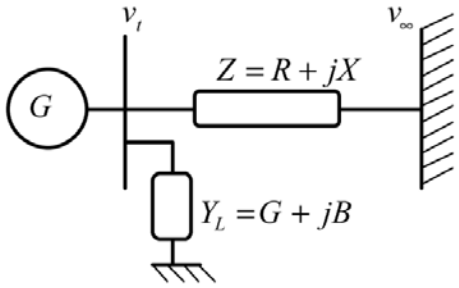

Figure 3.2: Single machine infinite bus system with local load

From Philips Heffron block diagram Fig. 3.2, I addition with the supplementary excitation control U_{PSS}, the state space equations may be written as

$$\dot{X} = AX + BU_{PSS} \tag{3.5}$$

The 4th order model of SMIB will becomes,

$$\begin{bmatrix} \Delta\dot{\delta} \\ \Delta\dot{\omega} \\ \Delta\dot{e}'_q \\ \Delta\dot{E}_{fd} \end{bmatrix} = \begin{bmatrix} 0 & \omega_b & 0 & 0 \\ -\frac{K_1}{M} & -\frac{D}{M} & -\frac{K_2}{M} & 0 \\ -\frac{K_4}{T'_{do}} & 0 & -\frac{1}{K_3 T'_{do}} & \frac{1}{T'_{do}} \\ -\frac{K_A K_5}{T_A} & 0 & -\frac{K_A K_6}{T_A} & -\frac{1}{T_A} \end{bmatrix} \begin{bmatrix} \Delta\delta \\ \Delta\omega \\ \Delta e'_q \\ \Delta E_{fd} \end{bmatrix} + \begin{bmatrix} 0 \\ 0 \\ 0 \\ \frac{K_A}{T_A} \end{bmatrix} U_{PSS} \tag{3.6}$$

3.2 Multimachine Power System

In this section, the SMIB system model represented by Fig. 3.1 is extended to describe an *n*-machine *m*-bus multi-machine power system [97,98]. A typical block diagram of the i^{th} machine can be represented by Fig. 3.3. Because of the interaction among machines, the branches and loops become multiplied [99]; for instance, K_1 becomes K_{1ij}, T_A becomes T_{Ai}, etc. The state variables also become multiplied; for instance, $\Delta\delta$ becomes $\Delta\delta_i$, where, i = 1, ..., n, and j = 1, ... ,n.

A multimachine power system with i^{th} machines is modeled as:

$$\dot{\delta}_i = \omega_b(\omega_i - 1) \tag{3.7}$$

$$\dot{\omega}_i = (P_{mi} - P_{ei} - D_i(\omega_i - 1))/M_i \tag{3.8}$$

$$\dot{E}'_{qi} = (E_{fdi} - (x_{di} - x'_{di})i_{di} - E'_{qi})/T'_{doi} \tag{3.9}$$

$$\dot{E}_{fdi} = (K_{Ai}(V_{refi} - v_i + u_{PSSi}) - E_{fdi})/T_{Ai} \tag{3.10}$$

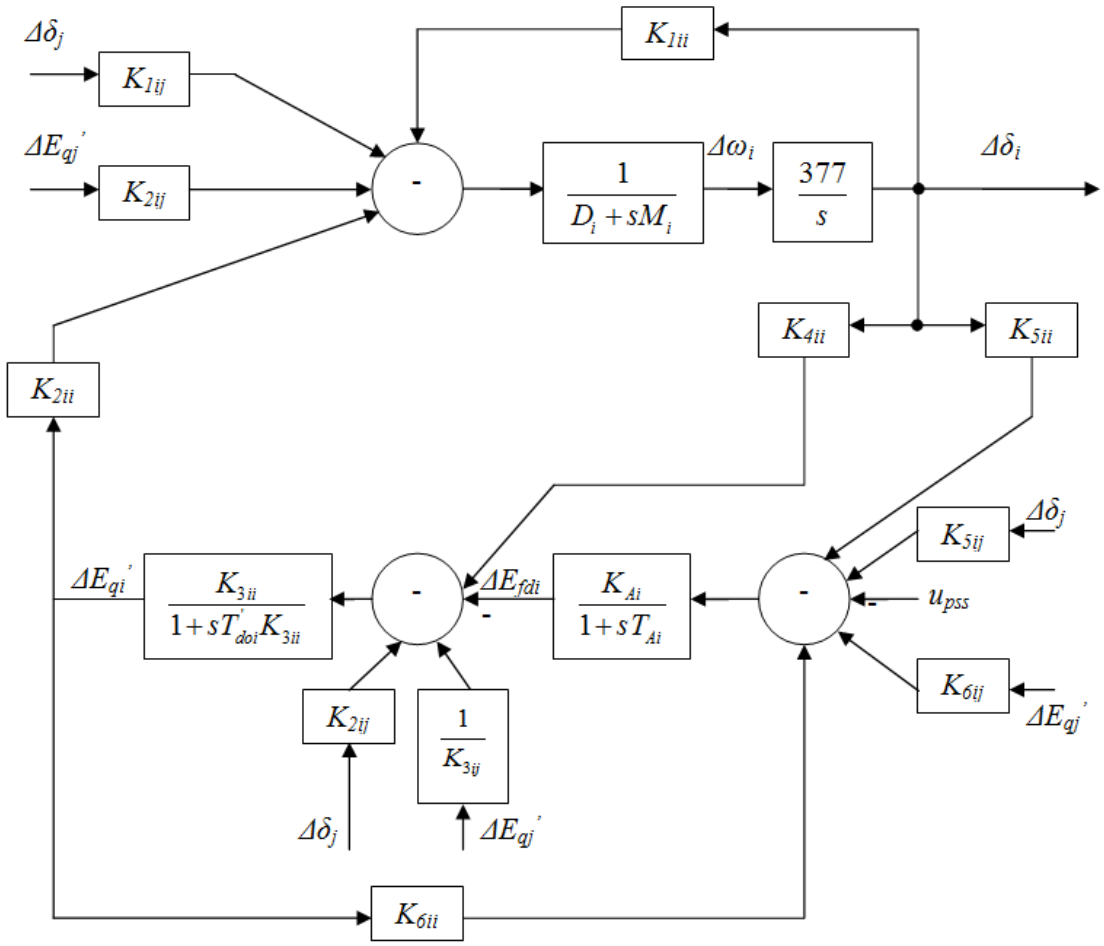

Figure 3.3: Linearized model of the ith machine in multi-machine power system

It is worth emphasizing that if a PSS is incorporated in the multimachine system, the *Y*-matrix is no longer constant. The PSS stabilizer is a widely used lead-lag controller, whose transfer function is

$$U_{PSS} = K_C \frac{sT_w}{1+sT_w}\left(\frac{1+sT_1}{1+sT_2}\right)\left(\frac{1+sT_3}{1+sT_4}\right)\Delta\omega \qquad (3.11)$$

where, $\Delta\omega$ and U_{PSS} are stabilizer input and output, K_C is stabilizer gain, T_w is washout time constant, T_1, T_2, T_3, and T_4 are stabilizer time constant. Since the state equation, is in the general form, it is applicable to any number of machines. So the system matrix will be as follows:

$$\dot{x} = Ax + Bu \tag{3.12}$$

$$\begin{bmatrix} \dot{x}_1 \\ \dot{x}_2 \\ \dot{x}_3 \\ \vdots \\ \dot{x}_n \end{bmatrix} = \begin{bmatrix} A_{11} & A_{12} & A_{13} & \cdots & A_{1n} \\ A_{21} & A_{22} & A_{23} & \cdots & A_{2n} \\ A_{31} & A_{32} & A_{33} & \cdots & A_{3n} \\ \vdots & \vdots & \vdots & \ddots & \vdots \\ A_{n1} & A_{n2} & A_{n3} & \cdots & A_{nn} \end{bmatrix} + [B] \begin{bmatrix} u_1 \\ u_2 \\ u_3 \\ \vdots \\ u_n \end{bmatrix} \tag{3.13}$$

where $\dot{x}_1, \ldots, \dot{x}_n$ are the state variable vectors of *n* machines, $u_1, \ldots, u_n$ are the controls; B is the control matrix; $A_{11}, A_{22}, \ldots, A_{nn}$ are the local system matrices of the individual machines; and the off-diagonal matrices A_{12}, A_{23} and so on, represent the paths of dynamic interaction between machines. Note that (3.13) can be expanded to any number of machines using high-or low-order machine and control models.

3.3 Excitation system

The excitation system considered in this study by the IEEE type-ST1 system shown in Fig. 3.4, and is described by

$$\dot{E}_{fd} = (K_A(V_{ref} - V_t + U_{PSS}) - E_{fd})/T_A \tag{3.14}$$

$$V_t = (V_d^2 + V_q^2)^{1/2} \tag{3.15}$$

$$V_d = x_q i_q \tag{3.16}$$

$$V_q = E_q^{'} - x_d^{'} i_d \tag{3.17}$$

Where, $E_q^{'}$, E_{fd} are the generator internal and field voltages, x_d, $x_d^{'}$ are d-axis reactance and d-axis transient reactances, i_d, i_q are d- and q-axis armature currents respectively. V_t

is generator terminal voltage and U_{PSS} is the PSS control signal. A conventional lead-lag PSS is installed in the feedback loop to generate a supplementary stabilizing signal U_{PSS}, see Fig. 3.2. The PSS input is the change in the machine speed.

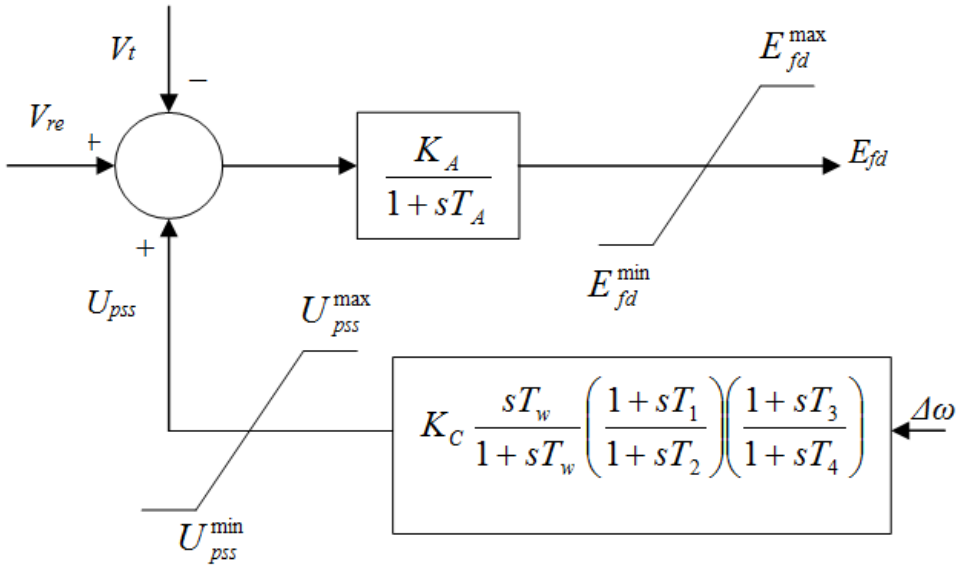

Figure 3.4: IEEE type-ST1 excitation system with lead-lag PSS

3.4 Power System Stabilizers

The supplementary excitation control of the low-frequency oscillations is currently known as the power system stabilizer (PSS). The idea of supplementary excitation is to apply a signal through the excitation system to increase the damping torque of the generator in a power system [100]. A generic PSS block diagram is shown in Fig. 3.5. It consists of three blocks: a gain block, a washout block and a phase compensation block [101]. The output signal of any PSS is a voltage signal, noted here as U_{PSS}, and added as an input signal to the AVR/exciter. This particular controller structure contains a washout block, $sT_\omega/(1+sT_\omega)$ used to reduce the over-response of the damping during severe events.

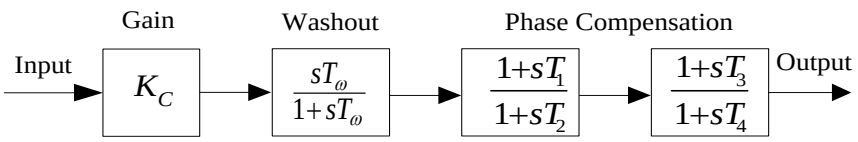

Figure 3.5: General PSS block diagram

Since the PSS must produce a component of electrical torque in phase with the speed deviation, phase 'lead-lag' block is used to compensate for the lag between the PSS output and the control action, the electrical torque. In Figs. 3.5, 3.6 and 3.7, K_C is the gain of PSS, T_W is the washout time constants and T_1, T_2, T_3 and T_4 are the time constants of lead-lag blocks which are needed to be tuned. While the inputs of these PSSs are deviation in rotor speed and real power. The number of lead-lag blocks needed depends on the particular system and the tuning of the PSS. The PSS gain *Kc* is an important factor as the damping provided by the PSS increases in proportion to an increase in the gain up to a certain critical gain value, after which the damping begins to decrease. All of the variables of the PSS must be determined separately for each type of generator because of the mutual interaction of the machines and shown in Fig. 3.3.

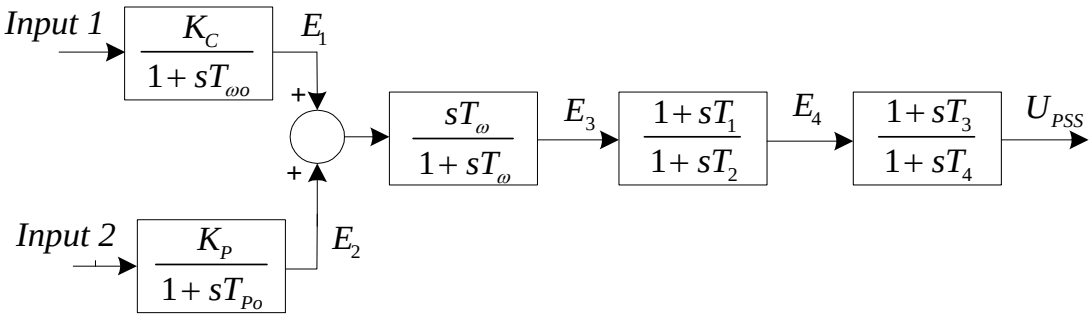

Figure 3.6: IEE2ST type PSS

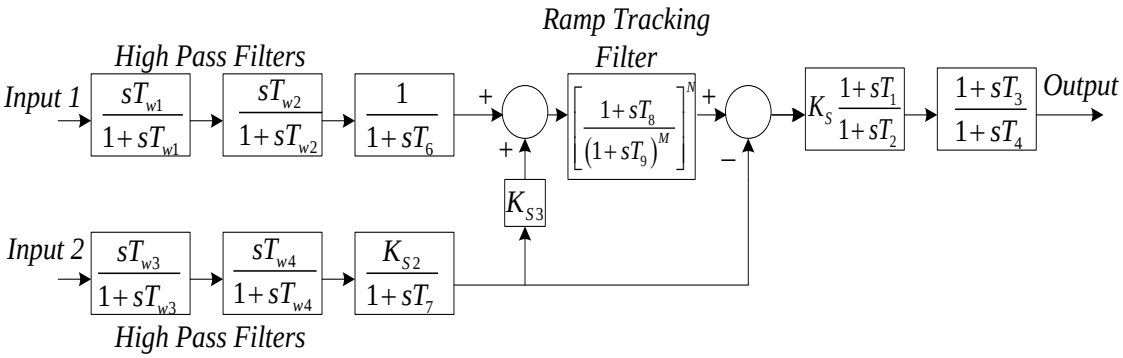

Figure 3.7: PSS2A type PSS

IEE2ST and PSS2A type PSSs are illustrated in Fig. 3.6 and Fig. 3.7 respectively. where T_6, T_7 and T_8,T_9 are the time constants for input filters and ramp tracking filter respectively. Both are multi-input PSSs but PSS2A consist of complex structure have more time delay that is not compatible for PMU real-time damping control operations. So IEE2ST type PSS is best suitable for local and remote signal applications.

Now, the proposed approach will be discussed in next chapter, where the proposed solution to deal with inter-area oscillation and the strategy to damp out these oscillations will be discussed in detail by considering the models presented in this chapter.

CHAPTER 4

PROPOSED APPROACH

Inter-area oscillations are the main concern for bulk power transfer on weak tie lines on large connected power systems. In this chapter we will discuss the proposed approach for the damping of inter-area oscillations based on modern wide area measurements, PMUs, that provides real-time dynamics of a wide area network.

For the application of proposed wide-area measurement and control WAMAC the test systems are first linearized, optimized and then simulated on Matlab. After that, these are tested one further in real-time using RTDS. Selection of optimal placement of power system stabilizers is done through eigen value based participation factor. IEEEST single input and IEE2ST dual input type PSS are used for damping control. PSS controller gains and time constants are optimized by differential evolution optimization technique. This thesis is a contribution for inter-area oscillations such that, Phasor Measurement Unit integrated with dual input IEE2ST type PSS in synchronism with GPS clock, is used to damp inter-area low frequency oscillations.

4.1 Optimal Location for Power System Stabilizer

Optimal placement of PSS is identified by dominant roots located near to the imaginary axis. This approach enhances the power system stability and reduces the cost of number of PSS installed [102]. State variables, affecting the dominant root are also identified. Consider a linear time-invariant system, with the system matrix $A(n \text{ x } n)$, the right eigenvectors ϕ_i, i = l, 2, ..., n, which are the conventional indices for the identification of stabilizer locations, are defined by the following equation

$$A \cdot \phi_i = \lambda_i \cdot \phi_i \qquad , \qquad i = 1, 2, \ldots, n \tag{4.1}$$

where λ_i are the eigenvalues of the system. On the other hand the left eignvector is defined as follows

$$\psi_i \cdot A = \lambda_i \cdot \psi_i \qquad , \qquad i = 1, 2, \ldots, n \tag{4.2}$$

Then the participation factor P_{ij} (the j-th state variable xj in the i-th eigenvalue λ_i) is expressed as:

$$P_{ij} = \phi_{ij} \text{ x } \psi_{ij} \tag{4.3}$$

The matrices Φ and Ψ are related as $\Phi \text{ x } \Psi^T = I$; therefore:

$$\sum_{j=1}^{n} P_{ij} = \sum_{j=1}^{n} \phi_{ij} \text{ x } \psi_{ij} = 1.0 + j0.0 \tag{4.4}$$

Similarly,

$$\sum_{i=1}^{n} P_{ij} = 1.0 + j0.0 \tag{4.5}$$

The participation factor P_{ij} expresses effect of i^{th} state variable against the eigenvalue λ_j; the participation factor found to be more effective than normal eigenvectors

method, and useful for the eigenvalue analysis. In this thesis, the state variable affecting the dominant root is identified by participation factor; which tell us that which generator should be equipped with the PSS controller in order to enhance the system stability and optimal use of stabilizers [103,104]. Once, the stabilizers are optimally located, their parameters are optimized and tuned by an intelligent optimization technique, differential evolution.

4.2 Power System Stabilizers Structure

In this thesis, the synchronous generator and the exciter are described by the 4th order model outlined in chapter 3, which is widely accepted for analyzing power system dynamics. In this controller structure, T_w is usually predetermined. The controller parameters to be specified, are K_C, T_1, T_2, T_3, and T_4.

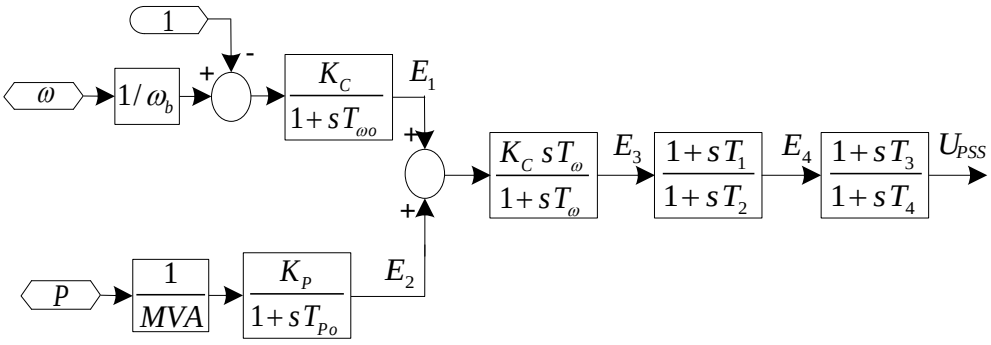

Figure 4.1: Proposed IEE2ST type PSS

For the proposed damping controller IEE2ST type PSS is considered as shown in Fig. 4.1, with local and remote input signals in coordination with PMU, to damp and settle down the transients of inter-area oscillations quickly, maintaining system stability. Equation 4.6, represents the state space representation of the proposed IEE2ST PSS integrated with PMU for a dual input PSS. As shown below:

$$\dot{W} = A_C W \tag{4.7}$$

where,

$$A_C = \begin{bmatrix}
0 & \omega_b & 0 & 0 & 0 & 0 & 0 & 0 & 0 \\
-\frac{K_1}{M} & -\frac{D}{M} & -\frac{K_2}{M} & 0 & 0 & 0 & 0 & 0 & 0 \\
-\frac{K_4}{T'_{do}} & 0 & -\frac{1}{K_3 T'_{do}} & \frac{1}{T'_{do}} & 0 & 0 & 0 & 0 & 0 \\
-\frac{K_A K_5}{T_A} & 0 & -\frac{K_A K_6}{T_A} & -\frac{1}{T_A} & 0 & 0 & 0 & 0 & \frac{K_A}{T_A} \\
0 & \frac{K_C}{T_{\omega o}} & 0 & 0 & -\frac{1}{T_{\omega o}} & 0 & 0 & 0 & 0 \\
\frac{K_P K_1}{T_{PO}} & 0 & \frac{K_P K_2}{T_{PO}} & 0 & 0 & -\frac{1}{T_{PO}} & 0 & 0 & 0 \\
\frac{K_P K_1}{T_{PO}} & \frac{K_C}{T_{\omega o}} & \frac{K_P K_2}{T_{PO}} & 0 & -\frac{1}{T_{\omega o}} & -\frac{1}{T_{PO}} & -\frac{1}{T_W} & 0 & 0 \\
\frac{K_P K_1 T_1}{T_{PO}} & \frac{K_C T_1}{T_{\omega o}} & \frac{K_P K_2 T_1}{T_{PO}} & 0 & -\frac{T_1}{T_{\omega o}} & -\frac{T_1}{T_{PO}} & \left(1-\frac{T_1}{T_W}\right) & 1 & 0 \\
\frac{K_P K_1 T_1 T_3}{T_4 T_{PO}} & \frac{K_C T_1 T_3}{T_4 T_{\omega o}} & \frac{K_P K_2 T_1 T_3}{T_4 T_{PO}} & 0 & -\frac{T_1 T_3}{T_4 T_{\omega o}} & -\frac{T_1 T_3}{T_4 T_{PO}} & \left(\frac{T_3}{T_4}-\frac{T_1 T_3}{T_4 T_W}\right) & \left(\frac{1}{T_4}-\frac{T_3}{T_4}\right) & -\frac{1}{T_4}
\end{bmatrix} \tag{4.6}$$

4.3 Power System Stabilizer Tuning

To increase the system damping to electromechanical modes, the following eigenvalue based objective function is considered [105].

$$J = max\left\{\zeta_1 : \zeta_i \in \zeta s \text{ of electromechanical modes}\right\} \tag{4.8}$$

where ζ_1 is the damping ratio of the i^{th} electromechanical mode eigen value respectively. In the optimization process, it is aimed to maximize J in order to increase the damping of electromechanical modes. The problem constraints are the optimized parameter bounds. Therefore, the design problem can be formulated as the following optimization problem.

Maximize *J* subject to,

$$\begin{aligned} K_i^{\min} \le K_i \le K_i^{\max} \\ T_{1i}^{\min} \le T_{1i} \le T_{1i}^{\max} \\ T_{2i}^{\min} \le T_{2i} \le T_{2i}^{\max} \\ T_{3i}^{\min} \le T_{3i} \le T_{3i}^{\max} \\ T_{4i}^{\min} \le T_{4i} \le T_{4i}^{\max} \end{aligned} \tag{4.9}$$

Typical ranges of the optimized parameters are [0.001-100] for K_i, [0.06-1.5] for T_{1i} and T_{3i}, and [0.01-0.1] for T_{2i} and T_{4i}. The time constant T_W is set to [3-10]sec. Considering the objective functions given in (4.8), the proposed approach employs DE algorithm to solve this optimization problem and search for optimal set of PSS parameters, { $K_i, T_{1i}, T_{2i}, T_{3i}, T_{4i}$, i=1,2,…, n_{PSS} }.

4.4 Optimization Technique

The parameters of the PSS, gains and time constants are optimized with differential

evolution optimization. The differential evolution algorithm is easy to use and fast converging. It optimizes the values of gain *Kc* and time constants of the lead-lag blocks based on minimizing the cost function. The DE is a population based optimization technique and is suited for solving non-linear and non-differentiable optimization problems. DE is a kind of searching technique and requires number (NP) of candidate solutions to form a population, where each solution consists of certain number of parameters depending on the problem dimension [106].

The strategy applied in this technique is to use the difference between randomly selected vectors to generate a new solution. For each solution in the original population, a trail solution is generated by performing process of mutation, recombination and selection operators. The old and new solutions are compared and the best solutions are emerged in the next generation. Initially the DE was developed to solve single objective optimization problem. The DE, as an evolutionary technique, generally performs three steps: initialization, creating new trail generation and selection [107].

A flowchart of DE algorithm is shown in Fig. 4.2. The algorithm begins by randomly initialize the controller parameters. The parameters to be optimized are the PSS controller gains and time constants. In order to diversify the search for the optimal solution mutation and crossover functions are applied. Objective function is then evaluated. The selected values of controller parameters are used to evaluate the eigenvalues of the closed loop matrix. DE will try to push all those eigenvalues that have damping ratio less than the preselected one to have the desired damping. The proposed DE based approach was implemented using MATLAB. Initially, several runs have been done with different

values of DE key parameters such as mutation constant F, crossover constant CR, and size of population NP. In this thesis, the following values are selected: F=0.8; CR=0.9; NP=20; the search will be terminated if (a) the number of iterations since the last change of the best solution is greater than 50; or (b) the number of iterations reaches 500.

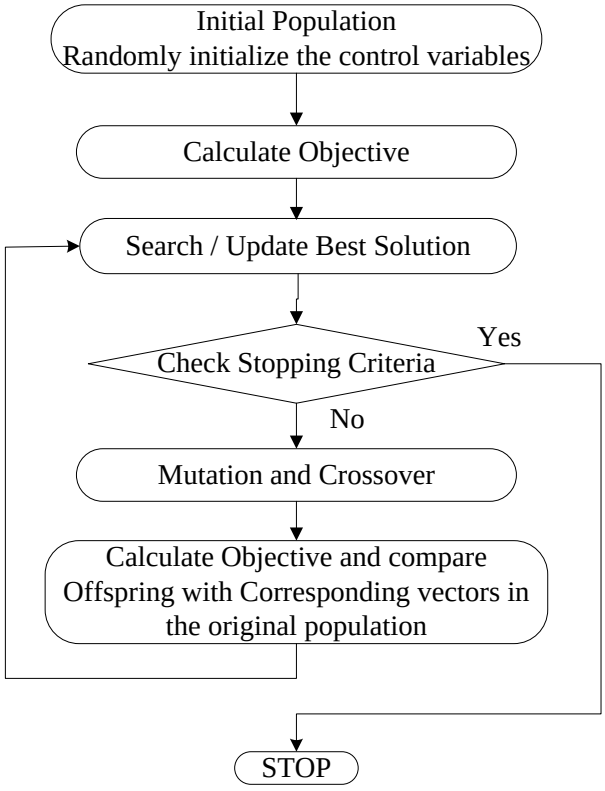

Figure 4.2: Flowchart of DE optimization method

4.5 Eigenvalue Analysis and non-linear Time Domain Simulations

The eigenvalues of the state matrix A determine the time domain response of the system to small perturbations and therefore provide valuable information regarding the stability characteristics of the system. The stability of the system is determined by the eigenvalues as follows: *The Eigen value analysis*, a real eigenvalue corresponds to a non-oscillatory mode. A negative real eigenvalue represents a decaying mode. A positive real eigen value represents a periodic instability. *Complex eigenvalues;* occur in conjugate

pairs, and each pair corresponds to an oscillatory mode. If all eigenvalues have a negative real part then all oscillatory modes decay with time and the system is said to be stable. The critical eigenvalues are characterized by being complex (also denominated swing modes or oscillatory modes) and located near the imaginary axis of the complex plane [108]. For a complex pair of eigenvalues $\lambda = \sigma \pm j\omega$, the real component of the eigenvalues (σ) gives the damping, and the imaginary component (ω) gives the frequency of oscillation. A negative value of σ represents a damped oscillation whereas a positive value of σ represents oscillation of increasing amplitude. The frequency of oscillation in Hz is given by $f = \omega / 2\pi$. The damping ratio (ζ) is given by $\zeta = -\sigma / \sqrt{\sigma^2 + \omega^2}$

4.6 Backup Protection for Transient Stabilities

To make the proposed model very near to the real scenario, a backup control is also considered as a backup protection for the proposed system. The frequency sensitivity based backup protection will trigger the braking resister to absorb the extra power. In case of fault disturbance, because it has low resistance and no inductance, it can be used to slow the system acceleration 'during' a fault. The role of the braking resistor is clear: it can be viewed as a fast load injection to absorb the excess transient energy. This thesis proposes an approach in which the braking resistor will be applied during the fault. This approach dramatically reduces the effect of the fault. The obvious question at this juncture is: how big should the braking resistor be? This is a hard question to answer with great precision. However, the preliminary studies [109,110] indicate that the total energy absorbing capacity of the brake in mega joules should be roughly ten per cent of the generator's rated output in megawatts.

CHAPTER 5

EXPERIMENTAL SETUP

5.1 Real time Digital Simulator

The proposed system is made on RSCAD program which is then compiled and sent for real-time simulations on RTDS. Real-time digital simulator (RTDS) is a combination of specialized computer hardware and software designed specifically for electromagnetic transient simulations in real-time. The system is used for high speed simulations, closed-loop testing of protecting and control equipment and hardware in the loop (HIL) applications. A proper RTDS lab is built under Power and Energy Group in the Electrical Engineering Department of King Fahd University of Petroleum and Minerals, Saudi Arabia. Where one rack of RTDS equipped with 3 GPC cards are installed with all accessories. The proposed system is simulated, tested and validated on RTDS.

RTDS is a real-time digital simulator specially designed for wide area power systems, its response are much nearer to the existing practical systems. The proposed system is first developed in RSCAD software which is then compiled and sent to the RTDS

processing and control unit. This unit consists of GPC cards, input output ports for hardware connection and high speed multi-processors. Following are the major components that are used in building RSCAD model.

5.2 Phasor Measurement Unit (PMU)

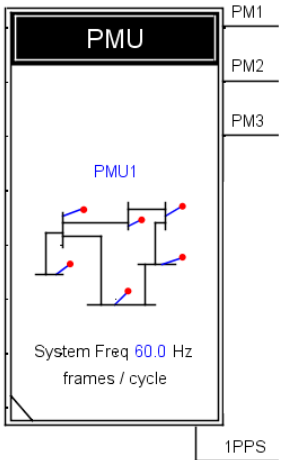

Figure 5.1: Representation of PMU Block in RTDS

PMU block is shown in Fig. 5.1, where each PMU block can take data from eight different remote locations PM1, PM2, …, PM8 with 1PPS, Pulse per signal . The PMU provides the phasor voltage, current and frequency of the remote location. Its reporting rate is 1frame per second to 60 frames per second. This data can be used for wide are measurement as well as for control purpose.

5.3 Power System Stabilizers Model

IEEEST and IEE2ST power system stabilizers with single and multi-input respectively are shown in Fig. 5.2, where IEEEST is a conventional PSS, while IEE2ST is a modern dual-input PSS having rotor speed and real power as an input signal. The output of the

PSS, in terms of voltage, is feedback to the excitation system to stabilize the system by compensating the component of field voltage.

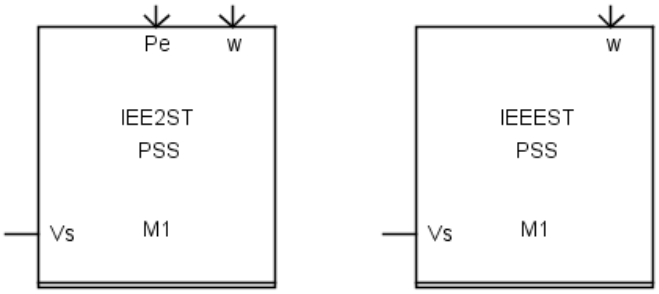

Figure 5.2: IEEEST and IEE2ST Power system stabilizers

Where, Pe is the real power, w is is the rotor speed and Vs is the output of PSS.

5.4 Transmission Line Model

Single circuit, three-phase transmission line with sending and receiving end is shown in Fig. 5.3. The transmission line connecting two areas in proposed system is a weak tie line, high reactance, with bulk power transfer, from one area to another area. A small disturbance will induce inter-area oscillations of 0.1-0.8 Hz, that could lead the system collapse.

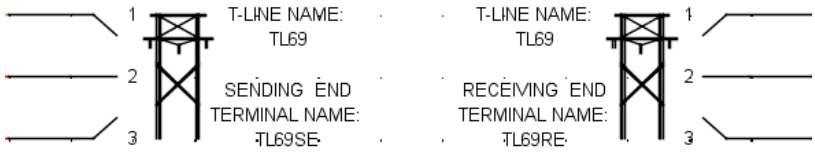

Figure 5.3: Transmission line model

5.5 Generator Model

A complete three-phase, synchronous generator model in RSCAD is shown in Fig. 5.4, it consist of generator transformer model, excitation system, PSS, and a governor. The

stabilizer input signal is a local speed of the generator to keep the generator in steady state. The power transfer to the grid is step up through ye-delta step-up transformer.

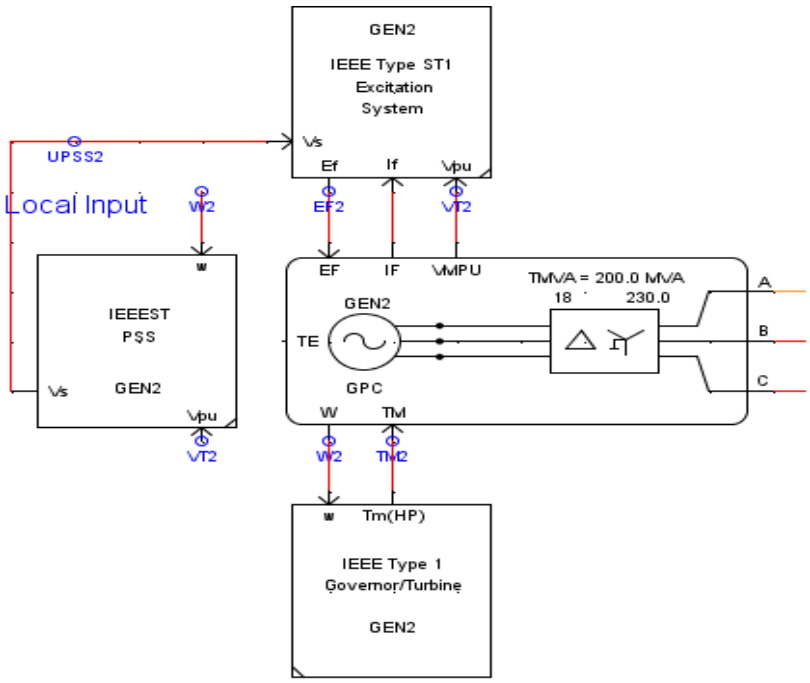

Figure 5.4: Synchronous generator model with governor, exciter and PSS

5.6 IEE2ST PSS Integrated with PMU

Multi input IEE2ST PSS controller is of great interest for damping local as well as inters area oscillation. A complete generator model with IEE2ST PSS integrated with PMU for damping inter-area oscillations is illustrated in Fig. 5.5. The remote signal ω is provided by PMU from distant locations in synchronism with GPS clock. Whereas, the local signal is the real power measured from generator terminal. These local and remote signals are injected in dual input IEE2ST PSS, whose output is then feedback to the exciter, to damp out low frequency inter-area oscillations.

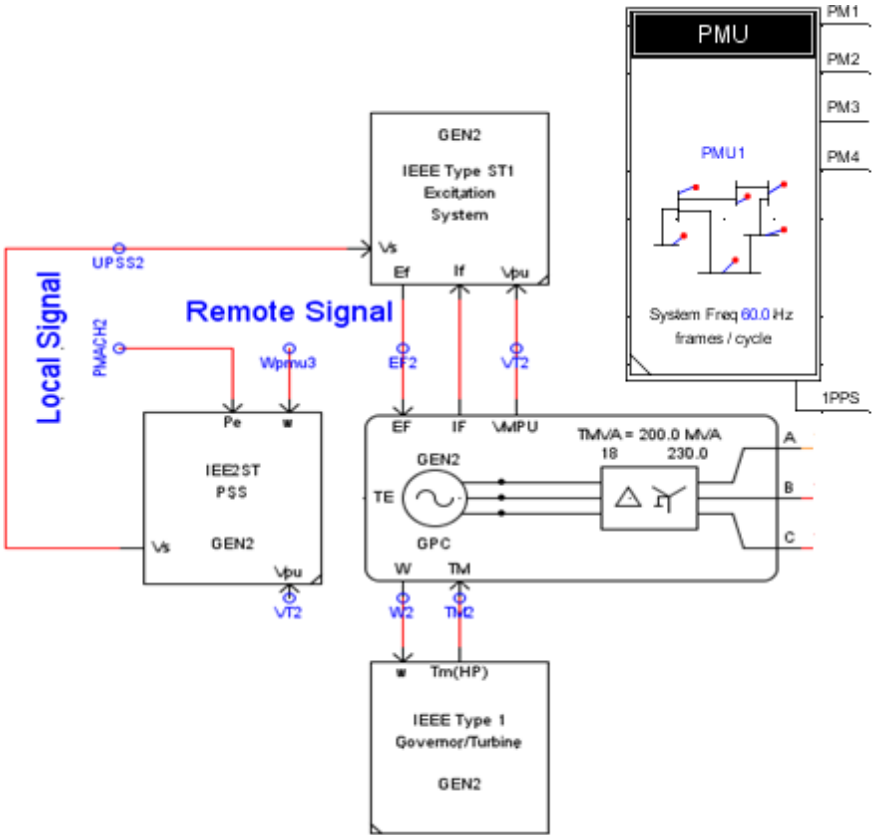

Figure 5.5: Generator model with IEE2ST PSS integrated with PMU for damping inter-area oscillations

CHAPTER 6

RESULTS AND TESTING

Proposed wide area monitoring and control (WAMAC) system that aims to mitigate the power system transient instabilities is simulated and tested on two test systems with Matlab and RTDS. 3-Machine 9-Bus test system and 5-Machine 14-Bus system are built, tested and validated to properly investigate the damping of low frequency inter-area oscillations quickly and efficiently.

6.1 Test Case 1: 3-Machine 9-Bus system

3-Machine 9-Bus system [111] as shown in Fig. 6.1, is used to test the proposed system response on three different conditions for inter-area oscillations. First, when no PSS is connected to the test system. Second, when the system is connected with IEEEST type PSS. Third, when system is connected with IEE2ST type PSS integrated with PMUs. The PSS are optimally located using participation factor method, PSS gains and time constants are optimized by differential evolution intelligent technique. At the end

eigenvalue analysis is carried out for all three conditions.

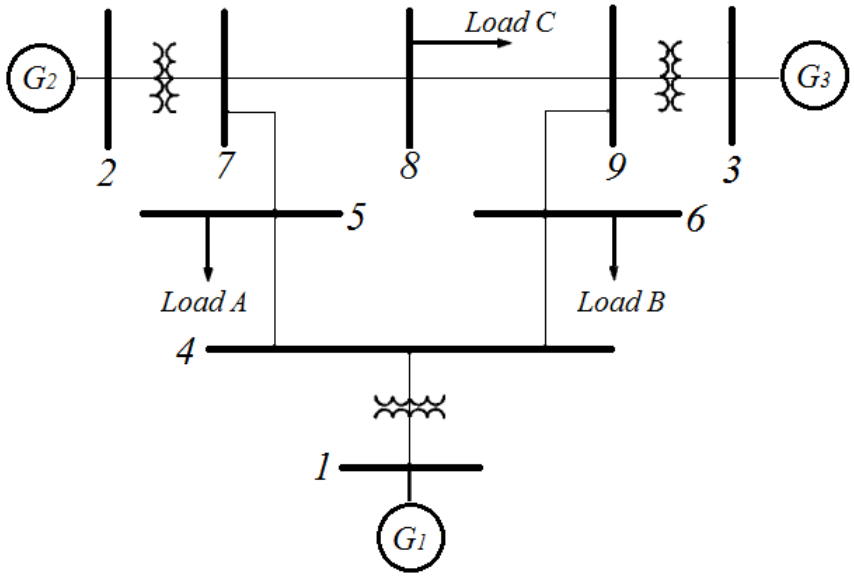

Figure 6.1: Bus diagram of three-machine nine-bus system

6.1.1 Optimal placement of PSS

Optimal placement of PSS is done with eigenvalue based participation factor. Table 6.1, indicates the electromechanical modes against the generator locations of the system which causes low frequency inter-area oscillations. The generators that are more affecting the electromechanical modes are highlighted in Table 6.1. It is obvious that generator 2 and generator 3 have more contribution in creating inter-area oscillations so PSS should be installed on these optimal locations for best performance with economical use.

Table 6.1: Optimal Location Identification for PSS Installation (Test Case-1)

Electromechanical Modes	Generator Busbar Number		
	1	2	3
-0.0521 ± 9.1547i	-0.0497	0.7964	-0.2185
-1.0898 ± 13.1915i	-0.2748	0.0196	0.6165

6.1.2 Stabilizer Design

Once the optimal location for placing PSS is known, the differential evolution is employed to optimize the controller gains and time constant of the power system stabilizers. Table 6.2, indicates the optimal values of controller gains and the time constants for single input type PSS (IEEEST) and multi-input type PSS (IEE2ST) integrated with PMUs' where the time constants are in seconds.

Table 6.2: Optimal PSS Controller Gains for 3-Machine 9-Bus system

Constants	IEEEST PSS		IEE2ST PSS	
	G2	G3	G2	G3
K_1	14.871	5.212	50.43	30. 27
K_2	-	-	0.05	0.05
T_1	0.298	0.631	0.049	0.047
T_2	0.05	0.05	0.05	0.05
T_3	0.406	0.629	10	10
T_4	0.05	0.05	10	10
T_5	5	5	0.25	0.514
T_6	5	5	0.05	0.05
T_7	-	-	0.313	0.25
T_8	-	-	0.05	0.05
T_9	-	-	0.0	0.0
T_{10}	-	-	0.001	0.001

6.1.3 Eigenvalue Analysis

Once the stabilizer parameter are known, case-1 is tested under 3 different conditions for computing system eigenvalues without PSS, with IEEEST type PSS and with the proposed PMU integrated dual-input IEE2ST type PSS controllers, given in Tables 6.3. The bold rows of these tables represent the electromechanical mode eigenvalue. It is evident that, using the proposed coordinated stabilizers design, the electromechanical mode eigenvalue is greatly shifted to the left of the s-plane. Hence, it can be concluded that it considerably enhances the system stability.

Table 6.3: Three-machine nine-bus system eigenvalues for without PSS, IEEEST PSS and IEE2ST PSS

No Control	*IEEEST*	*IEE2ST*
-0.0521 ± 9.1547i	**-1.2698 ± 11.6134i**	**-1.8025 ± 2.0920i**
-1.0898 ± 13.1915i	**-2.3340 ± 1.6948i**	**-3.6029 ± 9.9730i**
-12.3690 ± 23.5035i	-24.0237 ± 14.9438i	-24.0197 ± 14.95488i
-23.2068 ± 18.4090i	-18.1694 ± 30.2023i	-18.1959 ± 30.1626i
-29.0511	-8.3640 ± 21.37619i	-7.07457 ± 17.6017i
-19.2370	-4.8998 ± 9.4526i	-4.2885 ± 16.0329i
-0.0904	-106.7382	-106.7387
0.0001	-2.2214	-2.2172
--	-0.6688	-1.5315
--	-0.2014	-0.8733
--	-0.0273	-0.2016
--	-0.0006	-0.0184

6.1.4 Simulation Results for Test Case 1

In this case 3-phase 6-cycle fault is applied to verify the proposed IEE2ST integrated with PMU for damping inter-area oscillations. First, the system is examined with no PSS connected and the system responses are monitored. The system is found to be unstable and the oscillations continue for long period of time. In case two, single input type PSS (IEEEST), using rotor speed as local input signal, installed on generator 2, and generator 3 as computed from the optimal placement of PSS. It is observed that the oscillations are damped efficiently. In third case, generator 2 and generator 3 are optimally equipped with dual-input type PSS (IEE2ST) integrated with PMUs', where *Pe* is used as a local signal and *w* as a remote signal. This remote signal is provided by PMUs in synchronism with GPS clock, with optimized tuned parameters of PSS, the proposed controller is capable to provide good damping to the system.

Simulation results shows the performance for each case as discussed before, for no PSS, for IEEEST type PSS and for proposed IEE2ST type PSS. For a 3-phase 6-cycle fault on bus 7, the response of rotor speed of generator 1, 2 and 3 for each case are shown in Figs. 6.2-6.4 respectively. Without control, oscillations takes longer time to damp, with IEEEST control; rotor speed also increases but settles in about 4 seconds. However, it is evident that with proposed scheme, rotor speed effectively damped within 2 seconds. This is the fact that proposed wide-area damping controller can quickly damp local as well as inter-area modes.

With the three-phase line to ground fault, for 100msec. It is considered that the generator 1 is a reference one, with rotor angle zero. The variation in rotor angle for generator 2 and 3 is presented in Fig. 6.5 and Fig. 6.6. The IEEEST controller restores the operating condition within 6 seconds. However, the proposed IEE2ST controller provides good damping to generator rotor angle and so the transient's oscillations have been effectively suppressed within 3 seconds. The responses of the real power of all three generators under the 6-cycle fault are shown in Figs. 6.7-6.9. Without control the peak values reaches 500MW, and continue to oscillate over the period of time. With IEEEST controller, it settles down in 4 seconds with peak value of 400MW. However, with proposed IEE2ST controller, it is observed that it takes less time of 1.5sec and less overshoots to reach steady state value. From simulation results it is concluded that IEE2ST having input signal *w* from remote locations provides high level of damping with minimum transients to inter-area oscillations as compared with IEEEST. The proposed dual-input IEE2ST stabilizer outperforms the conventional IEEEST in terms of reduction

of overshoot and settling time of low frequency inter-area oscillations.

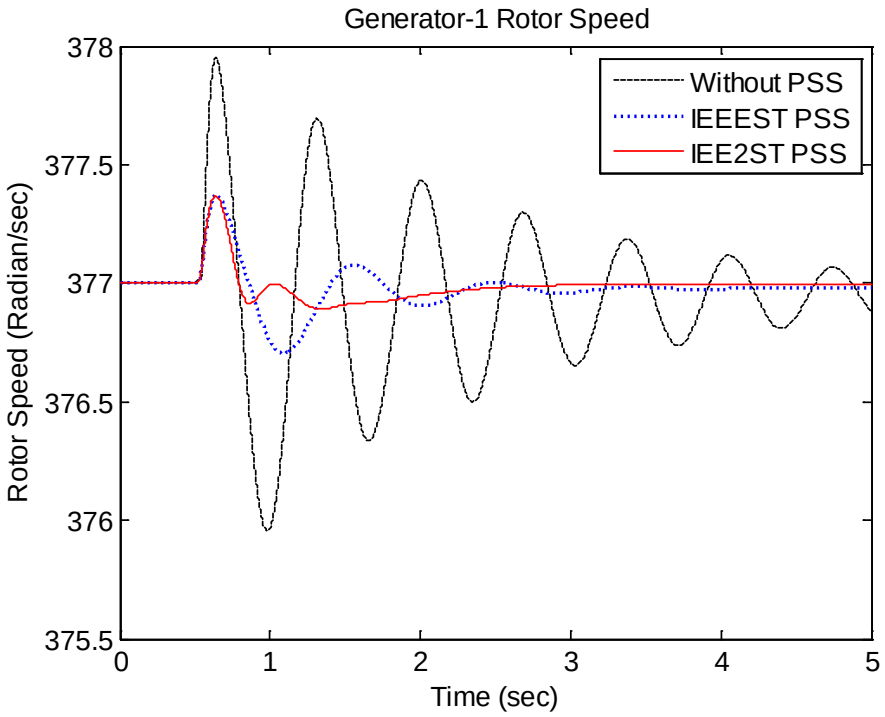

Figure 6.2: Simulated response of rotor speed at generator-1 under three-phase six-cycle fault at t=0.5sec (a) Without PSS (b)With IEEEST type single input PSS and (c) With IEE2ST type multi-input PSS

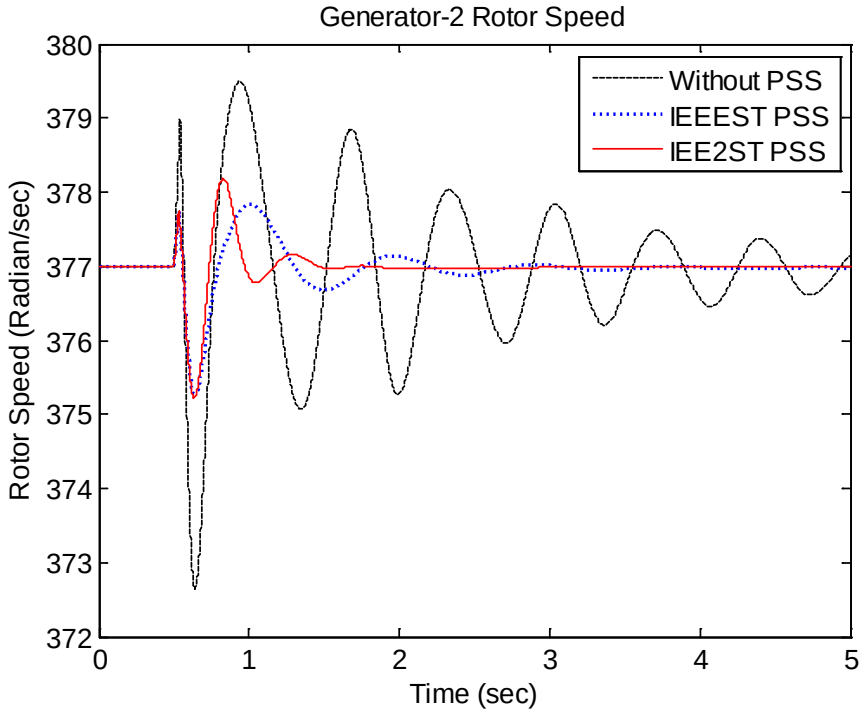

Figure 6.3: Simulated response of rotor speed at generator-2 under three-phase six-cycle fault at t=0.5sec (a) Without PSS (b)With IEEEST type single input PSS and (c) With IEE2ST type multi-input PSS

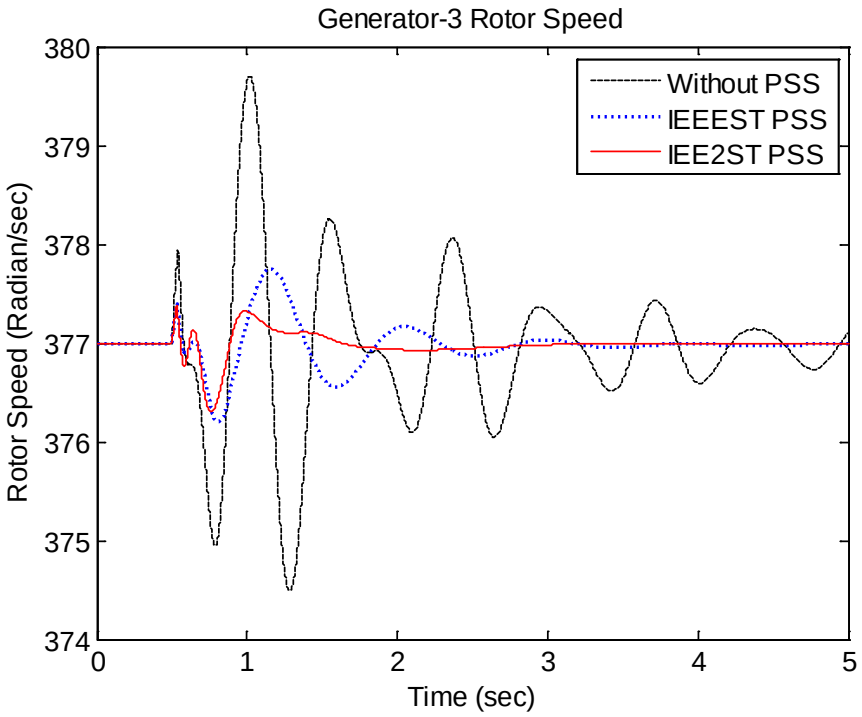

Figure 6.4: Simulated response of rotor speed at generator-3 under three-phase six-cycle fault at t=0.5sec (a) Without PSS (b)With IEEEST type single input PSS and (c) With IEE2ST type multi-input PSS

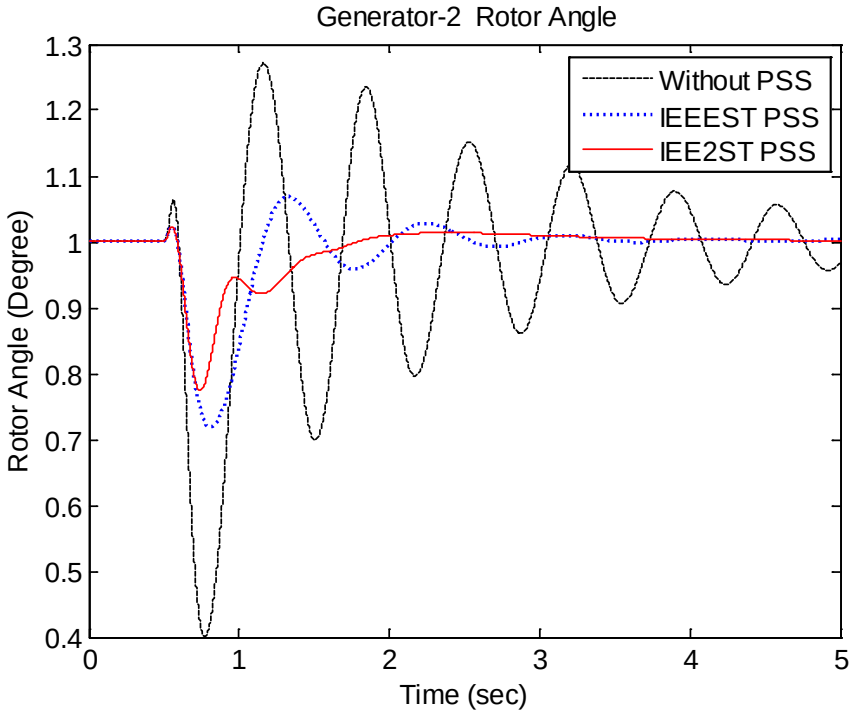

Figure 6.5: Simulated response of rotor angle at generator-2 under three-phase six-cycle fault at t=0.5sec (a) Without PSS (b)With IEEEST type single input PSS and (c) With IEE2ST type multi-input PSS

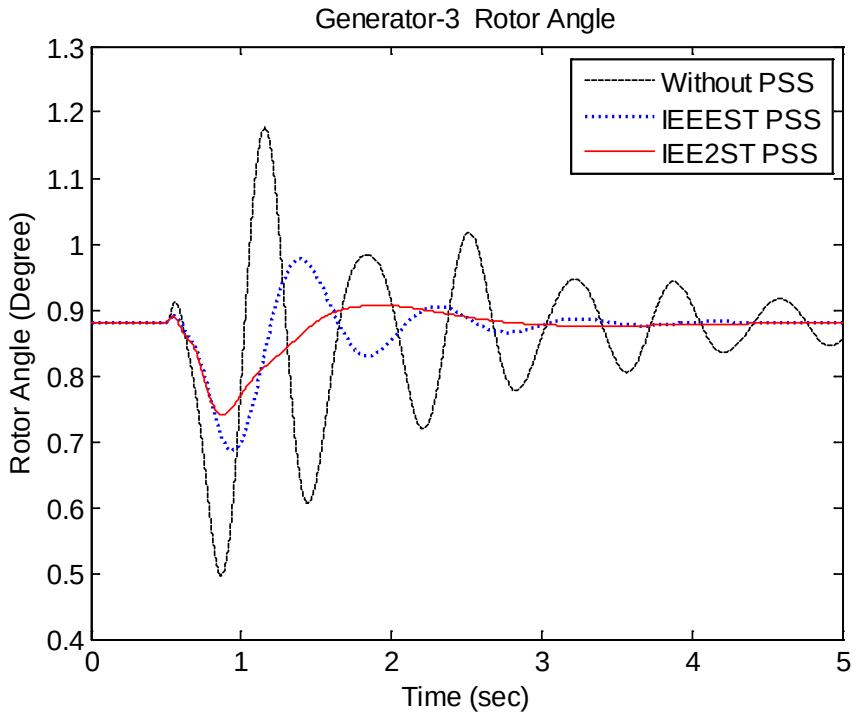

Figure 6.6: Simulated response of rotor angle at generator-3 under three-phase six-cycle fault at t=0.5sec (a) Without PSS (b)With IEEEST type single input PSS and (c) With IEE2ST type multi-input PSS

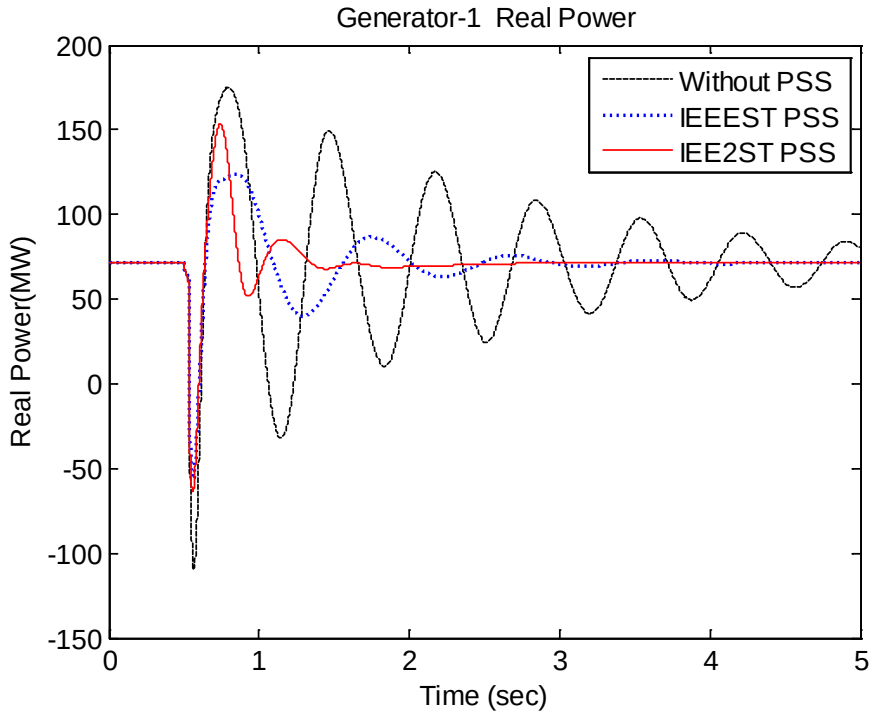

Figure 6.7: Simulated response of real power at generator-1 under three-phase six-cycle fault at t=0.5sec (a) Without PSS (b)With IEEEST type single input PSS and (c) With IEE2ST type multi-input PSS

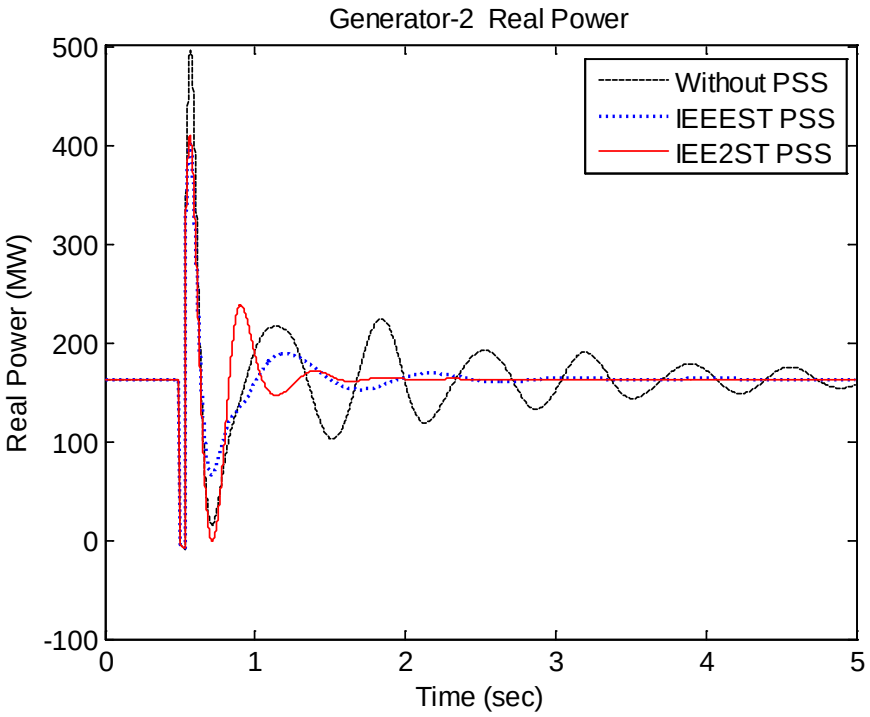

Figure 6.8: Simulated response of real power at generator-2 under three-phase six-cycle fault at t=0.5sec (a) Without PSS (b)With IEEEST type single input PSS and (c) With IEE2ST type multi-input PSS

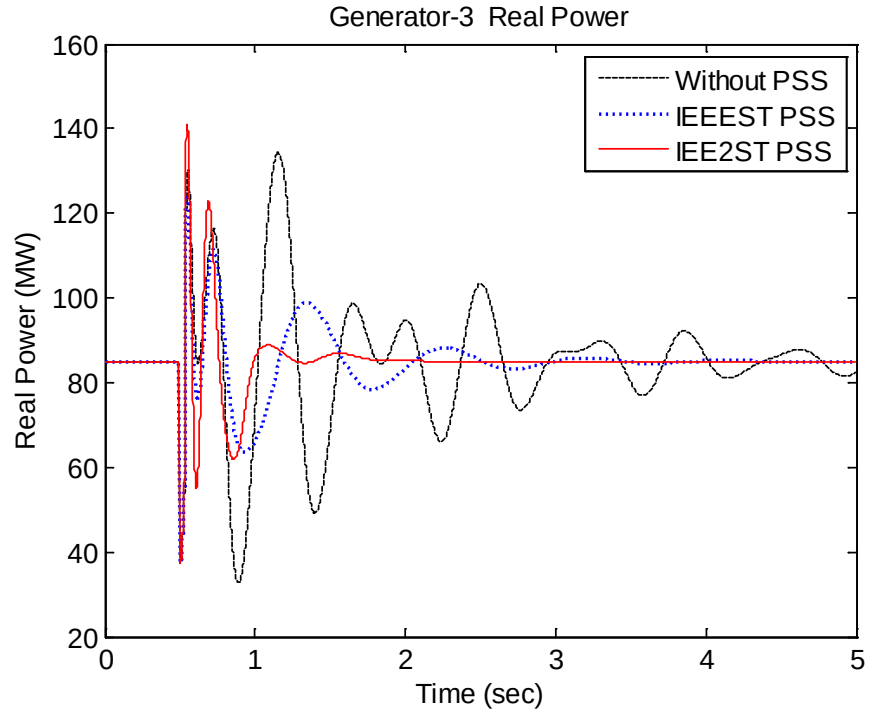

Figure 6.9: Simulated response of real power at generator-3 under three-phase six-cycle fault at t=0.5sec (a) Without PSS (b)With IEEEST type single input PSS and (c) With IEE2ST type multi-input PSS

6.1.5 RTDS Results for Test Case 1

The power system test model is built on RSCAD, the graphical user interface, consist of vast library of all modern components of power system. The test model is then simulated on high speed real-time digital simulator RTDS. The 3-Machine 9-Bus system is built on the simulator as shown in Fig. 6.10, the complete system data is available in [111]. First the test system is simulated for the case when no PSS connected to the system, and all the critical states are monitored in real-time. Second, the IEESET type PSS is used to damp out the oscillations. Third, the PMU is installed to collect the remote signal from distant generator in synchronism with the GPS signal. This remote signal is sent to the IEE2ST type multi input PSS. Literature review shows that PSS equipped with both local and remote signal, effectively damp out the inter-area oscillations.

A three-phase six-cycle fault occurred on bus 7 of the 3-Machine 9-Bus system. The voltage response on bus 7 is shown in Fig. 6. 11, where all the phases become zero for the duration of fault and afterwards they are trying to stabilize over the time. The experimental response of the rotor speed under three-phase six-cycle fault for all the three generator for without PSS, with IEEEST and with proposed multi input IEE2ST damping controller integrated with PMU are shown in Fig. 6.12-6.14. From graphs, the major affected generators are the same as those recommended for installing PSS by optimal placements of PSS in Table 6.1.

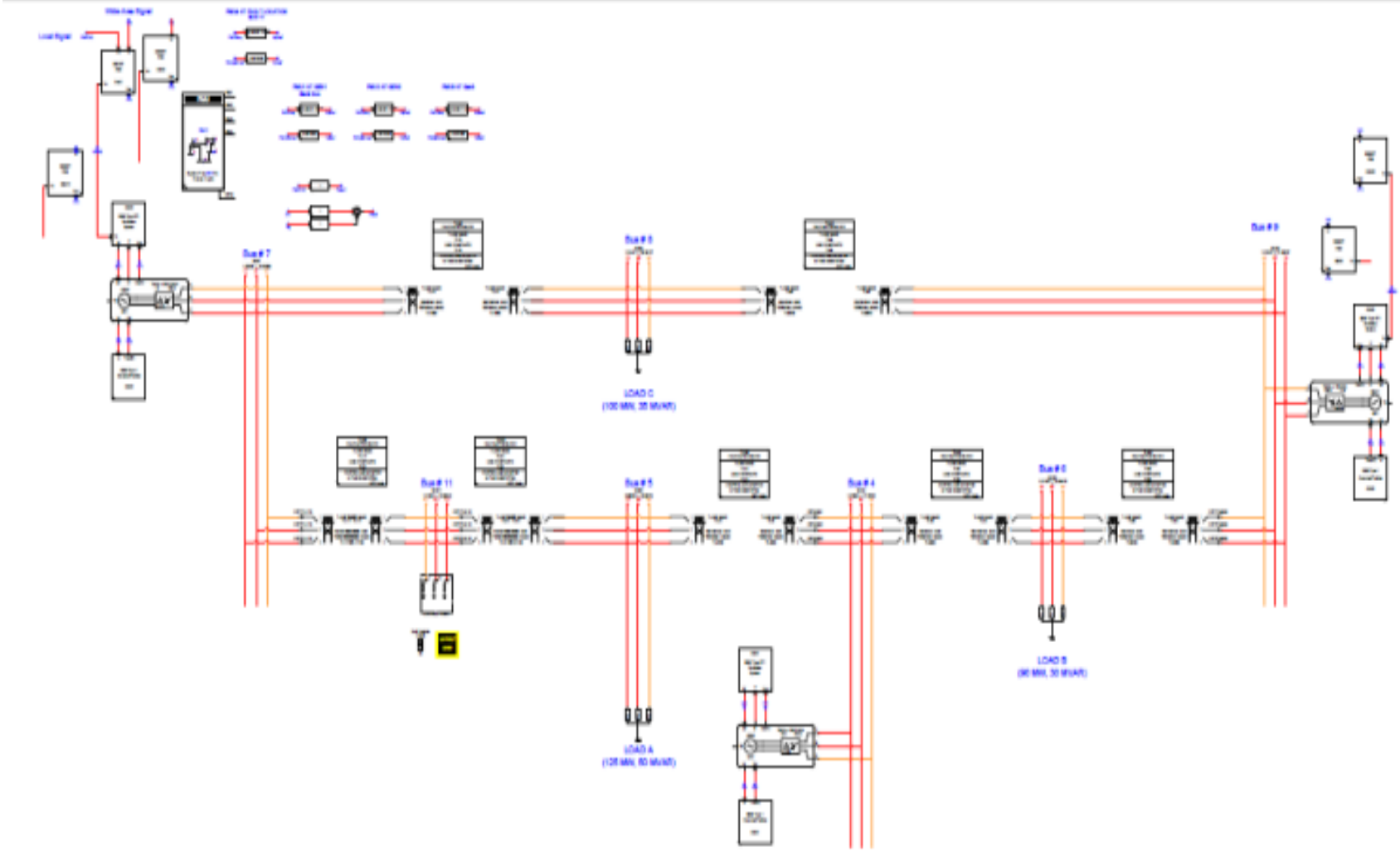

Figure 6.10: RTDS model of three-machine nine-bus system

In Fig. 6.12-6.14, with no controller, the oscillations are increasing with the passage of time, with IEEEST controller, the oscillations settles in 5 seconds. However, proposed IEE2ST controller quickly damps the transients with less overshoots within 5 seconds. The rotor angle responses are presented in Fig. 6.15 - 6.17, without controller, the rotor angle is not damped even in 15 sec, with IEEEST control it restores the system to its nominal operating condition in 6 sec, and with the proposed IEE2ST controller using wide are measurements quickly damp within 5 sec. The responses of real power of all three generators are shown in Figs. 6.18-6.20. With no control the oscillations damps afterr a long period of time, IEEEST controller bring the system to steady state in 4 seconds. IEE2ST controller provides good damping to the generator power so transient oscillation efficiently suppressed within 3 seconds.

The responses of terminal voltages for all three generators are shown in Fig. 6.21-6.23. Generator 2 is near to the fault location; its voltage is more affected with peak values 1.05pu and 0.7pu. With no controller, the oscillations are increasing with the passage of time, with IEEEST controller, the oscillations settles down in 5 seconds. However, proposed IEE2ST controller quickly damps the transients with less overshoots of 0.8pu within 4 seconds. From simulation results it is concluded that IEE2ST having input signal *w* from remote locations can effectively damp inter-area oscillations as compared to conventional IEEEST PSS. The proposed multi input IEE2ST stabilizer outperforms the conventional IEEEST in terms of reduction of overshoot and settling time of low frequency inter-area oscillations.

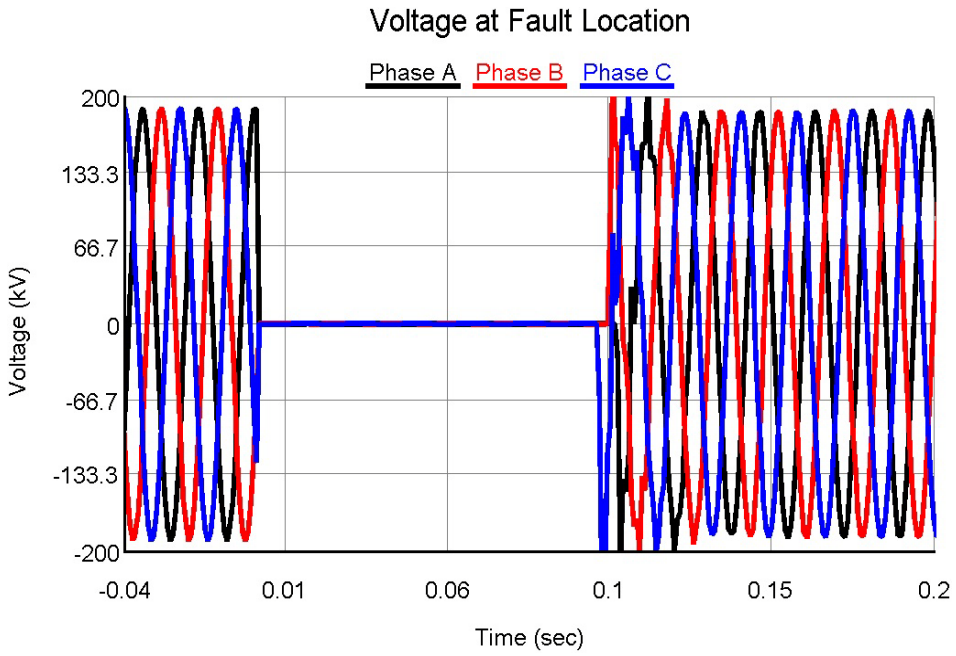

Figure 6.11: RTDS response of three-phase six-cycle fault on three-machine nine-bus system

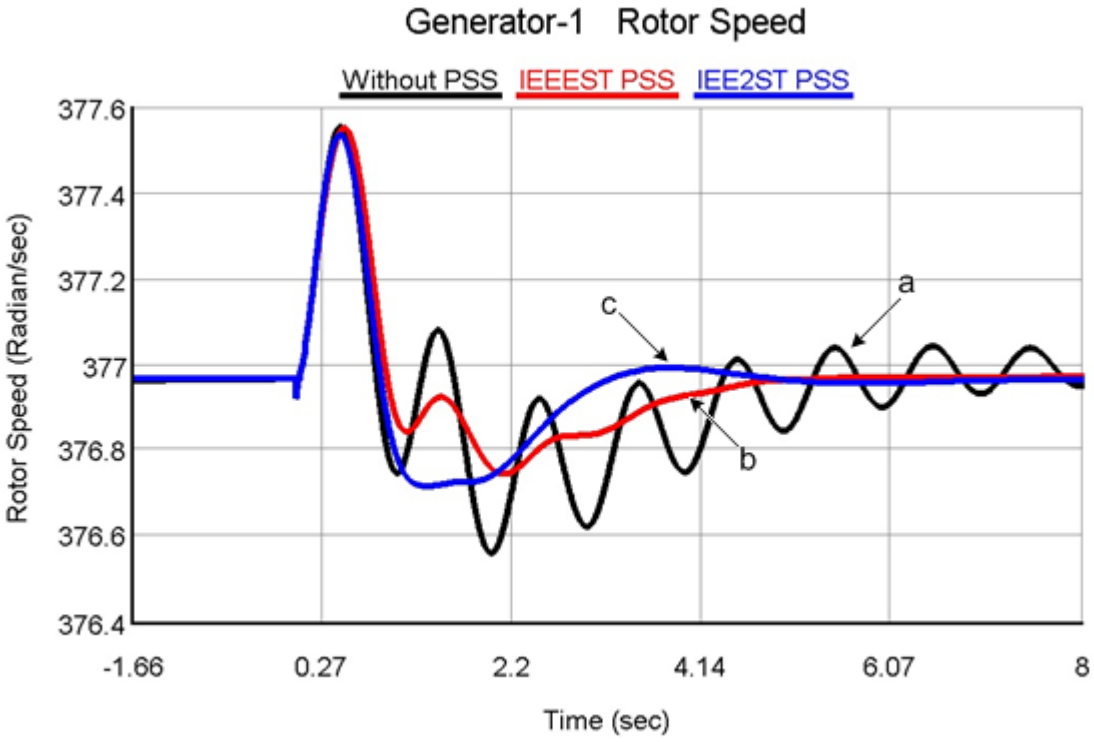

Figure 6.12: RTDS response of rotor speed at generator-1 under three-phase six-cycle fault at t=0sec (a) Without PSS (b)With IEEEST type single input PSS and (c) With IEE2ST type multi-input PSS

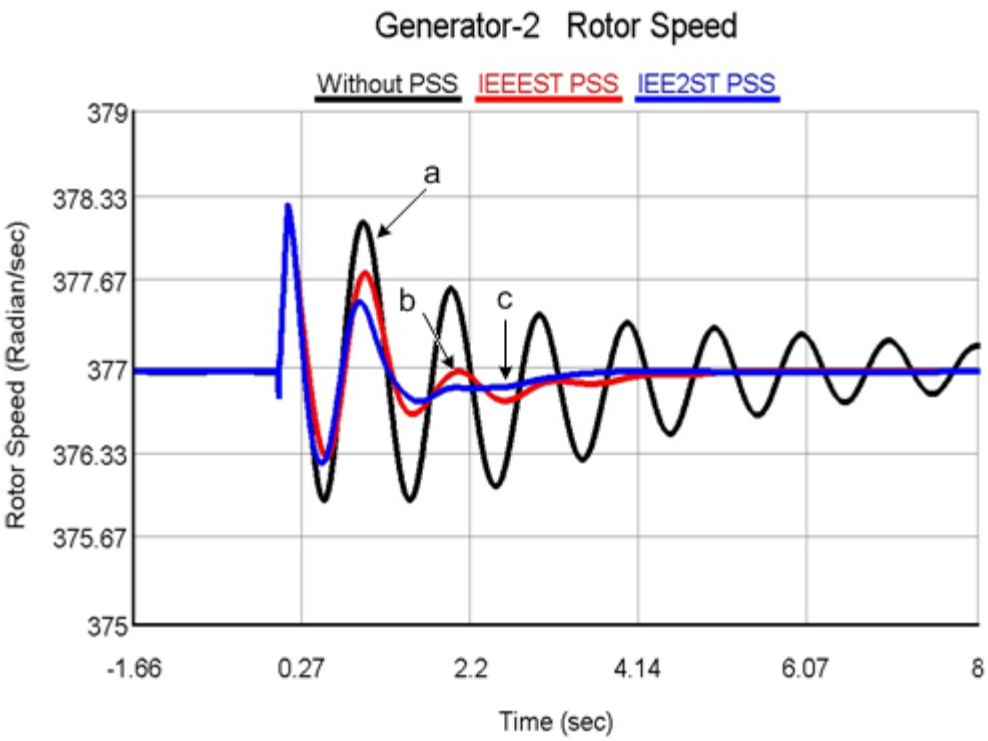

Figure 6.13: RTDS response of rotor speed at generator-2 under three-phase six-cycle fault at t=0sec (a) Without PSS (b)With IEEEST type single input PSS and (c) With IEE2ST type multi-input PSS

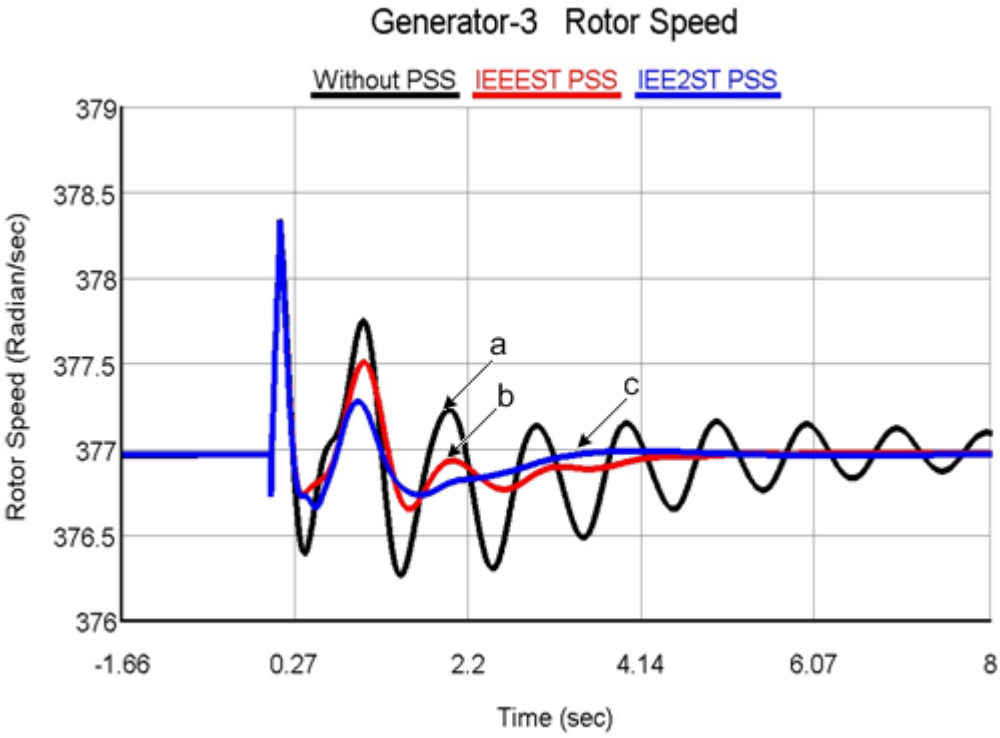

Figure 6.14: RTDS response of rotor speed at generator-3 under three-phase six-cycle fault at t=0sec (a) Without PSS (b)With IEEEST type single input PSS and (c) With IEE2ST type multi-input PSS

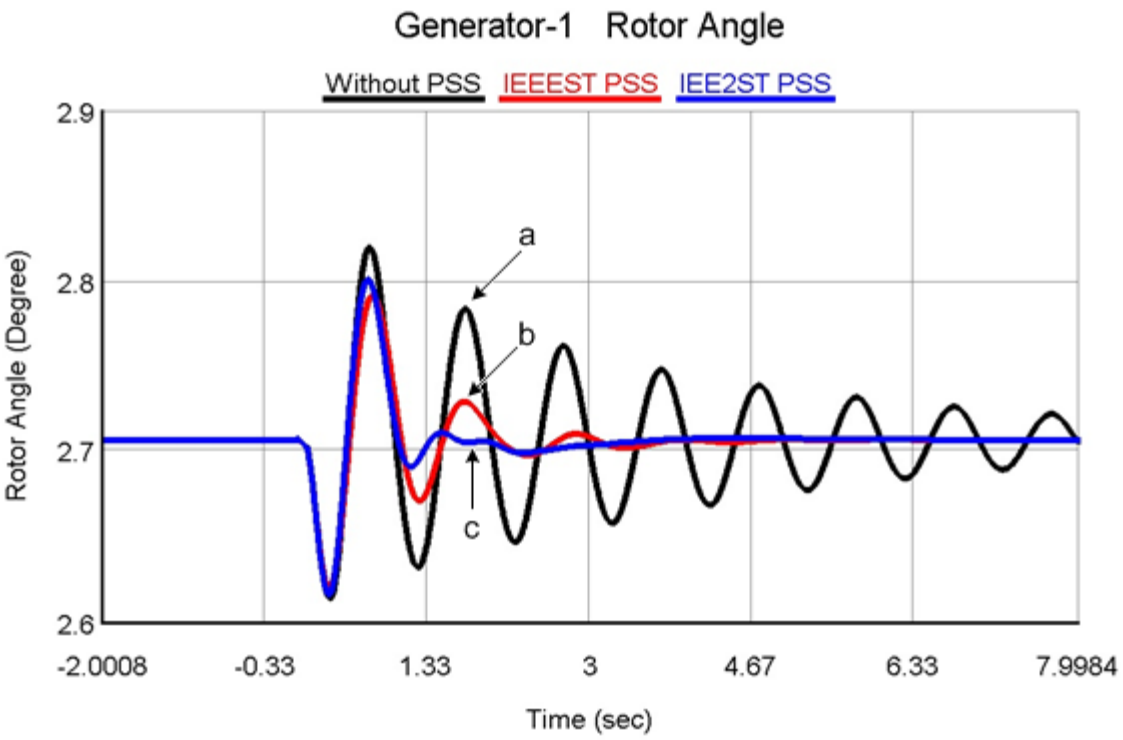

Figure 6.15: RTDS response of rotor angle at generator-1 under three-phase six-cycle fault at t=0sec (a) Without PSS (b)With IEEEST type single input PSS and (c) With IEE2ST type multi-input PSS

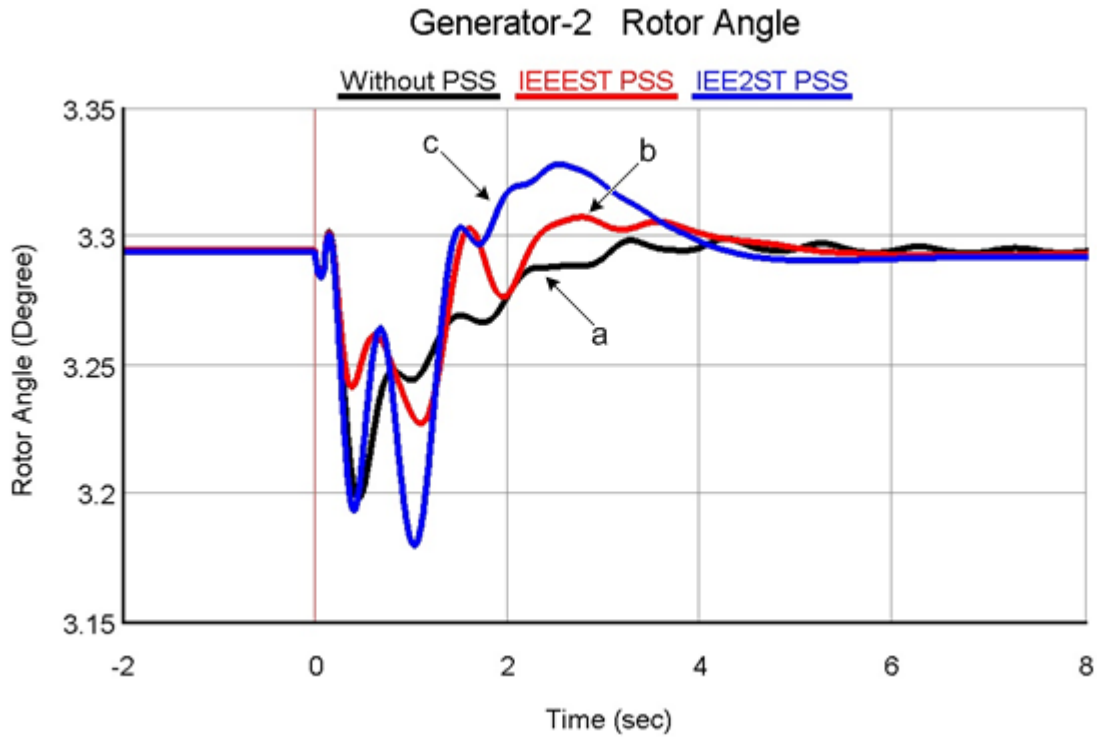

Figure 6.16: RTDS response of rotor angle at generator-2 under three-phase six-cycle fault at t=0sec (a) Without PSS (b)With IEEEST type single input PSS and (c) With IEE2ST type multi-input PSS

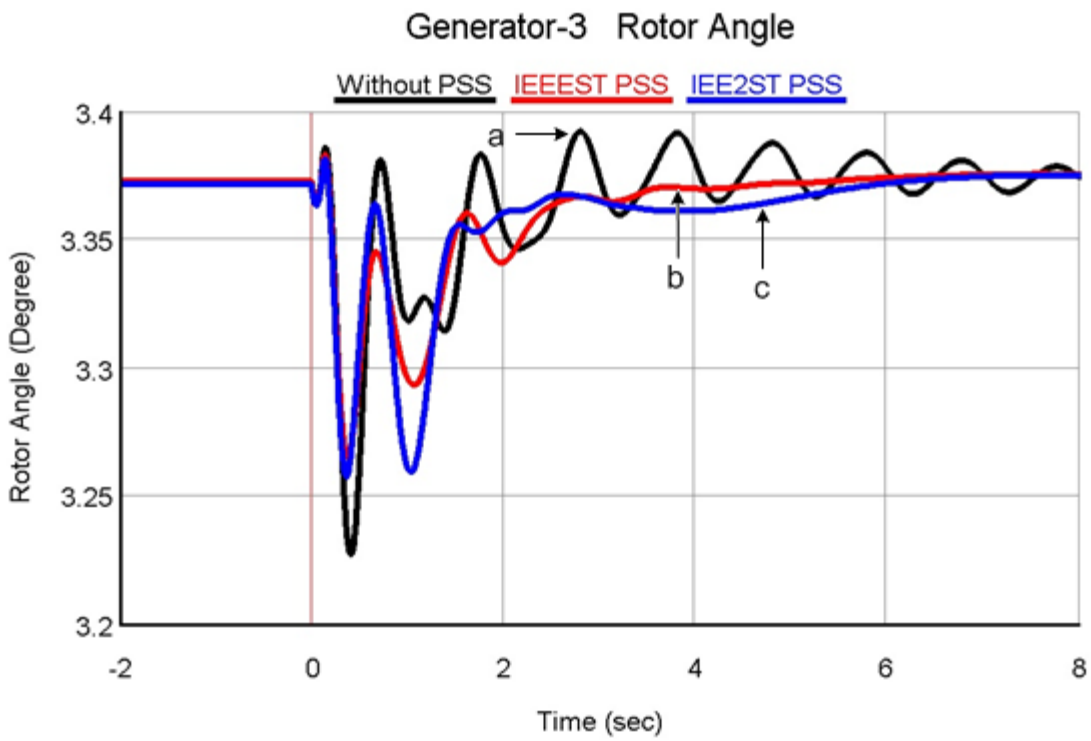

Figure 6.17: RTDS response of rotor angle at generator-3 under three-phase six-cycle fault at t=0sec (a) Without PSS (b)With IEEEST type single input PSS and (c) With IEE2ST type multi-input PSS

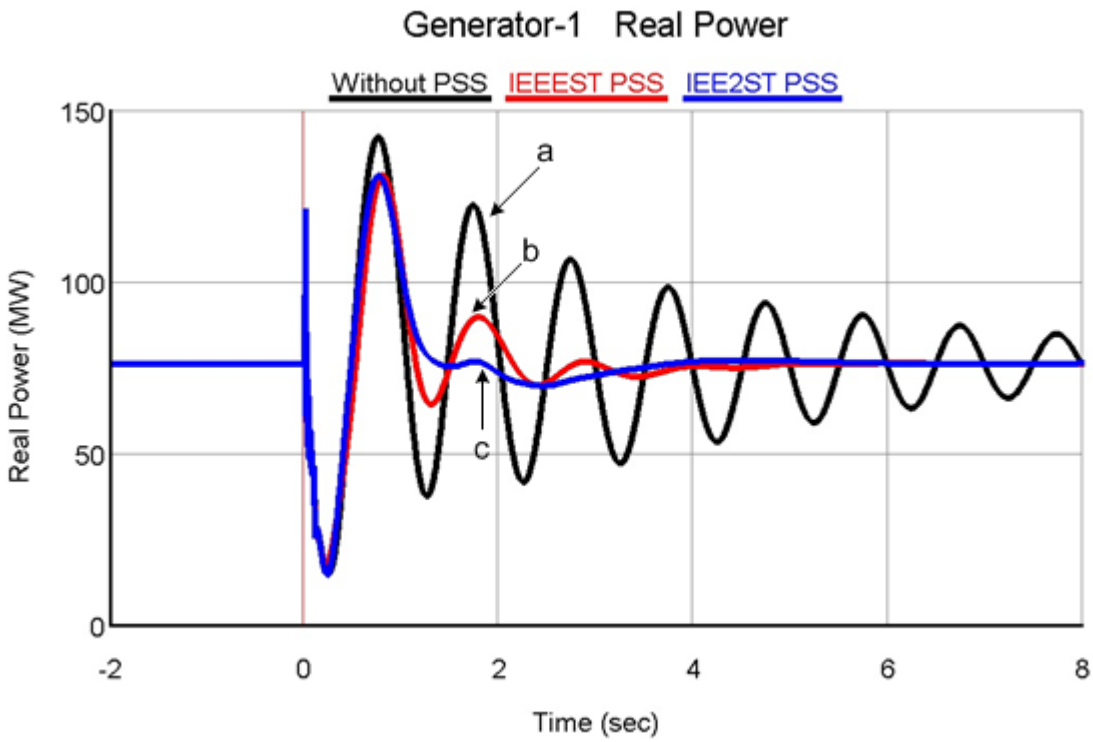

Figure 6.18: RTDS response of real power at generator-1 under three-phase six-cycle fault at t=0sec (a) Without PSS (b)With IEEEST type single input PSS and (c) With IEE2ST type multi-input PSS

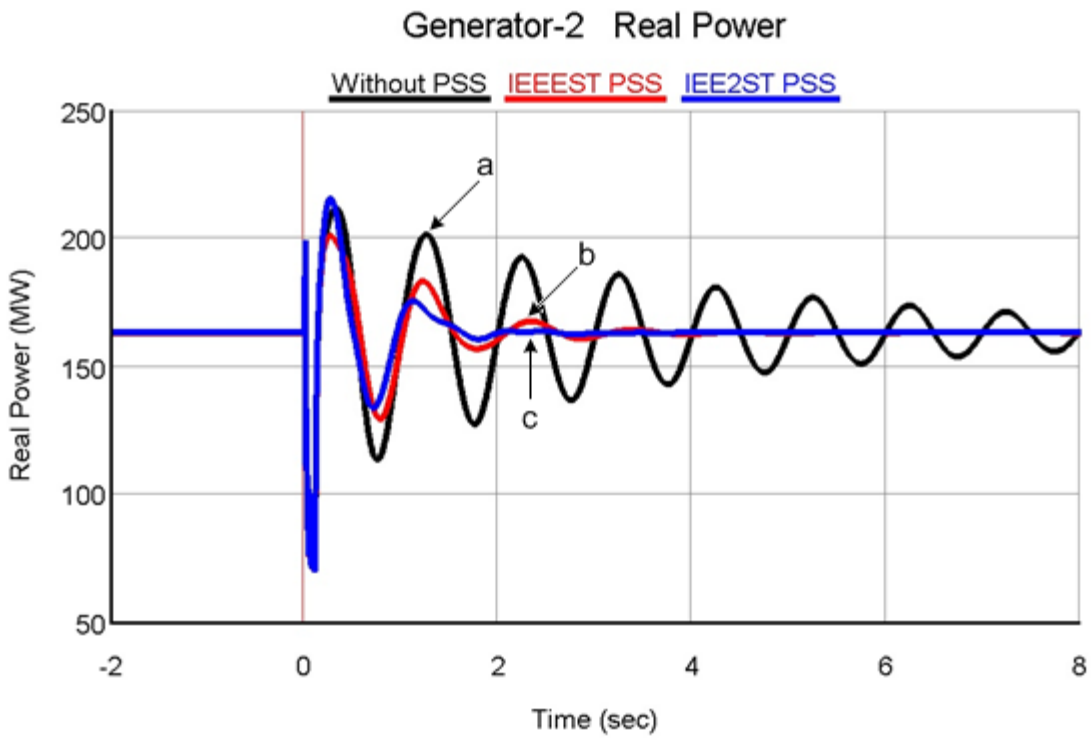

Figure 6.19: RTDS response of real power at generator-2 under three-phase six-cycle fault at t=0sec (a) Without PSS (b)With IEEEST type single input PSS and (c) With IEE2ST type multi-input PSS

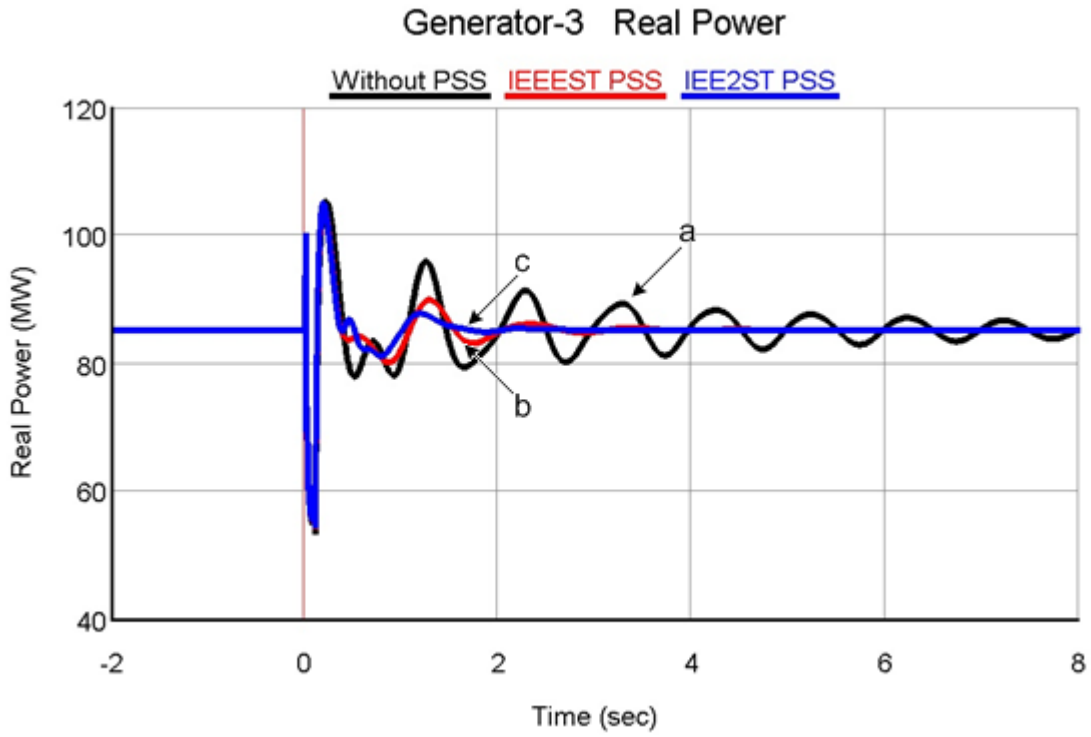

Figure 6.20: RTDS response of real power at generator-3 under three-phase six-cycle fault at t=0sec (a) Without PSS (b)With IEEEST type single input PSS and (c) With IEE2ST type multi-input PSS

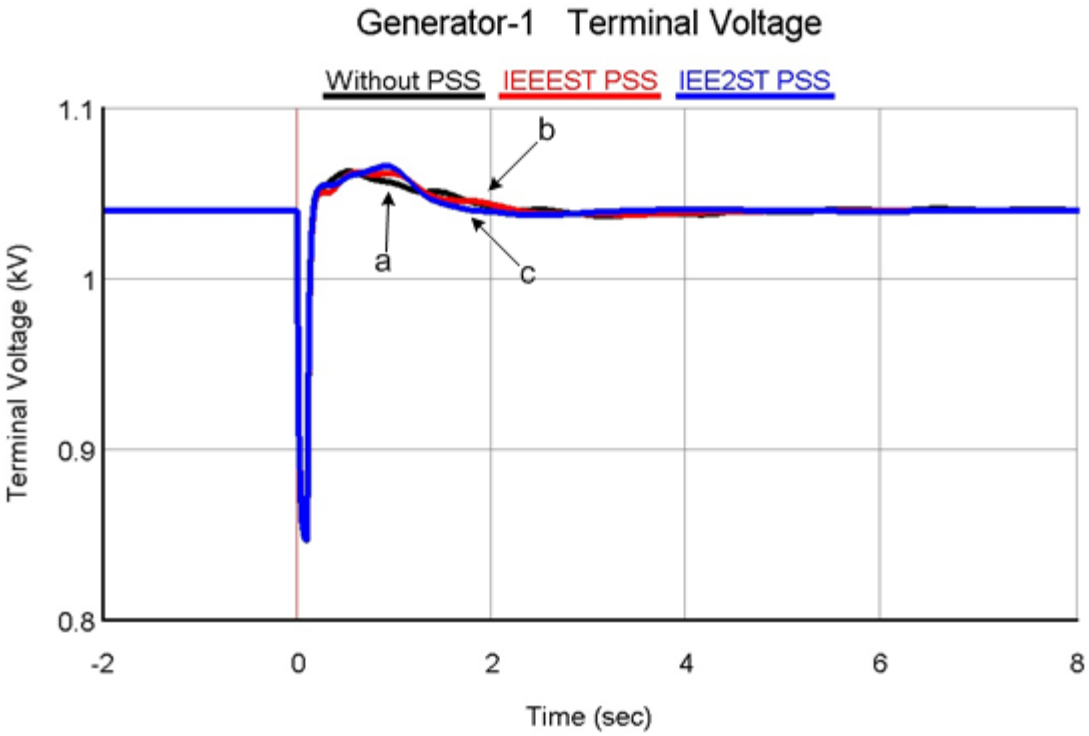

Figure 6.21: RTDS response of terminal voltage at generator-1 under three-phase six-cycle fault at t=0sec (a) Without PSS (b)With IEEEST type single input PSS and (c) With IEE2ST type multi-input PSS

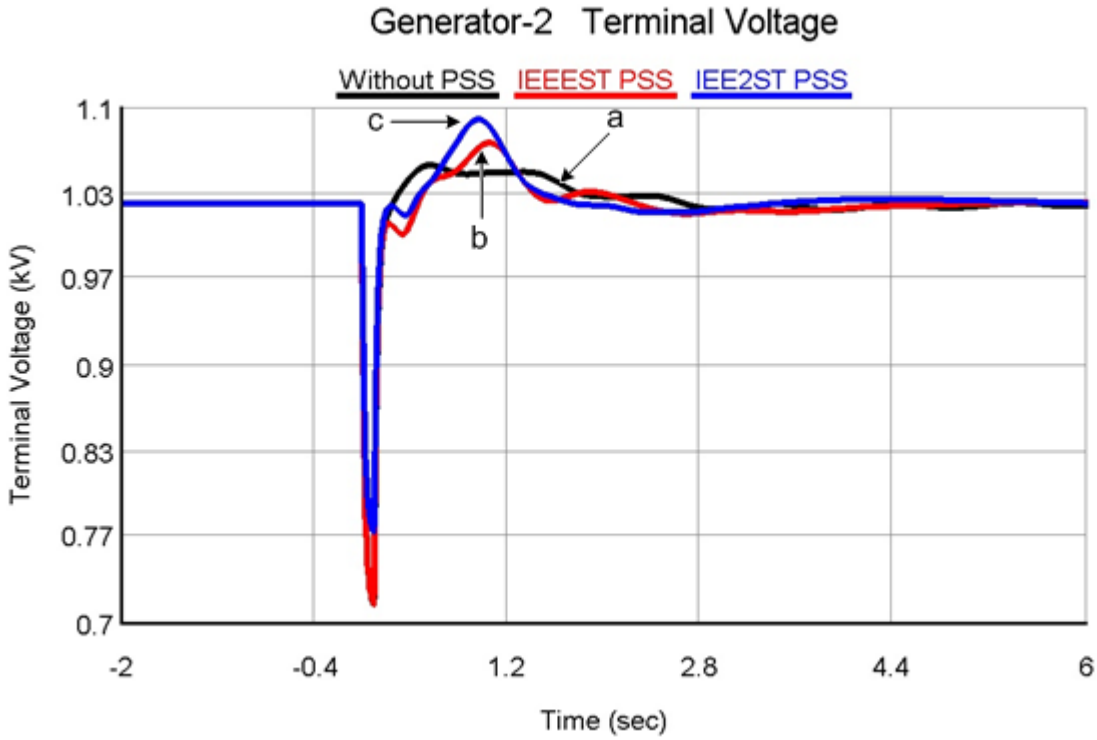

Figure 6.22: RTDS response of terminal voltage at generator-2 under three-phase six-cycle fault at t=0sec (a) Without PSS (b)With IEEEST type single input PSS and (c) With IEE2ST type multi-input PSS

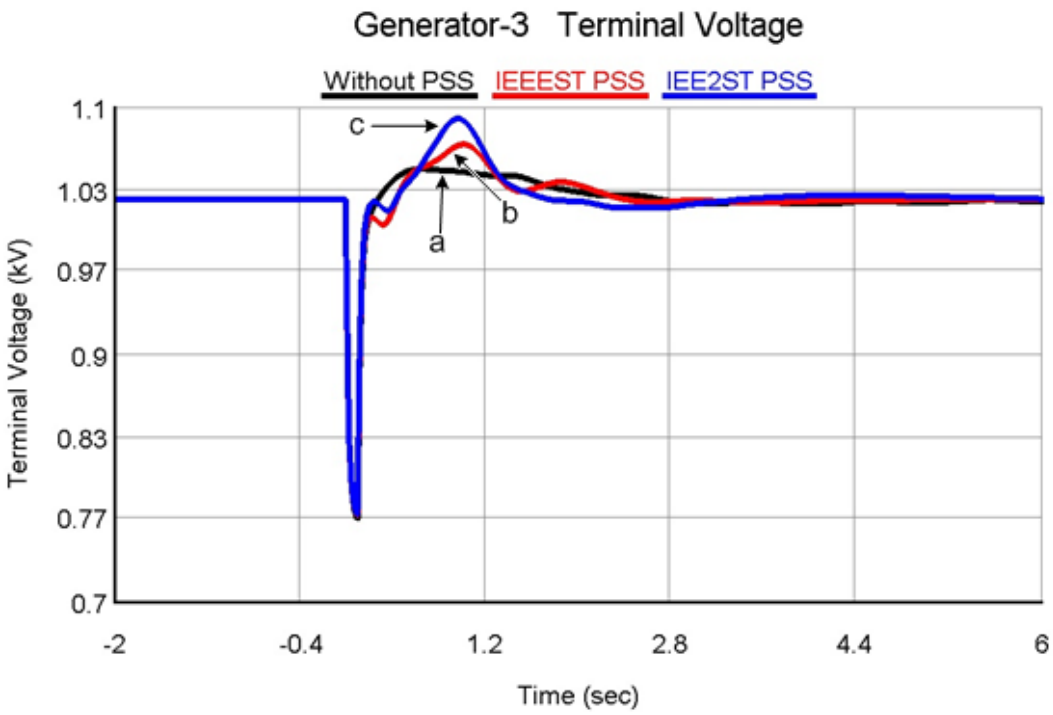

Figure 6.23: RTDS response of terminal voltage at generator-3 under three-phase six-cycle fault at t=0sec (a) Without PSS (b)With IEEEST type single input PSS and (c) With IEE2ST type multi-input PSS

6.1.6 Comparison of Simulated and RTDS results for test case 1

Comparing the simulated and RTDS results it is clear that response of both are approximately same following the same pattern. The simulated results of rotor angle and real power are very much near to simulated and RTDS results. But the RTDS result takes a little longer time, 0.5sec to 1sec. This is due to the fact that the RTDS is a practical application considering all environmental effects like temperature, electromagnetic field produced by the transmission lines, and even the sub-transient reactances and time constants for generators. RTDS also took some processing time for every block used. While in Matlab all the above parameter are usually not considered. Comparing the results with the recent literature using IEEEST PSS structure on 3-machine 9-Bus system under three-phase six-cycle fault, it is found that the proposed approach quickly damps the oscillations with less overshoot within 2 sec. However, in [112–114] it took around 2.5 sec to 4 sec in bringing the system to steady state.

6.2 Test Case 2: 5-Machine 14-Bus system

5-Machine 14-Bus system as shown in Fig. 6.24 is used to test the system response on three different cases for low frequency inter-area oscillations. First, when no PSS is connected to the test system. Second, when the system is connected with IEEEST type PSS. Third, when system is connected with IEE2ST type PSS integrated with PMUs.

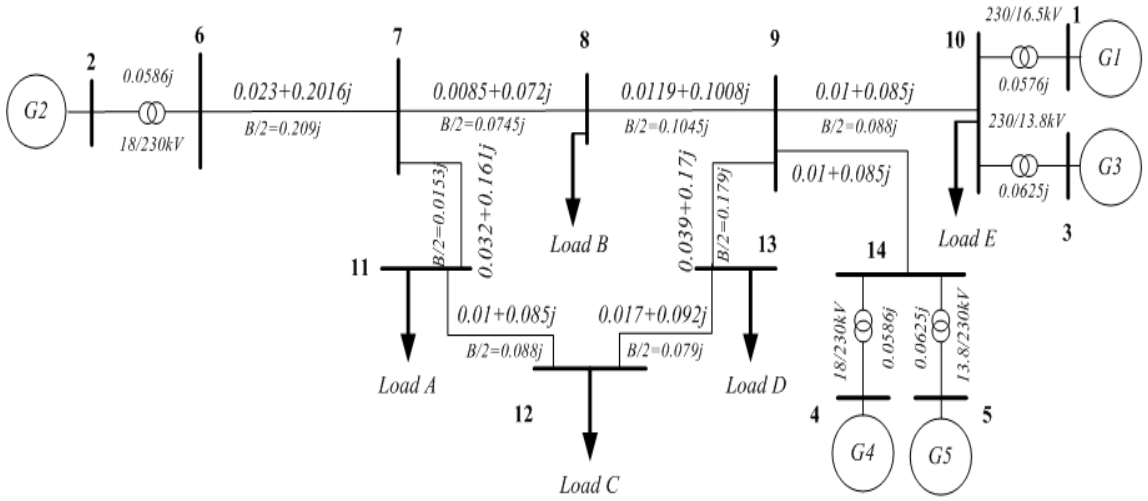

Figure 6.24: A detailed 5-Machine 14-Bus test system

6.2.1 Optimal placement of PSS

Optimal placement of PSS is done with eigenvalue based participation factor. Table 6.4, indicates the electromechanical modes against the generator locations of the system which causes low frequency inter-area oscillations. The generators those are more affecting the electromechanical modes are highlighted in Table 6.4. It is obvious that generator 1 and generator 2 have more contribution in creating inter-area oscillations so PSS should be installed on these optimal locations for best performance with economical use of PSSs.

Table 6.4: Optimal Location Identification for PSS Installation

Electromechanical Modes	Generator Busbar Number				
	1	2	3	4	5
0.1326 ± 5.0194i	-0.0005	0.7964	-0.0005	0.3585	-0.0005
0.0084 ± 9.5269i	0.8783	0.0196	0.0009	0.0271	0.4746
-0.4155 ±14.7843i	0.0398	0	0.0041	0.5241	0.0467
-0.8135 ±16.9739i	0.1869	0.0004	0.3881	0	0.0014

6.2.2 Stabilizer Design

Once the optimal location for placing PSS is known, the differential evolution is used to optimize the gains and time constant of the power system stabilizers. Table 6.5, indicates the optimal controller gains and the time constants for single input type PSS (IEEEST) and multi-input type PSS (IEE2ST) integrated with PMUs'.

Table 6.5: Optimal PSS Controller Gains for 5-Machine 14-Bus system

	IEEEST PSS		IEE2ST PSS	
	G1	G2	G1	G2
K_1	39.371	5.212	82.235	20.12
K_2	-	-	0.05	0.05
T_1	0.298	0.919	0.049	0.049
T_2	0.05	0.05	0.05	0.05
T_3	0.802	0.874	10	10
T_4	0.05	0.05	10	10
T_5	10	10	0.211	0.981
T_6	10	10	0.05	0.05
T_7	-	-	0.322	0.791
T_8	-	-	0.05	0.05
T_9	-	-	0.0	0.0
T_{10}	-	-	0.001	0.001

6.2.3 Eigenvalue Analysis

The system eigenvalues without PSS, IEEEST type PSS and with the proposed PMU integrated multi input IEE2ST type PSS controllers are given in Table 6.6. The bold rows of this table represent the electromechanical mode eigenvalue. It is evident that, using the proposed coordinated stabilizer design, the electromechanical mode eigenvalue is greatly shifted to the left of the s-plane. Hence, it can be concluded that it considerably enhances the system stability.

Table 6.6: 5-machine 14-bus system eigenvalues for without PSS, IEEEST PSS and IEE2ST PSS

No Control	IEEEST	IEE2ST
0.1326 ± 5.0194i	**-0.6665 ± 10.3275i**	**-0.5268 ± 10.3253i**
0.0084 ± 9.5269i	**-0.8141 ± 16.9737i**	**-0.8146 ± 16.9735i**
-0.4155 ±14.7843i	**-1.4018 ± 0.5070i**	**-0.8992 ± 17.5645i**
-0.8135 ±16.9739i	**-1.4082 ± 3.2469i**	**-1.3913 ± 3.083761i**
-25.0506 ±26.2149i	-26.6518 ± 28.3641i	-26.4844 ± 27.6586i
-25.1034 ±13.7743i	-22.957 ± 13.6536i	-23.1359 ± 13.9781i
-10.4524 ±28.6219i	-10.2260 ± 9.7065i	-12.2738 ± 7.3983i
-42.2282	-2.9054 ± 29.32761i	-1.6263 ± 30.0716i
-40.9692	-1.4314 ± 18.9210i	-1.5725 ± 0.6287i
-8.3796	-56.0228	-53.2949
-7.7889	-40.9690	-40.969
-0.0106	-16.2192	-18.1534
0.001	-8.3797	-8.3797
--	-3.3219	-3.5925
--	-0.1008	-0.1009
--	-0. 05	-.0102
--	-20	-20
--	-20	-20
--	-0.1	-0.1
--	-20	-20
--	-20	-20
--	-0.1	-0.1
--	-20	-20
--	-20	-20
--	-0.1	-0.1
--	-0.04	-0.03

6.2.4 Simulation Results for Test Case 2

In first case, 3-phase 6-cycle fault is applied to the test system with no PSS connected and monitor the system responses. The system is found to be unstable and the oscillations continue for system break down. In case two, single input type PSS (IEEEST), using rotor speed as a local input signal, installed on generator 1 and generator 2. Selection of these generators is based on Table 6.4 It is observed that the oscillations are damped efficiently. In third case, generator 2 and generator 3 are equipped with multi-input type PSS (IEE2ST) integrated with PMUs', where *Pe* is used as a local signal and *w* as a remote signal. This remote signal is provided by PMUs in synchronism with GPS clock.

Simulation results shows the performance for each case as discussed before, for no PSS, for IEEEST type PSS and for the proposed IEE2ST type PSS. For a 3-phase 6-cycle fault, response of rotor speed of all five generators, for each case is shown in Figs. 6.25-6.29 where low frequency inter-area oscillations of 0.66 Hz can be clearly observed. Without control, oscillations grow with the passage of time, with IEEEST control; rotor speed also increases but settles in about 4 seconds. However, it is evident that with proposed scheme, rotor speed effectively damped within 2 seconds. This is the fact that proposed wide-area damping controller can quickly damp local as well as inter-area modes. With the three-phase line to ground fault, for 100msec. It is considered that the generator is a reference one, with rotor angle zero. The variation in rotor angle for all generator are presented in Fig. 6.30-6.33. The IEEEST controller restores the operating condition within 5 seconds. However, the proposed IEE2ST controller provides good damping to generator rotor angle and so the transient's oscillations have been effectively

suppressed within 3 seconds. The responses of the real power of all five generators under the 6-cycle fault are shown in Figs. 6.34-6.38. Without control the peak values reaches 120 MW, and continue to oscillate over the period of time. With IEEEST controller, is settles down in 4 second with peak value of 80MW. However, with proposed IEE2ST controller, it is observed that it takes less time of 2.5sec and less overshoots to reach steady state value.

From simulation results it is concluded that IEE2ST having input signal *w* from remote locations provides high level of damping with minimum transients to inter-area oscillations as compared to IEEEST. The proposed multi input IEE2ST stabilizer outperforms the conventional IEEEST in terms of reduction of overshoot and settling time of low frequency inter-area oscillations.

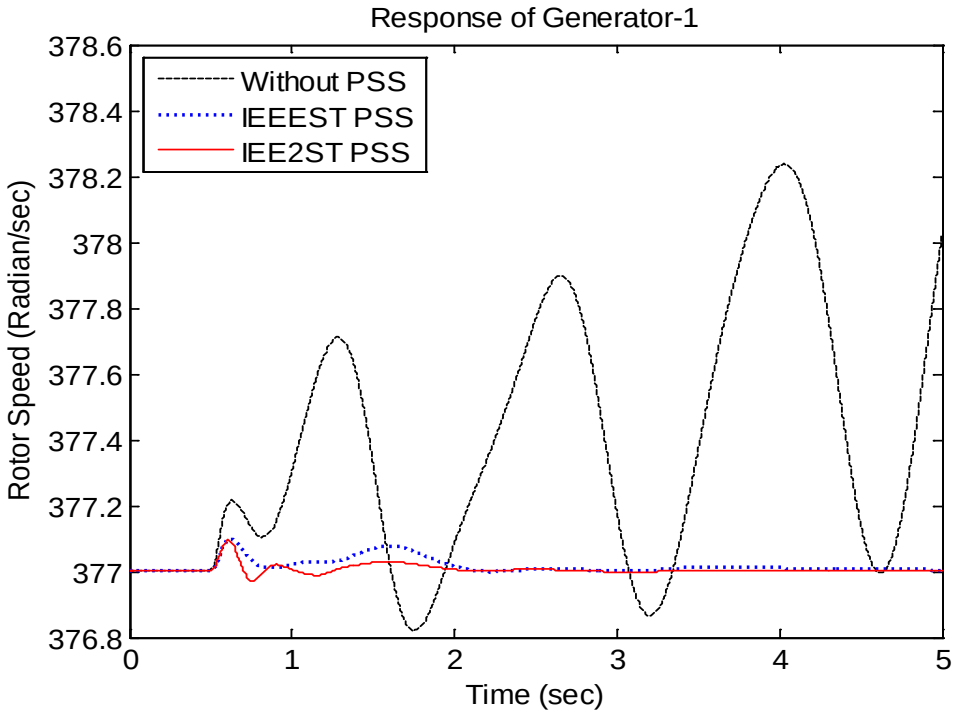

Figure 6.25: Simulated response of rotor speed at generator-1 under three-phase six-cycle fault at t=0.5sec (a) Without PSS (b)With IEEEST type single input PSS and (c) With IEE2ST type multi-input PSS

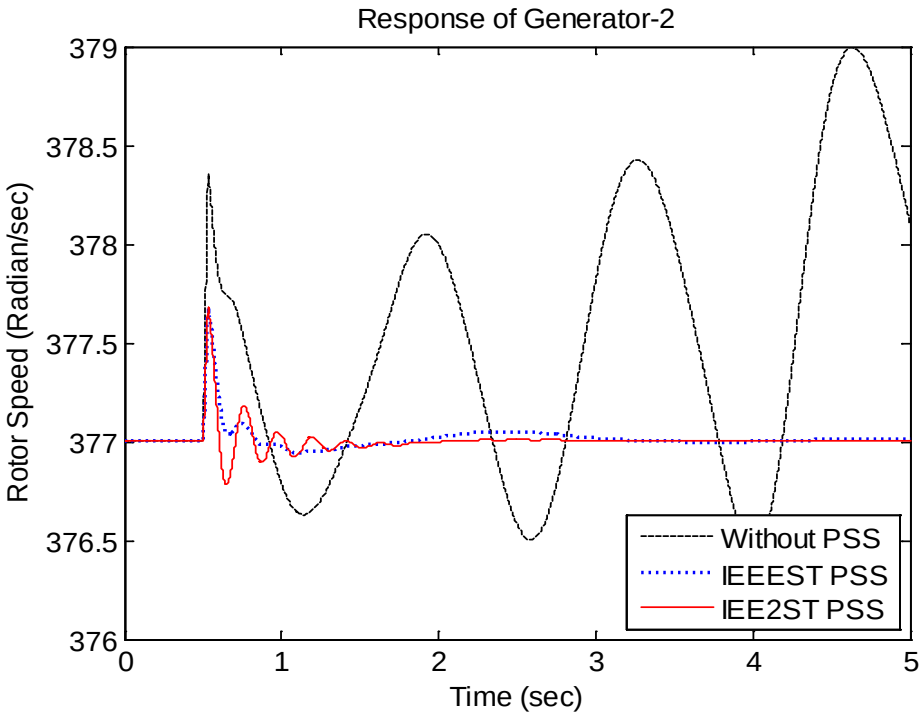

Figure 6.26: Simulated response of rotor speed at generator-2 under three-phase six-cycle fault at t=0.5sec (a) Without PSS (b)With IEEEST type single input PSS and (c) With IEE2ST type multi-input PSS

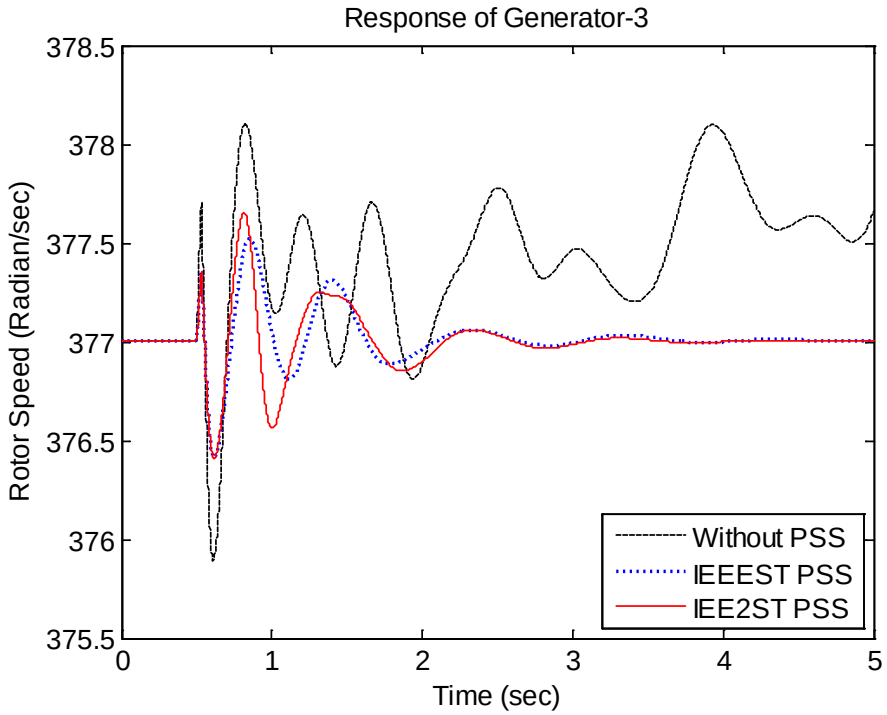

Figure 6.27: Simulated response of rotor speed at generator-3 under three-phase six-cycle fault at t=0.5sec (a) Without PSS (b)With IEEEST type single input PSS and (c) With IEE2ST type multi-input PSS

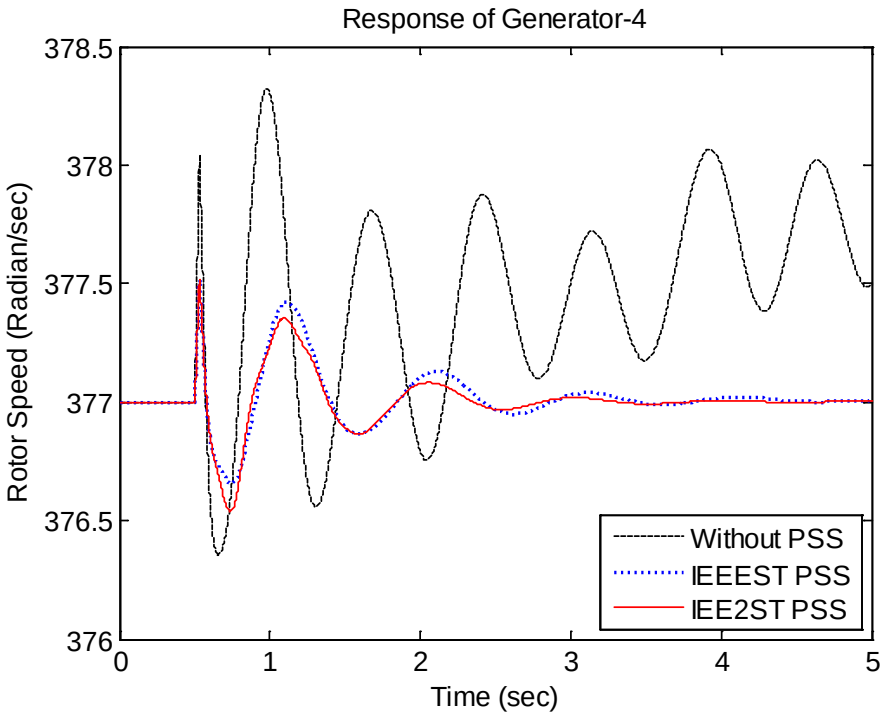

Figure 6.28: Simulated response of rotor speed at generator-4 under three-phase six-cycle fault at t=0.5sec (a) Without PSS (b)With IEEEST type single input PSS and (c) With IEE2ST type multi-input PSS

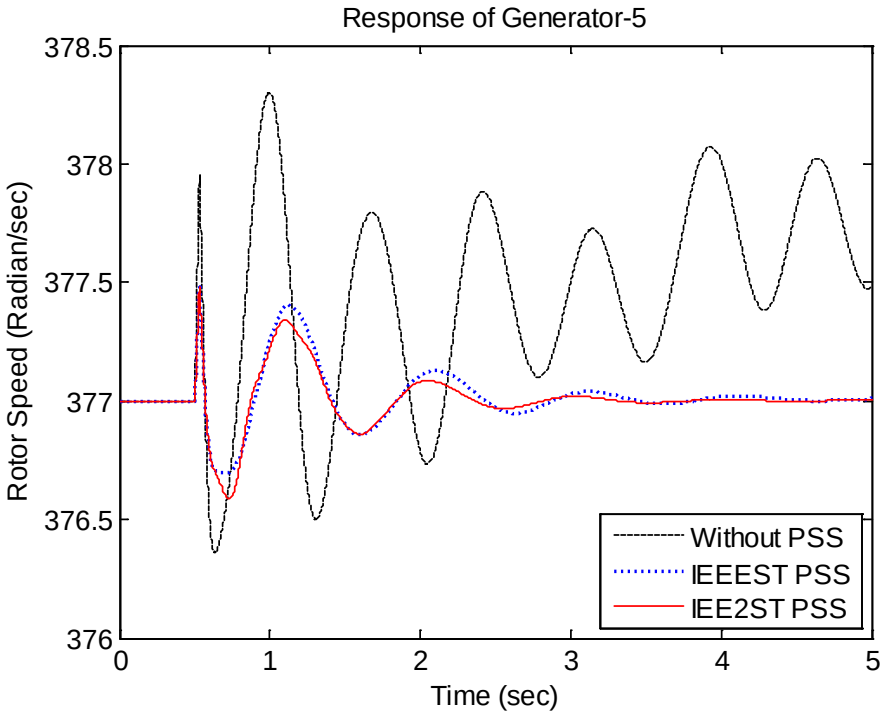

Figure 6.29: Simulated response of rotor speed at generator-5 under three-phase six-cycle fault at t=0.5sec (a) Without PSS (b)With IEEEST type single input PSS and (c) With IEE2ST type multi-input PSS

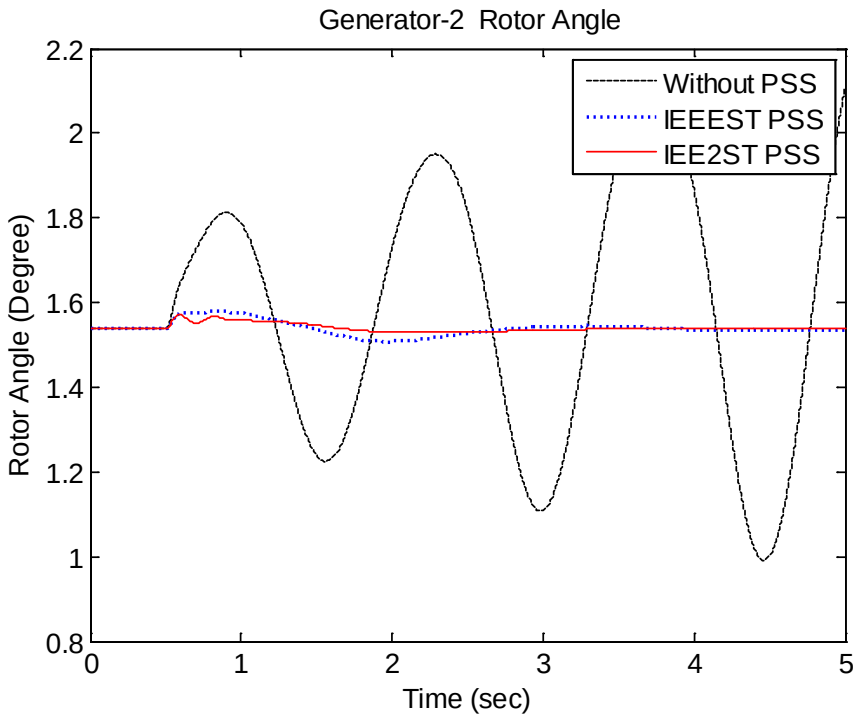

Figure 6.30: Simulated response of rotor angle at generator-2 under three-phase six-cycle fault at t=0.5sec (a) Without PSS (b)With IEEEST type single input PSS and (c) With IEE2ST type multi-input PSS

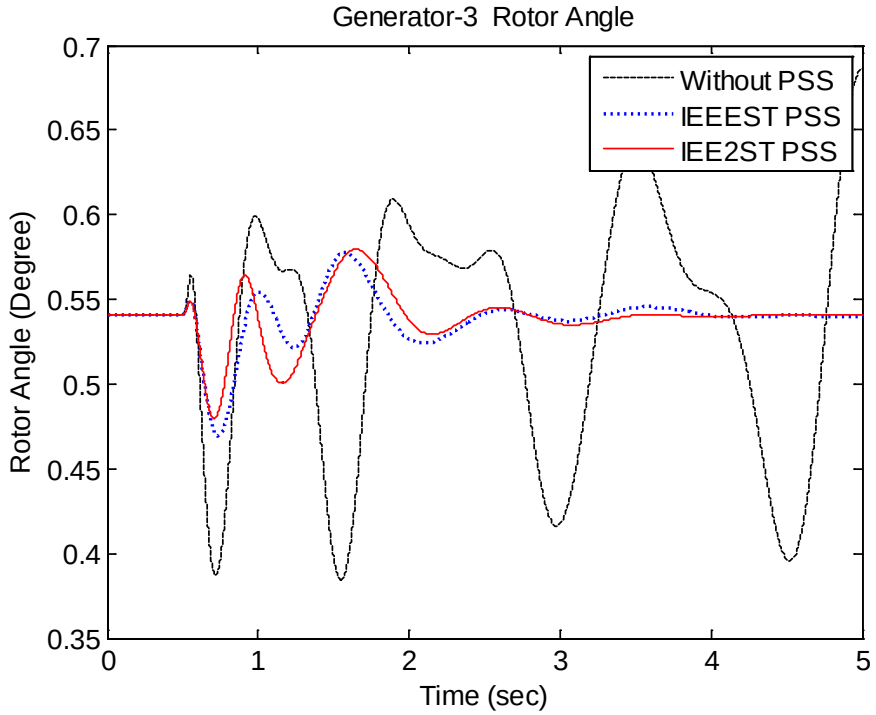

Figure 6.31: Simulated response of rotor angle at generator-3 under three-phase six-cycle fault at t=0.5sec (a) Without PSS (b)With IEEEST type single input PSS and (c) With IEE2ST type multi-input PSS

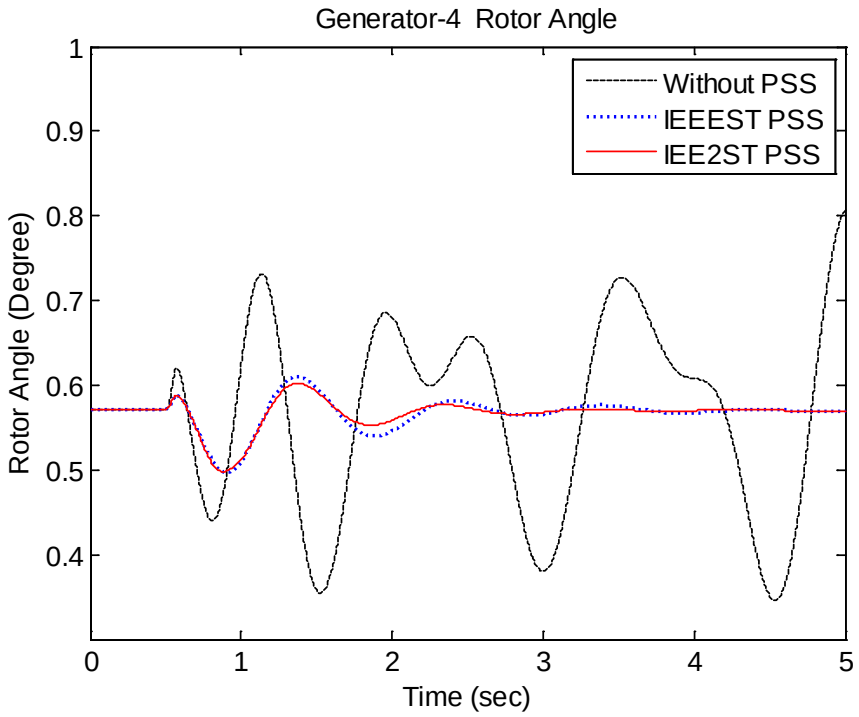

Figure 6.32: Simulated response of rotor angle at generator-4 under three-phase six-cycle fault at t=0.5sec (a) Without PSS (b)With IEEEST type single input PSS and (c) With IEE2ST type multi-input PSS

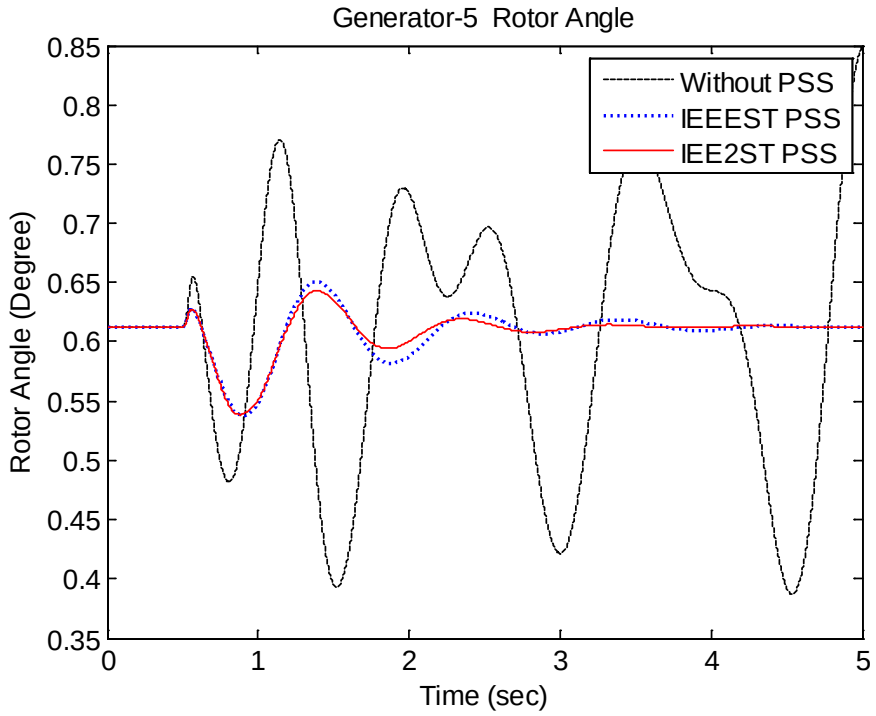

Figure 6.33: Simulated response of rotor angle at generator-5 under three-phase six-cycle fault at t=0.5sec (a) Without PSS (b)With IEEEST type single input PSS and (c) With IEE2ST type multi-input PSS

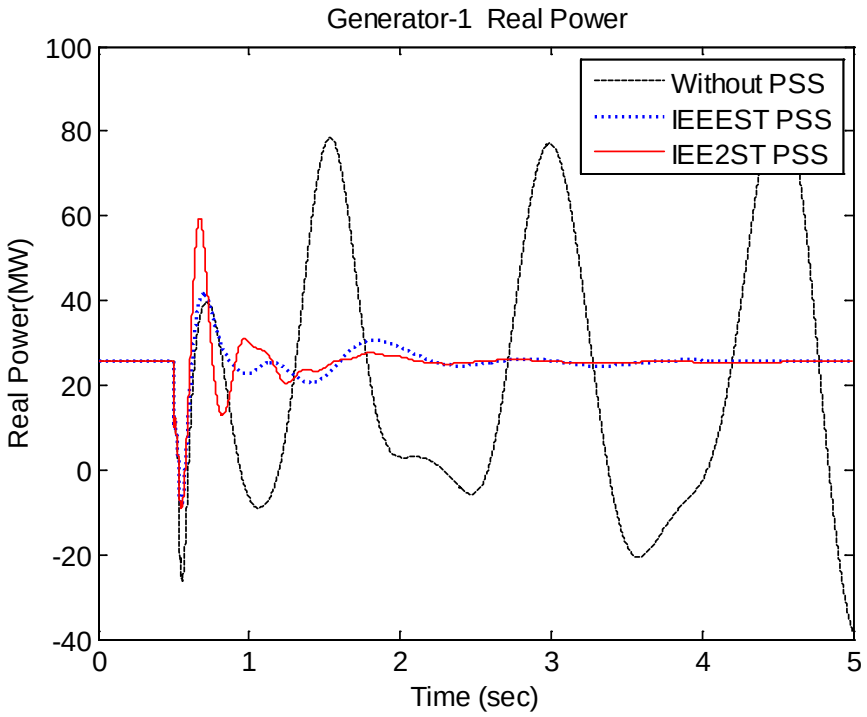

Figure 6.34: Simulated response of real power at generator-1 under three-phase six-cycle fault at t=0.5sec (a) Without PSS (b)With IEEEST type single input PSS and (c) With IEE2ST type multi-input PSS

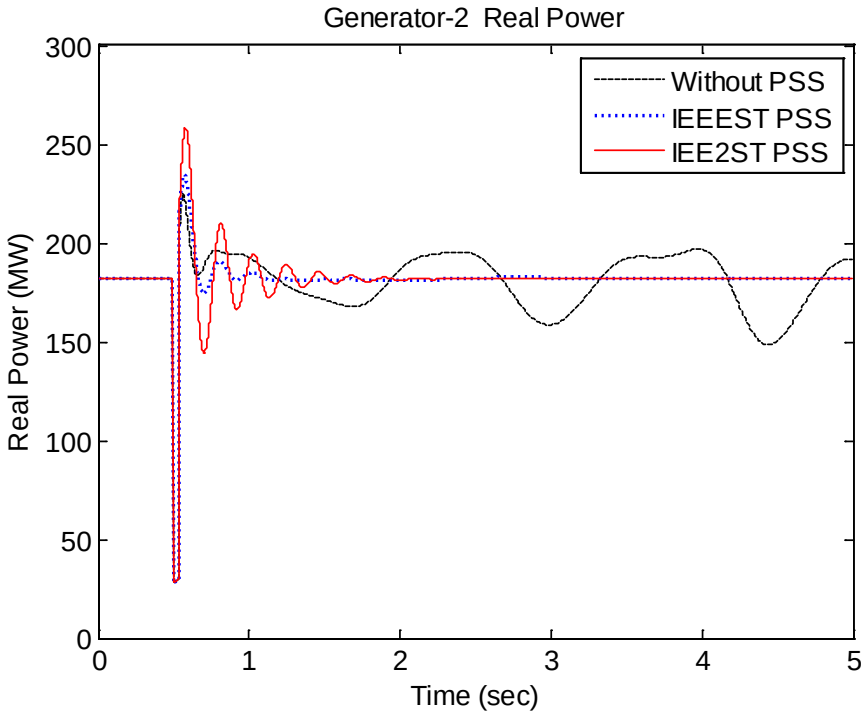

Figure 6.35: Simulated response of real power at generator-2 under three-phase six-cycle fault at t=0.5sec (a) Without PSS (b)With IEEEST type single input PSS and (c) With IEE2ST type multi-input PSS

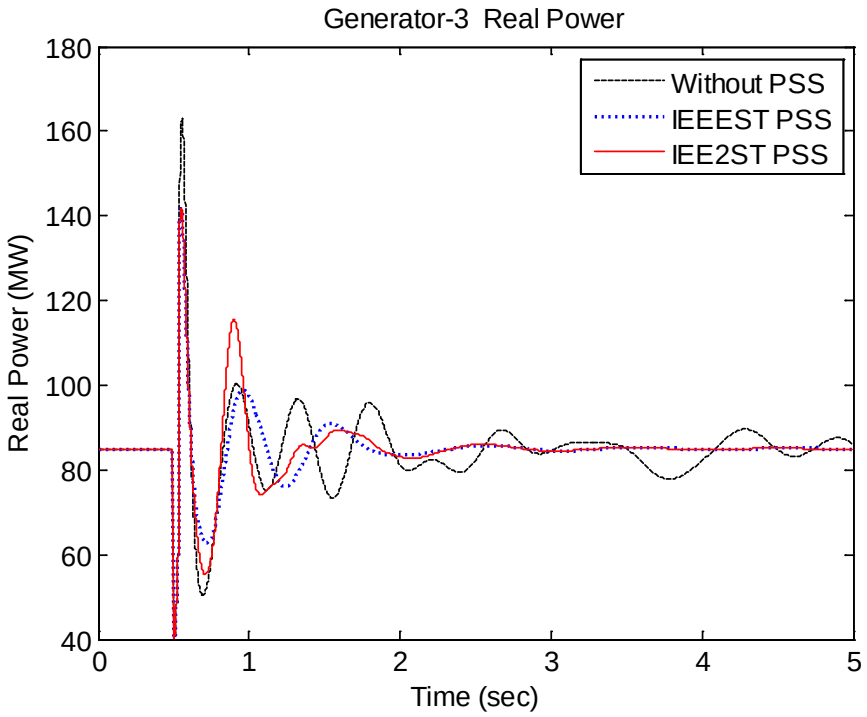

Figure 6.36: Simulated response of real power at generator-3 under three-phase six-cycle fault at t=0.5sec (a) Without PSS (b)With IEEEST type single input PSS and (c) With IEE2ST type multi-input PSS

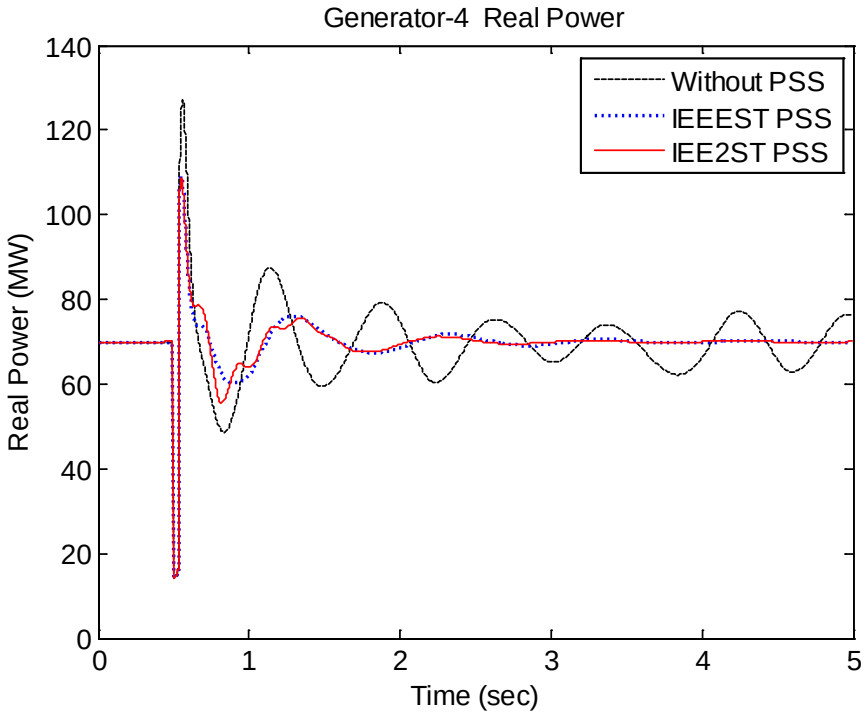

Figure 6.37: Simulated response of real power at generator-4 under three-phase six-cycle fault at t=0.5sec (a) Without PSS (b)With IEEEST type single input PSS and (c) With IEE2ST type multi-input PSS

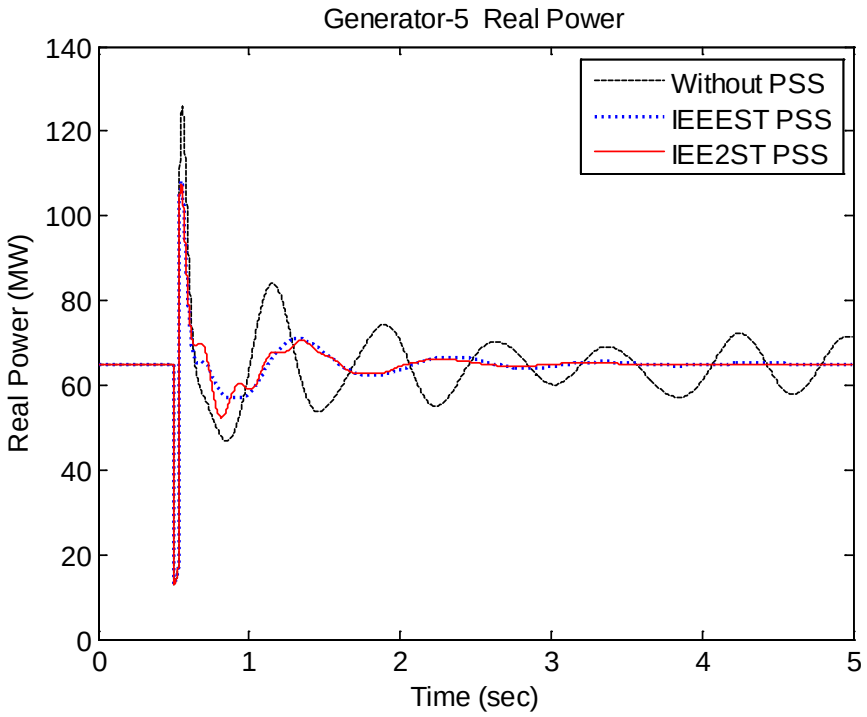

Figure 6.38: Simulated response of real power at generator-5 under three-phase six-cycle fault at t=0.5sec (a) Without PSS (b)With IEEEST type single input PSS and (c) With IEE2ST type multi-input PSS

6.2.5 RTDS Results for Test Case 2

The 5-Machine 14-Bus system is built on the RSCAD as shown in Fig. 6.39. The complete system data is available in the Appendix C. Where generator 2 is located on the left with a long transmission line. This case is considered to deeply focus on two area power system. Two area network is of high interest for testing weakly damped inter-area oscillations. First the test system is simulated for the case when no PSS connected to the system, and all the critical states are monitored in real-time. Second, the IEESET type PSS is used to damp out the oscillations. Third, the PMU is installed to collect the remote signal from distant generator in synchronism with the GPS signal. This remote signal is sent to the IEE2ST type multi input PSS. Literature review shows that PSS equipped with both local and remote signals, effectively damp out the inter-area oscillations.

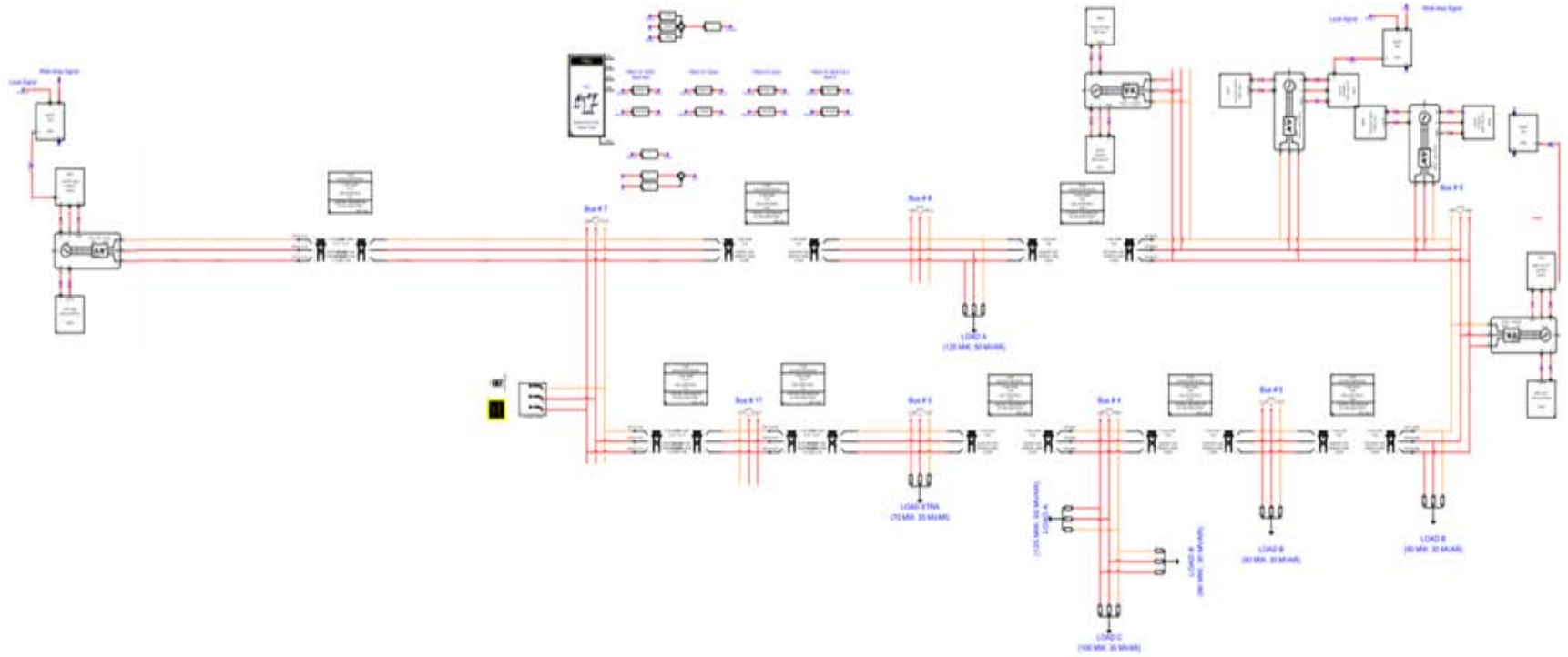

Figure 6.39: RTDS Model for 5-Machine 14-Bus system

A three-phase six-cycle fault occurred on bus 7 of the 5-Machine 14-Bus system. The voltage response on Bus 7 is shown in Fig. 6.40, where all of the phases become zero for the duration of fault and then trying to stabilize over the time.

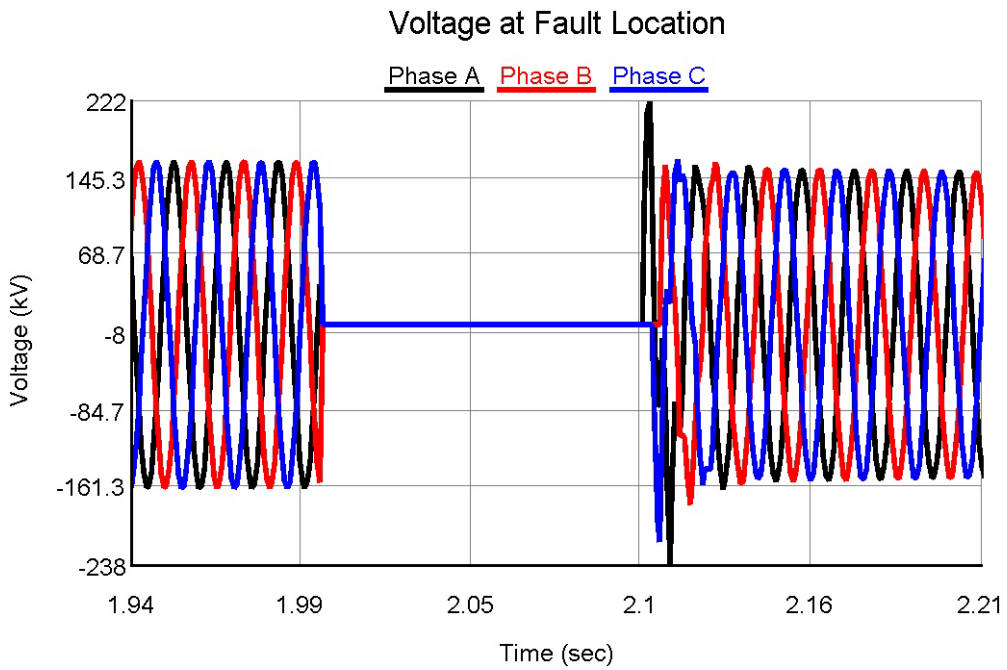

Figure 6.40: RTDS response of three-phase six-cycle fault on five-machine fourteen-bus system

The RTDS response of the rotor speed under three-phase six-cycle fault (100msec) for all five generator for without PSS, with IEEEST and with proposed multi input IEE2ST damping controller integrated with PMU are shown in Fig. 6.41-6.45. Since the fault is near to generator 2 it is affected most with the peak value 379.5 rad/sec. Inter-area oscillations of 0.58Hz are observed in Fig. 6.41-6.45. From graphs, the major affected generators are the same as those recommended for installing PSS by optimal placements of PSS in Table 6.4. Since generator 1 is the dominant generator among the group of generator 1,3,4 and 5 therefore, generator 3,4 and 5 follows the same pattern of oscillations. With no controller, the oscillations are increasing with the passage of time, With IEEEST controller, the oscillations settles in 6 seconds. However, proposed IEE2ST

controller quickly damp the transients with less overshoots within 3.5 seconds. These responses are very much near to the original system as it is obtained on a modern real-time digital simulator. The rotor angle responses are presented in Fig. 6.46-6.50, without controller the rotor angle is not damped even in 20 sec, with IEEEST control it restores the system to its nominal operating condition in 8 sec, and with the proposed IEE2ST controller using wide are measurements quickly damp within 4 sec. The responses of real power of all three generators are shown in Figs. 6.51-6.55. with no control the oscillations continues over a long period of time, IEEEST controller bring the system to steady state in 3sec. IEE2ST controller, provides good damping to the generator power so transient oscillation efficiently suppressed within 2 sec.

The responses of terminal voltages for all five generators are shown in Fig. 6.56-6.60. Generator 2 takes higher time for stabilizing its voltage with peak values of 1.1pu and 0.85pu. With no controller, the oscillations are increasing with the passage of time, With IEEEST controller, the oscillations settles down in 8 seconds. However, proposed IEE2ST controller quickly damps the transients with less overshoots within 6 seconds.

From simulation results it is concluded that IEE2ST having input signal *w* from remote locations can effectively damp inter-area oscillations as compared to IEEEST. The proposed multi input IEE2ST stabilizer outperforms the conventional IEEEST in terms of reduction of overshoot and settling time of low frequency inter-area oscillations.

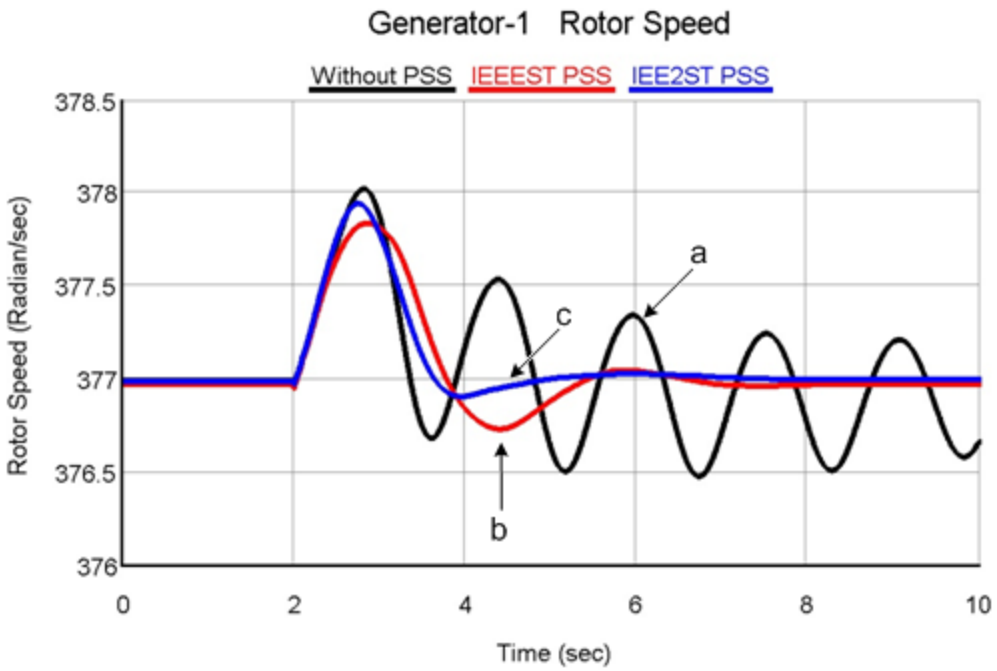

Figure 6.41: RTDS response of rotor speed at generator-1 under three-phase six-cycle fault at t=0sec (a) Without PSS (b)With IEEEST type single input PSS and (c) With IEE2ST type multi-input PSS

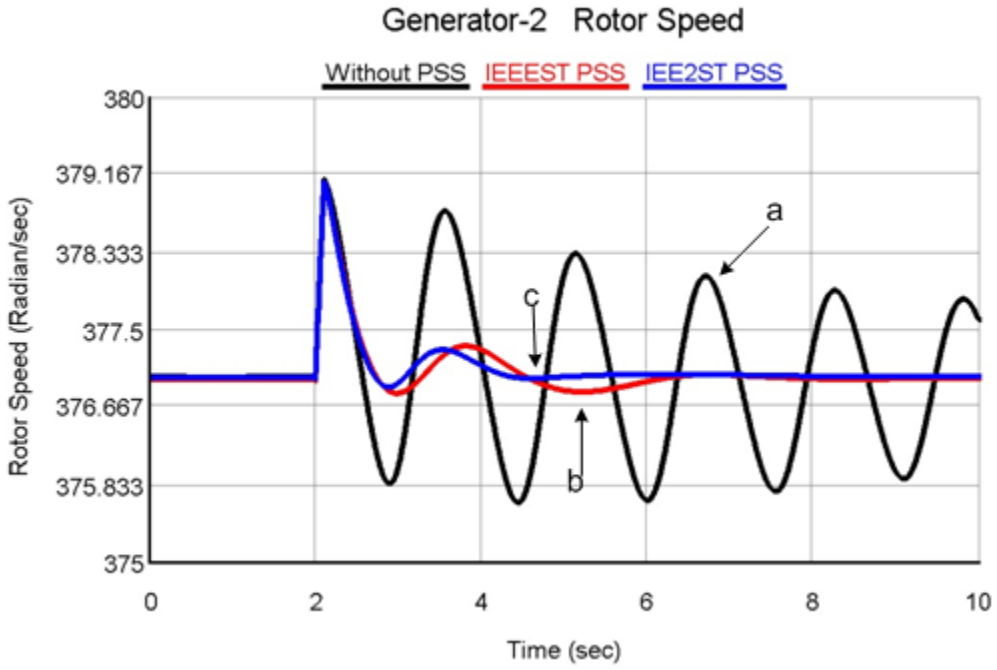

Figure 6.42: RTDS response of rotor speed at generator-2 under three-phase six-cycle fault at t=0sec (a) Without PSS (b)With IEEEST type single input PSS and (c) With IEE2ST type multi-input PSS

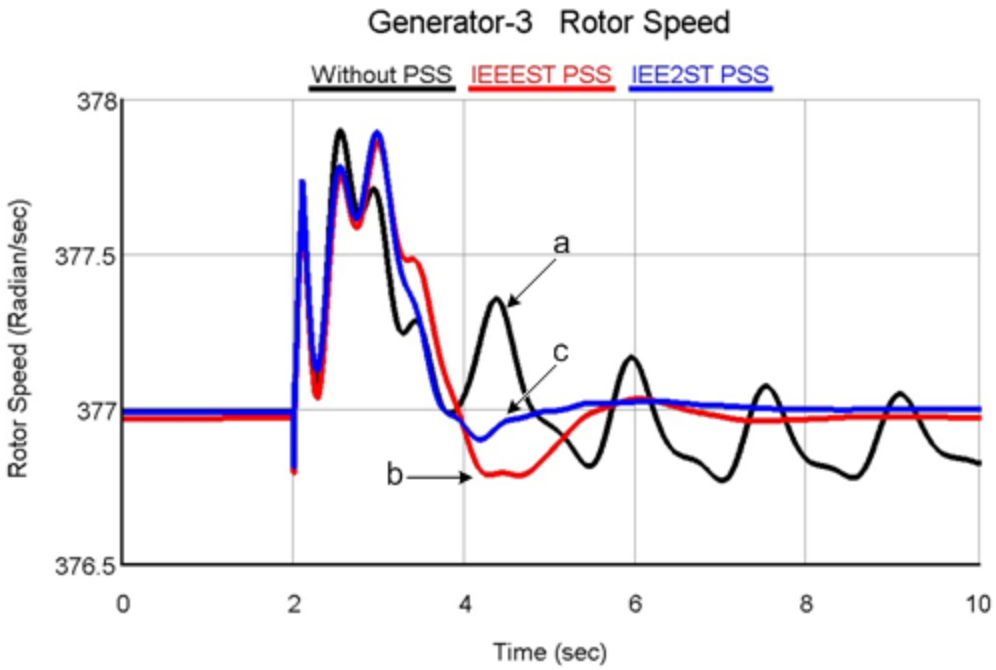

Figure 6.43: RTDS response of rotor speed at generator-3 under three-phase six-cycle fault at t=0sec (a) Without PSS (b)With IEEEST type single input PSS and (c) With IEE2ST type multi-input PSS

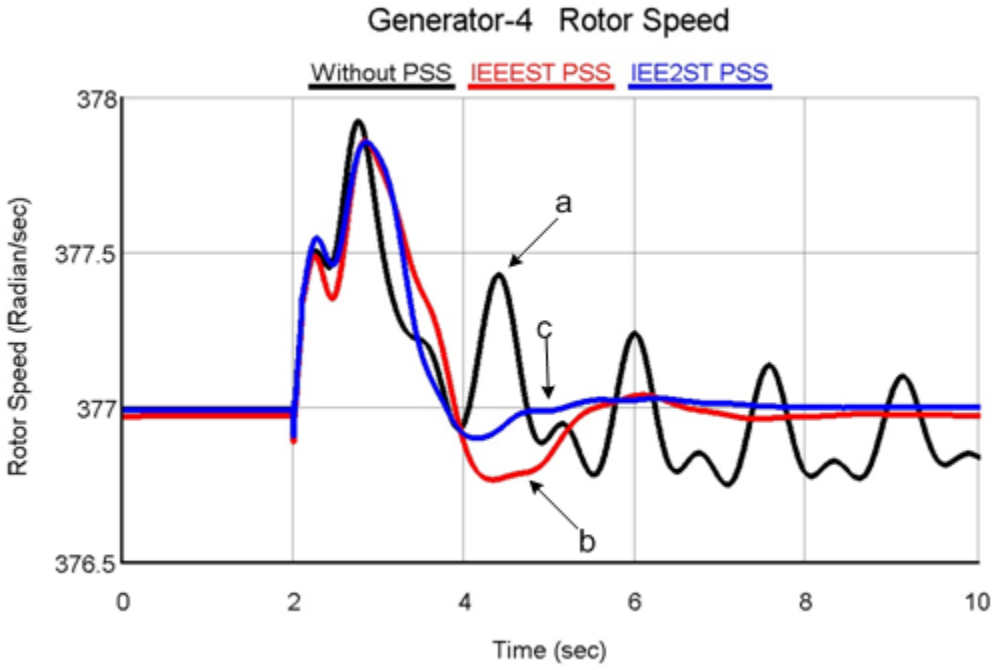

Figure 6.44: RTDS response of rotor speed at generator-4 under three-phase six-cycle fault at t=0sec (a) Without PSS (b)With IEEEST type single input PSS and (c) With IEE2ST type multi-input PSS

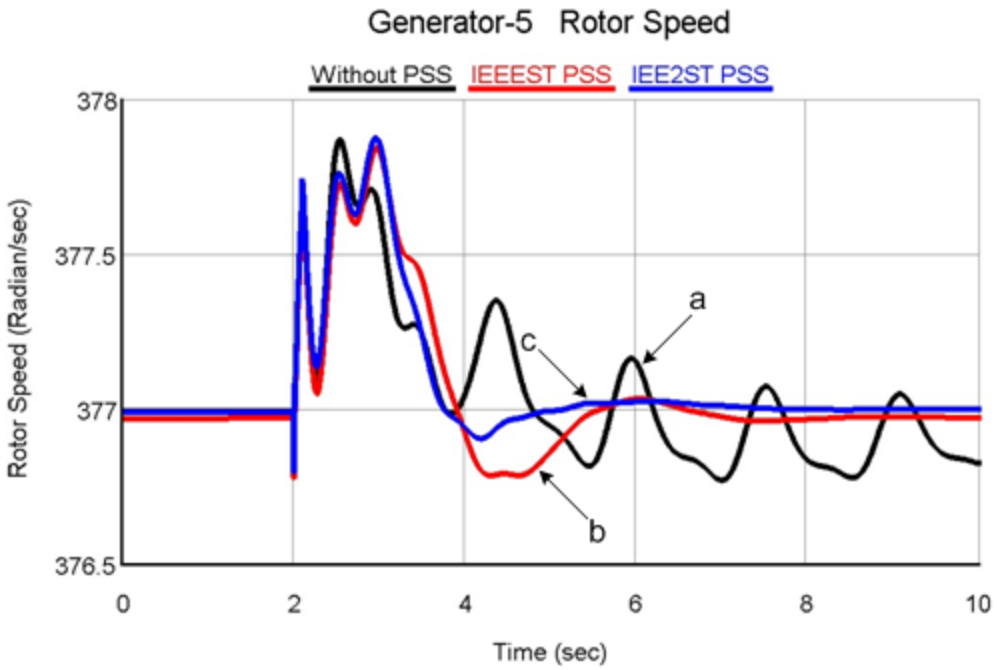

Figure 6.45: RTDS response of rotor speed at generator-5 under three-phase six-cycle fault at t=0sec (a) Without PSS (b)With IEEEST type single input PSS and (c) With IEE2ST type multi-input PSS

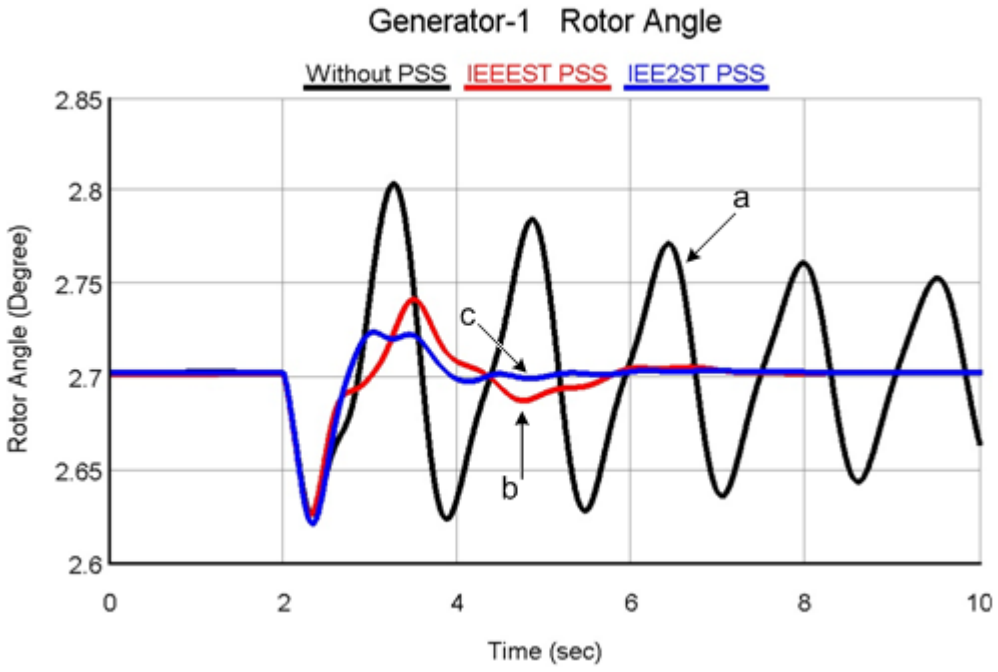

Figure 6.46: RTDS response of rotor angle at generator-1 under three-phase six-cycle fault at t=0sec (a) Without PSS (b)With IEEEST type single input PSS and (c) With IEE2ST type multi-input PSS

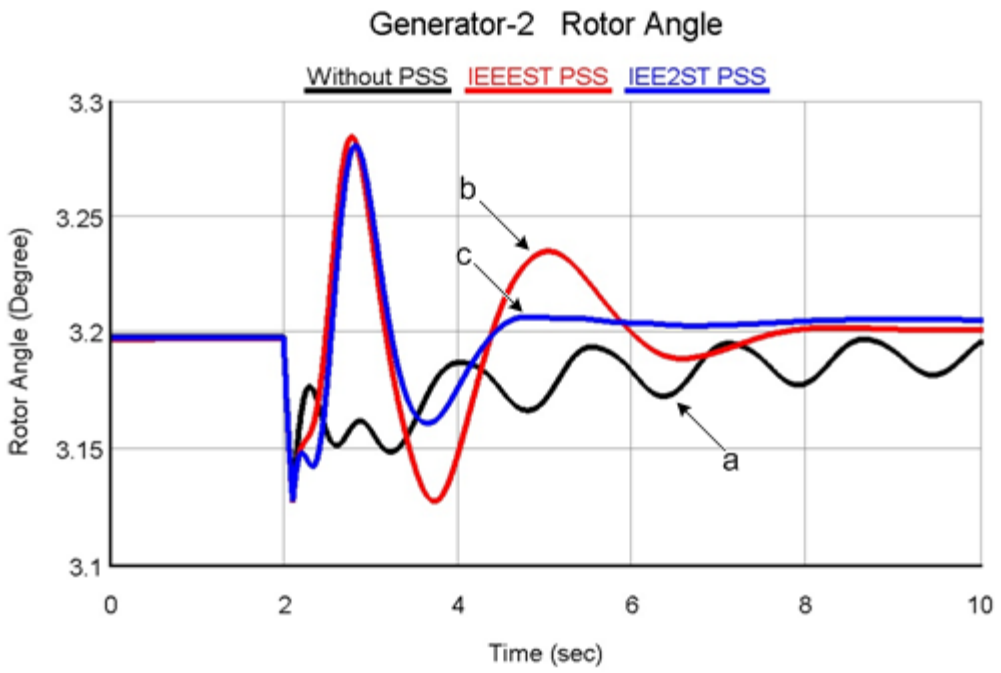

Figure 6.47: RTDS response of rotor angle at generator-2 under three-phase six-cycle fault at t=0sec (a) Without PSS (b)With IEEEST type single input PSS and (c) With IEE2ST type multi-input PSS

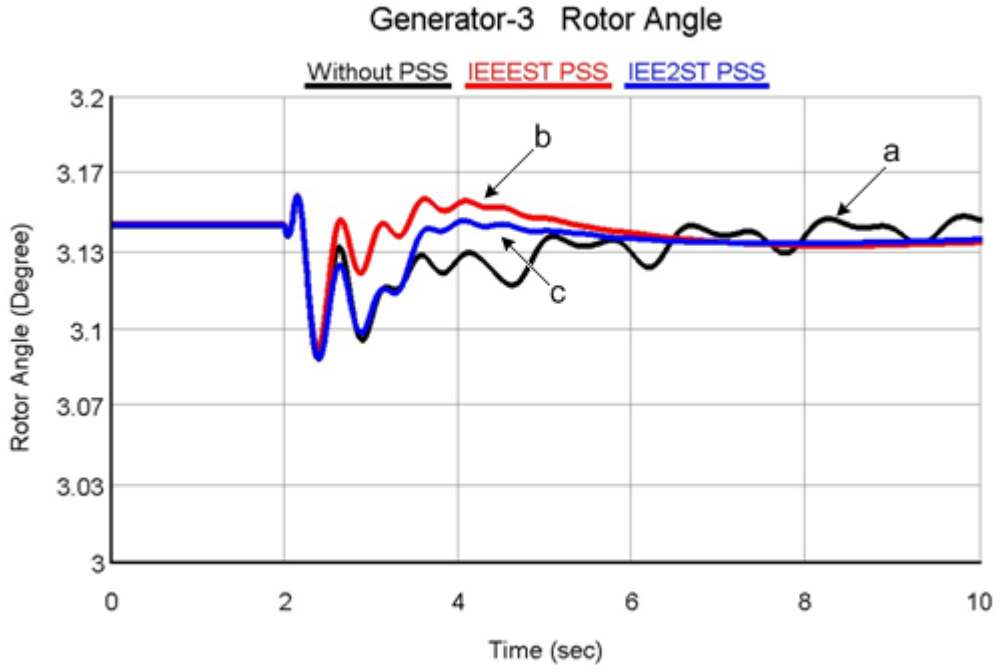

Figure 6.48: RTDS response of rotor angle at generator-3 under three-phase six-cycle fault at t=0sec (a) Without PSS (b)With IEEEST type single input PSS and (c) With IEE2ST type multi-input PSS

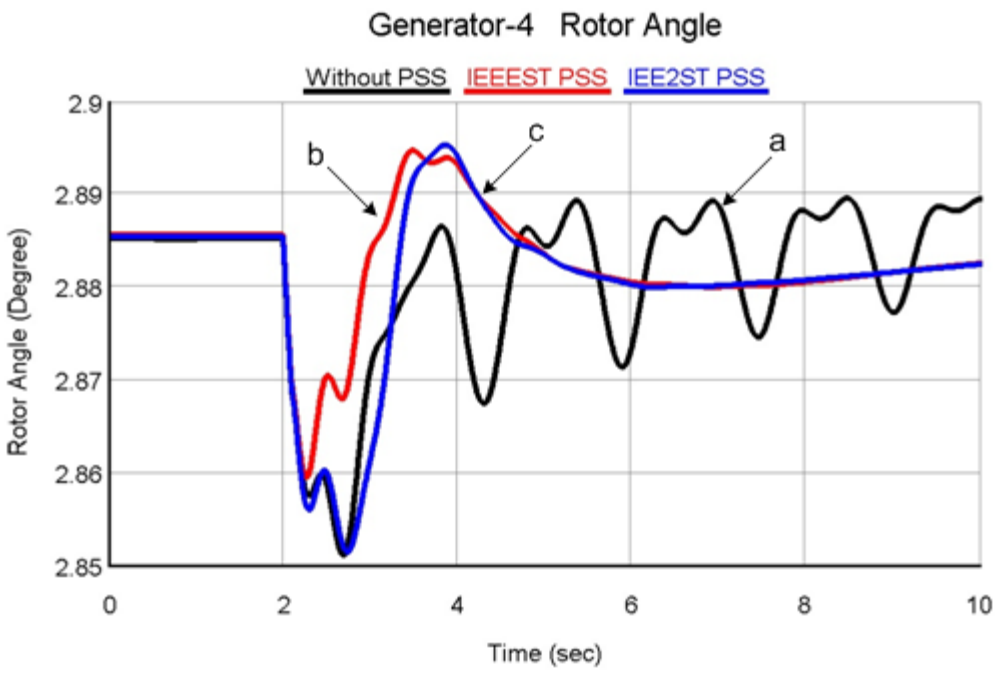

Figure 6.49: RTDS response of rotor angle at generator-4 under three-phase six-cycle fault at t=0sec (a) Without PSS (b)With IEEEST type single input PSS and (c) With IEE2ST type multi-input PSS

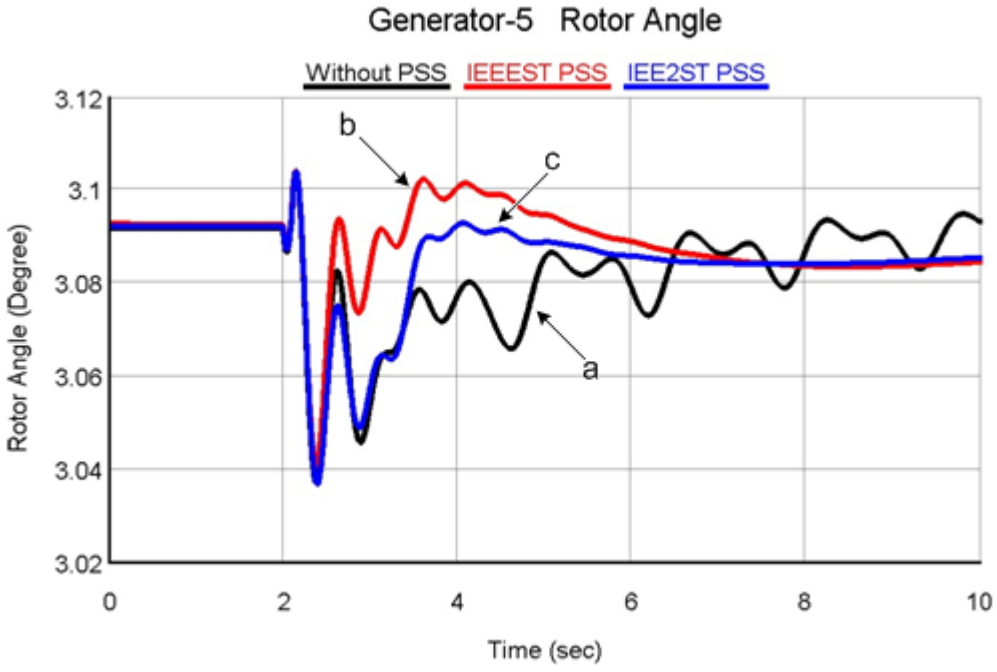

Figure 6.50: RTDS response of rotor angle at generator-5 under three-phase six-cycle fault at t=0sec (a) Without PSS (b)With IEEEST type single input PSS and (c) With IEE2ST type multi-input PSS

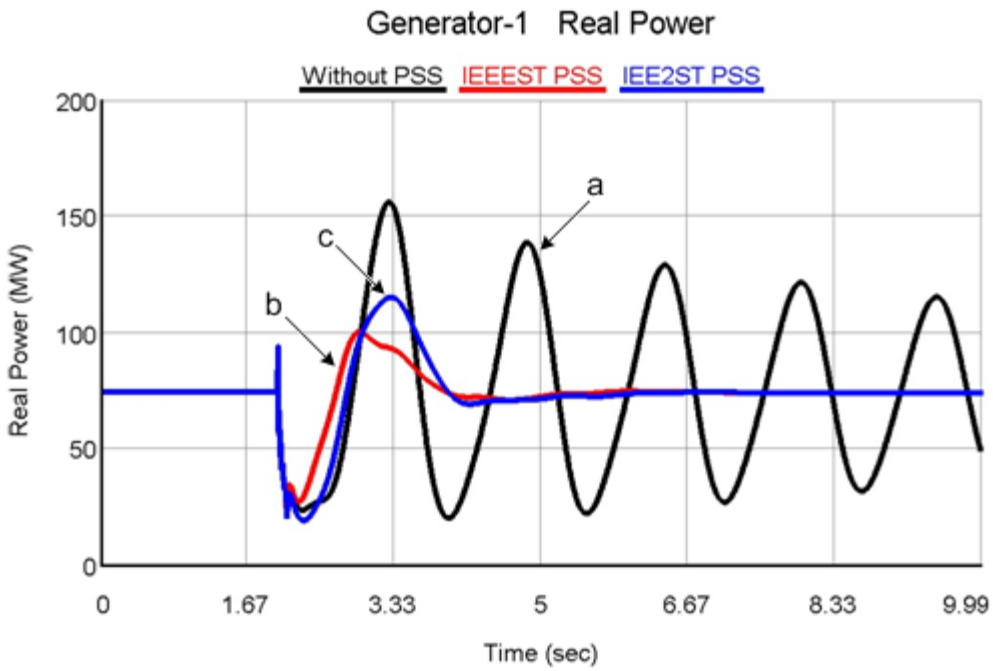

Figure 6.51: RTDS response of real power at generator-1 under three-phase six-cycle fault at t=0sec (a) Without PSS (b)With IEEEST type single input PSS and (c) With IEE2ST type multi-input PSS

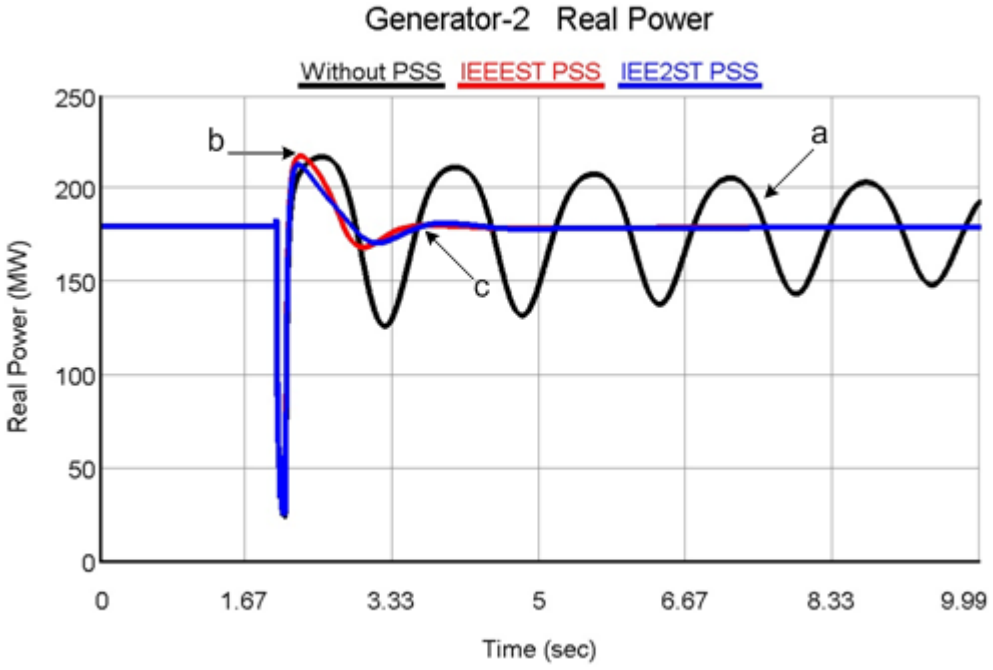

Figure 6.52: RTDS response of real power at generator-2 under three-phase six-cycle fault at t=0sec (a) Without PSS (b)With IEEEST type single input PSS and (c) With IEE2ST type multi-input PSS

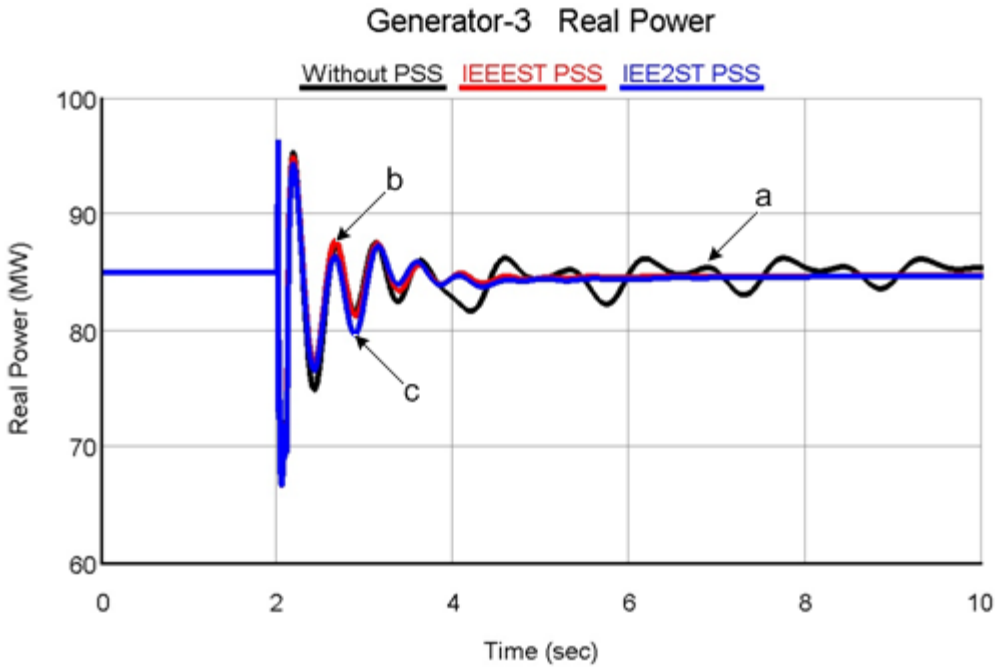

Figure 6.53: RTDS response of real power at generator-3 under three-phase six-cycle fault at t=0sec (a) Without PSS (b)With IEEEST type single input PSS and (c) With IEE2ST type multi-input PSS

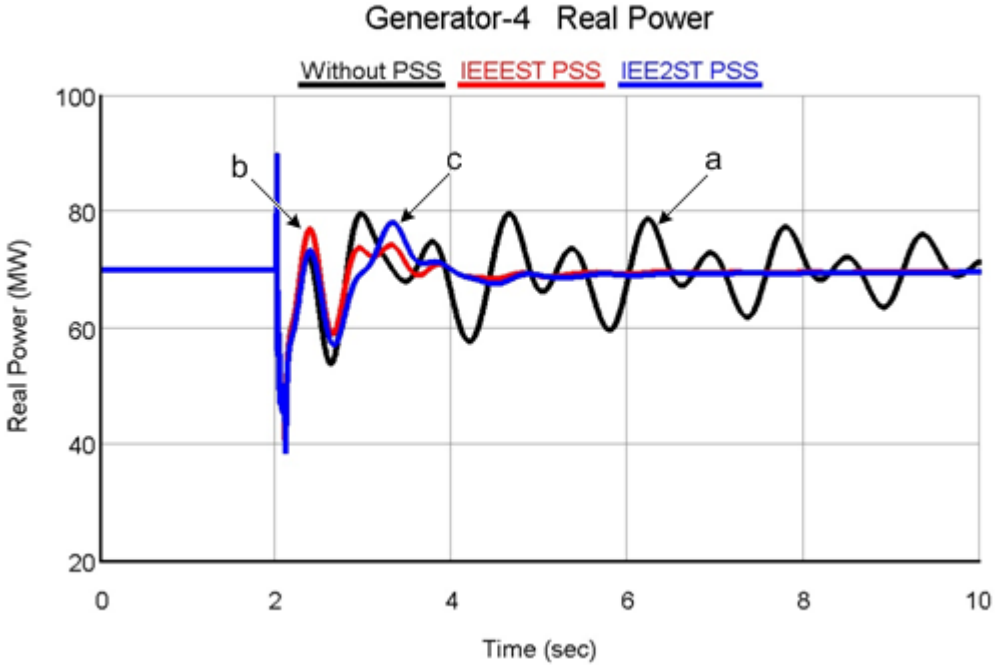

Figure 6.54: RTDS response of real power at generator-4 under three-phase six-cycle fault at t=0sec (a) Without PSS (b)With IEEEST type single input PSS and (c) With IEE2ST type multi-input PSS

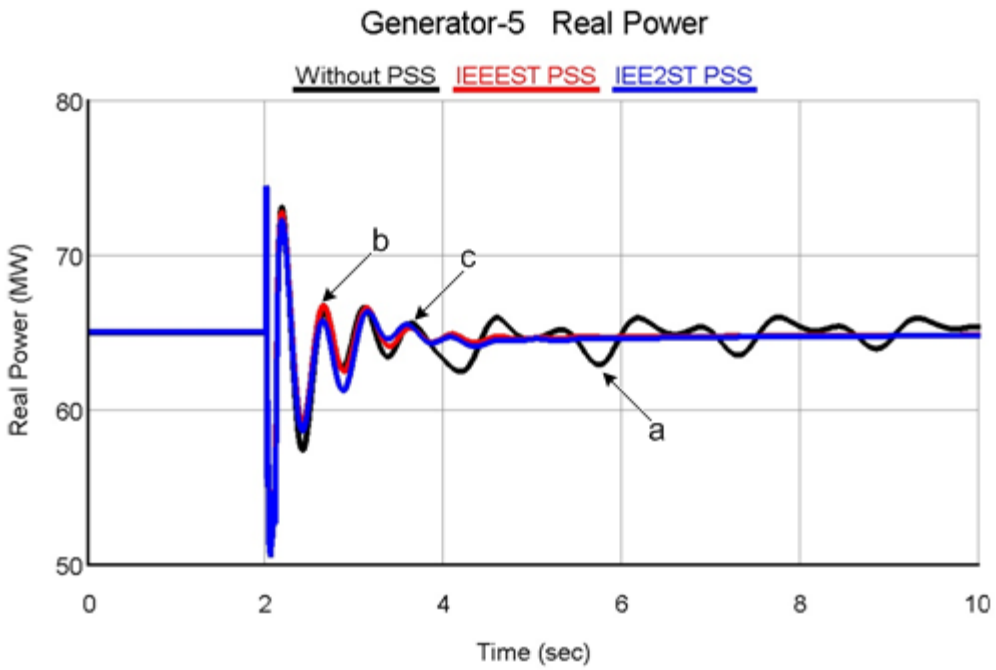

Figure 6.55: RTDS response of real power at generator-5 under three-phase six-cycle fault at t=0sec (a) Without PSS (b)With IEEEST type single input PSS and (c) With IEE2ST type multi-input PSS

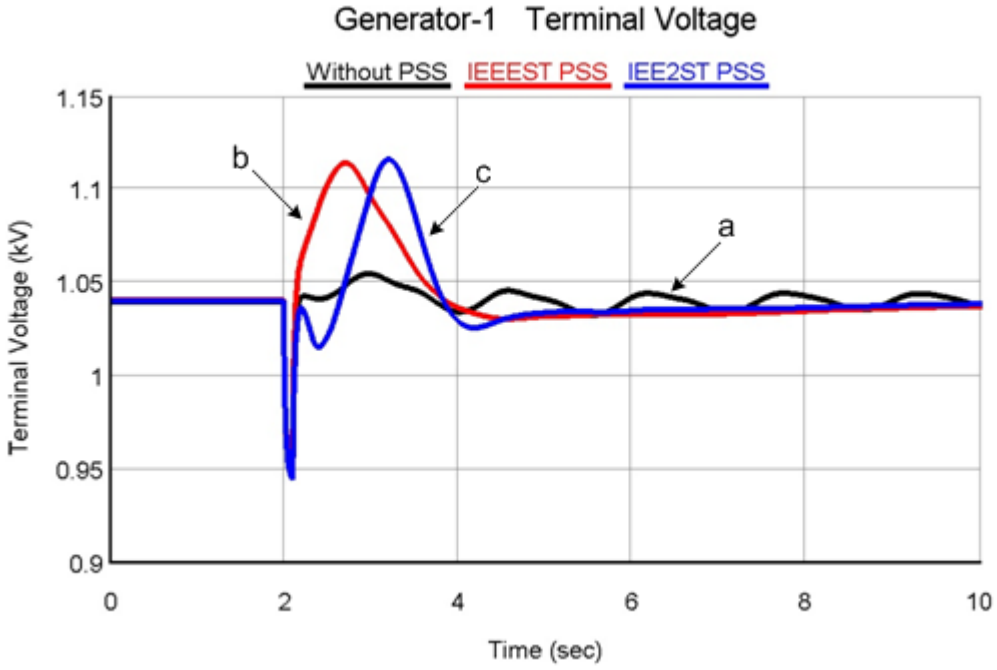

Figure 6.56: RTDS response of terminal voltage at generator-1 under three-phase six-cycle fault at t=0sec (a) Without PSS (b)With IEEEST type single input PSS and (c) With IEE2ST type multi-input PSS

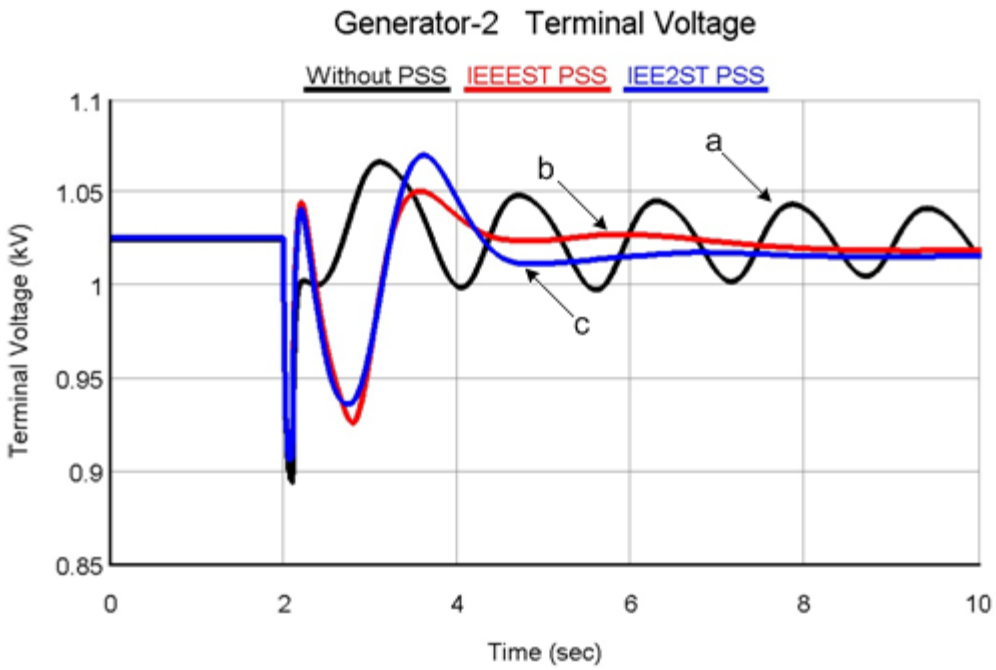

Figure 6.57: RTDS response of terminal voltage at generator-2 under three-phase six-cycle fault at t=0sec (a) Without PSS (b)With IEEEST type single input PSS and (c) With IEE2ST type multi-input PSS

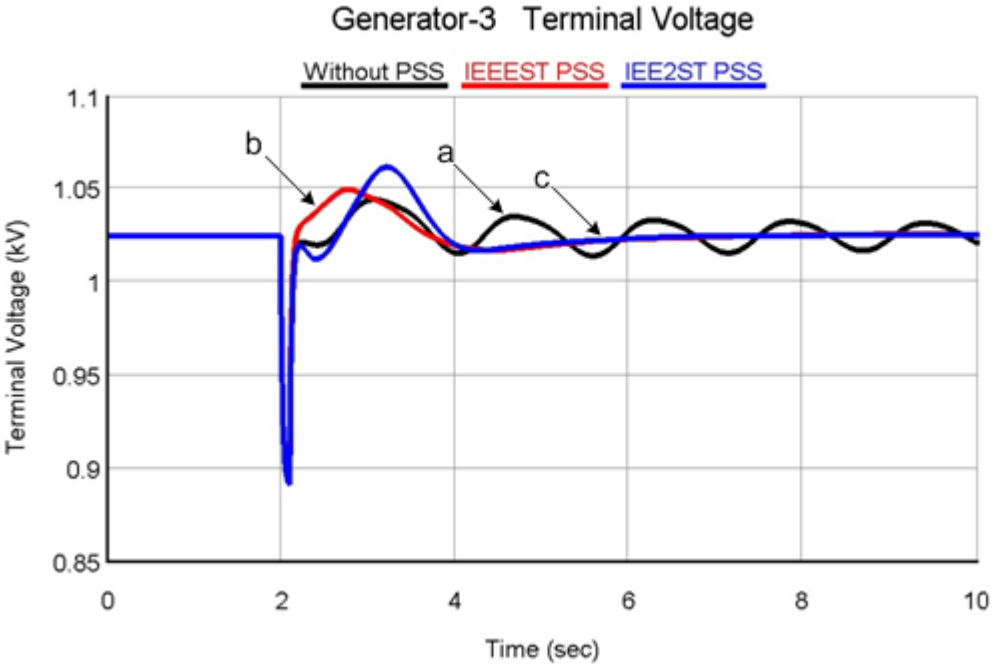

Figure 6.58: RTDS response of terminal voltage at generator-3 under three-phase six-cycle fault at t=0sec (a) Without PSS (b)With IEEEST type single input PSS and (c) With IEE2ST type multi-input PSS

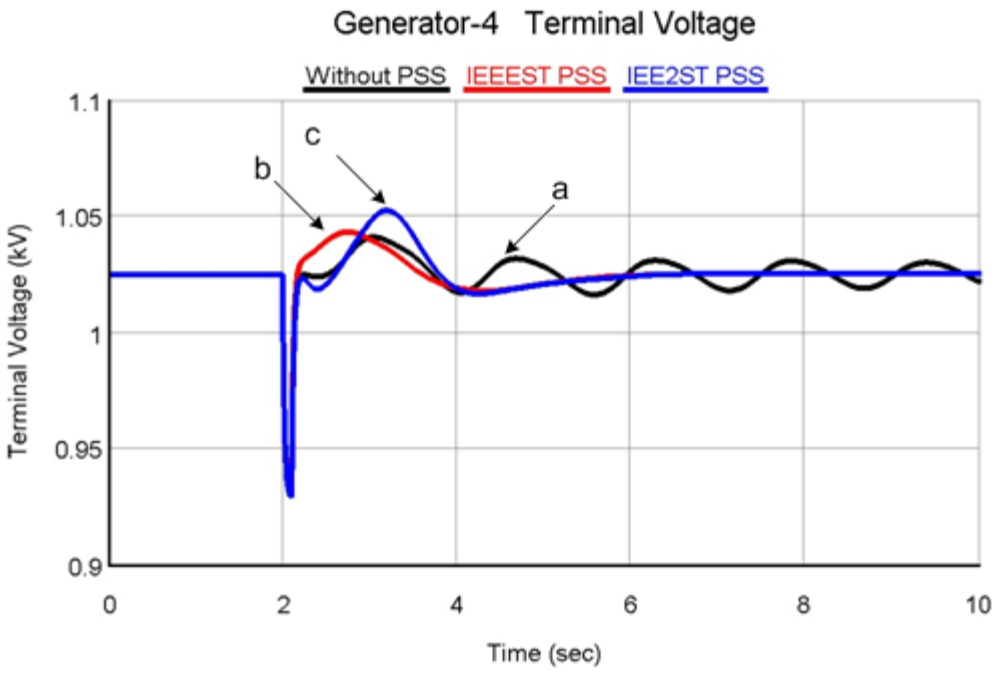

Figure 6.59: RTDS response of terminal voltage at generator-4 under three-phase six-cycle fault at t=0sec (a) Without PSS (b)With IEEEST type single input PSS and (c) With IEE2ST type multi-input PSS

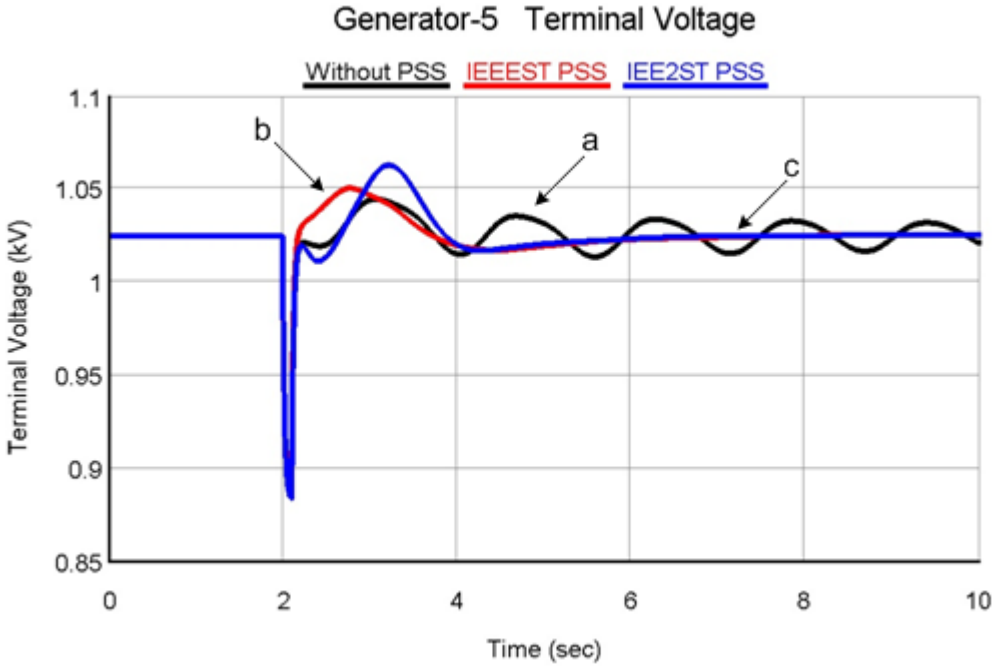

Figure 6.60: RTDS response of terminal voltage at generator-5 under three-phase six-cycle fault at t=0sec (a) Without PSS (b)With IEEEST type single input PSS and (c) With IEE2ST type multi-input PSS

6.2.6 Comparison of Simulated and RTDS results for test case 2

Comparing simulated and RTDS results it obvious that the responses are following the same pattern. The simulated results of rotor speed, rotor angle and real power are very much near to simulated and RTDS results. The voltage curves are within the limits of 5% regulation. However, RTDS result takes relatively more time, about 0.5sec to 1sec. This is because, RTDS is a real-time practical application, it considers the environmental effects like temperature and electromagnetic field produced by the transmission lines, transformers etc. and the sub-transient reactances and time constants for generators. RTDS works on higher order model of power system. Also it took some processing time for every block used. While in Matlab all the above parameter are usually not considered.

6.3 Development of Backup Damping Controller

To make the proposed model very near to the real scenario, A supervisory control backup is also considered as a backup protection for the proposed system. A worst scenario is considered with a three-phase 30-cycles fault, without any protection and damping control. The system oscillations start increasing and going towards the system collapse. Then there should be some backup loop for supervisory control.

In real system, the generator isolation relays activated if frequency goes beyond 60Hz $\pm$ 2.5Hz (or 360~392 radians per second). So the proposed backup control is designed to be activated before generators are isolated, i.e. 61.5Hz (or 385 radians per second). Based on the frequency sensitivity of the system, the backup control is developed such that whenever the rotor speed crosses 61.5Hz or 385 rad/sec, braking resistor will come into action and start damping the oscillations, and protect the system

from total collapse.

This scenario is shown in graphical form, where Fig. 6.61 represents the rotor speed of the 3-machine 9-bus system under the said fault conditions without any protection and damping control. The rotor speed transients for generator 2 and 3 reaches 395 and 408 rad/sec respectively, within 2 seconds. Fig 6.62 represents the supervisory controlled system, keeping the rotor speed of 3-machine 9-bus system in a safe region avoiding system collapse due to 30-cyle three-phase fault. A braking resistor of 10% rated power of overall system, 56 mega-joules is installed near to the tie line at Bus 7. The total amount of energy taken up by the brake is not large, only for the transients, but it is enough to slow the generator so that the normal turbine/governor and excitation controls can take effect. And the rotor speed transients for generator 2 and 3 are with a peak value of 385 and 388 rad/sec within 1.2 seconds. Fig. 6.63 represents the switching action of braking resistor such that if the transients go beyond a preset limit of 385 radian/sec it will activate the braking resistor keeping the system in a safe region. Results show that backup supervisory control, significantly damps the transients, maintaining system stability without generators isolation.

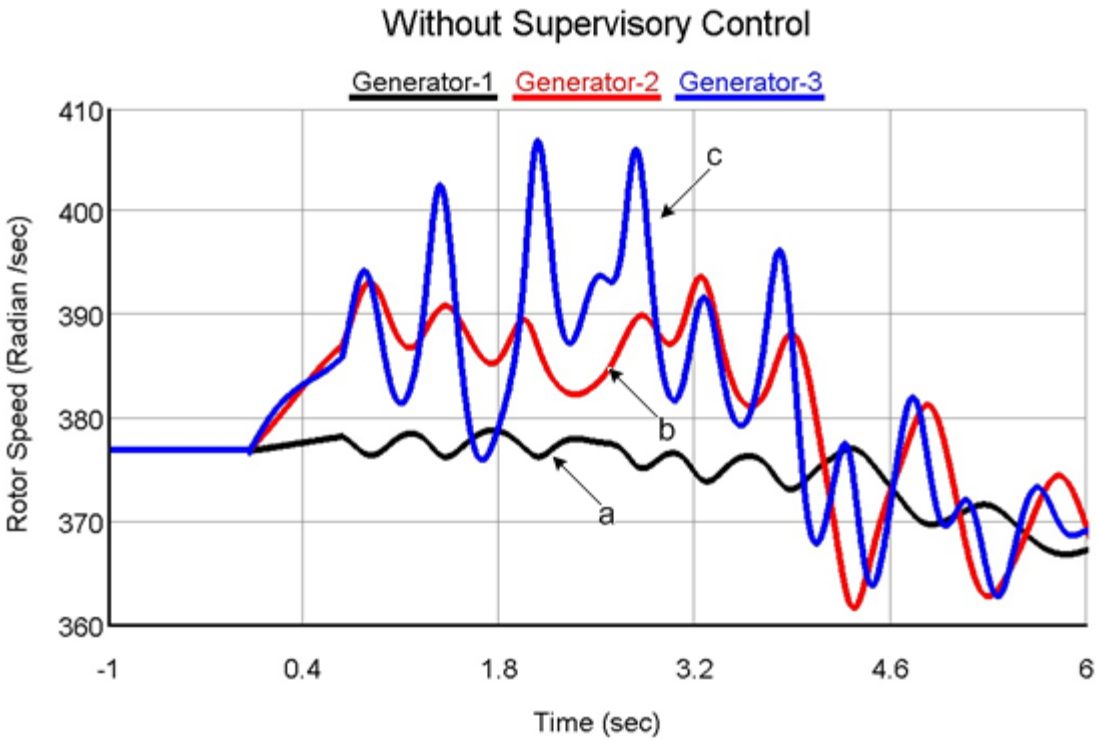

Figure 6.61: Rotor speed response of 3-Machine 9-Bus system for three-phase 30-cycle fault at t=0sec without supervisory control (a) Generator 1 (b) Generator 2 and (c) Generator 3

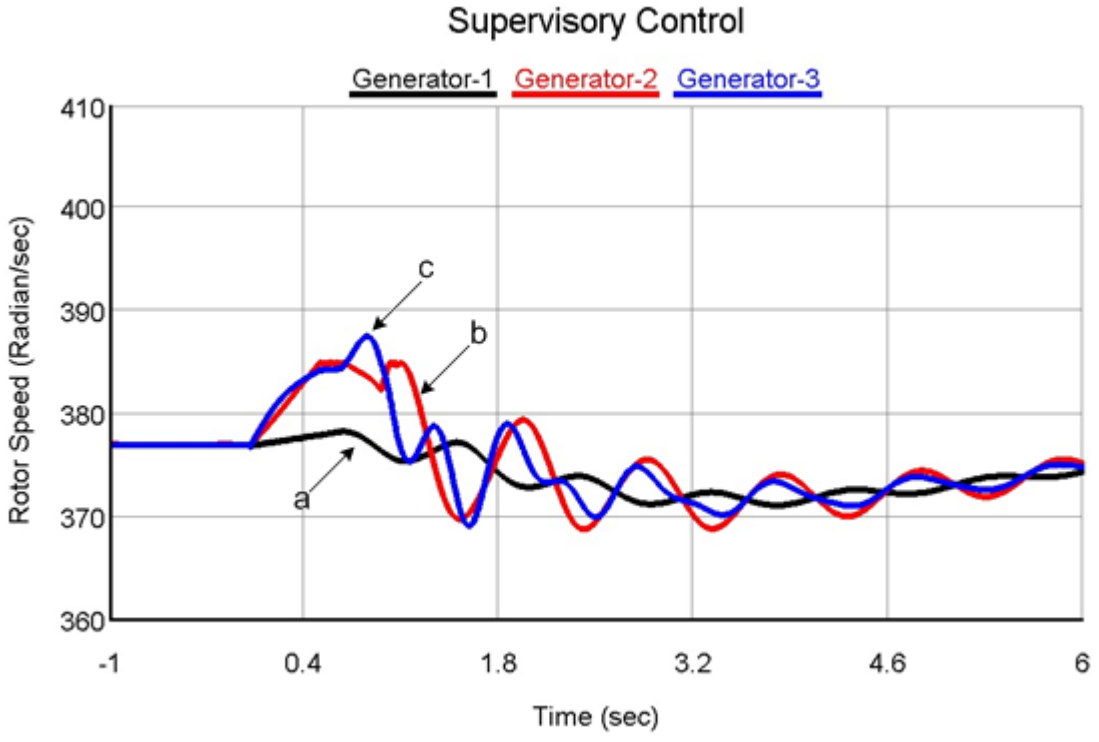

Figure 6.62: Rotor speed response of 3-Machine 9-Bus system for three-phase 30-cycle fault at t=0sec with supervisory control (a) Generator 1 (b) Generator 2 and (c) Generator 3

Figure 6.63: Braking resistor control response of 3-Machine 9-Bus system for three-phase 30-cycle fault at t=0sec with supervisory control

CHAPTER 7

CONCLUSION AND FUTURE WORK

7.1 Conclusion

Power system stability enhancement through wide area measurements is presented in this thesis. Low frequency inter-area oscillations are of main concern for wide area power system. System stability can be enhanced by using modern type of PSS controllers integrated with PMUs. IEE2ST PSS controller is used in combination with PMUs to damp out inter-area modes. A supervisory control strategy, as a backup protection, is developed for the designed system. The proposed system is designed, tested and validated on RTDS.

Single input IEEEST and multi input IEE2ST type PSS integrated with PMU are used to damp the inter-area oscillations. IEEEST type PSS input signal is limited to local measurements. However, IEE2ST type PSS integrated with PMU is based on local as

well as remote signals, providing greater visibility over a larger area of the network to efficiently damp the inter-area modes. For this purpose two multi machine power systems have been considered. Following is the summary of this thesis:

- Dual-input PSSs integrated with PMUs are used to damp out inter-area oscillations to a wide extent.
- PSSs are optimally placed by using participation factor for efficient damping and economic point of view.
- Gains and time constants of PSSs are optimized using differential evolution due to its simplicity and fast convergence.
- Eigenvalue analysis is performed regarding the stability characteristics of the system.
- Supervisory backup damping controller is considered as a backup protection using braking resistor.
- Experimental setup is build-up on RSCAD for real-time digital simulations.
- Simulations are carried out on Matlab and then compared with RTDS results it is observed that both follows the same pattern.
- Comparing local and wide-area PSSs, it has been clearly shown that the coordinated design of IEE2ST PSSs integrated with PMU outperforms the individual design of these stabilizers.

This work is a contribution in power system stability enhancement through wide area measurements that had not been previously addressed. The proposed

inter area IEE2ST PSS integrated with PMU constitute a systematic and powerful approach to simultaneously improve the inter area oscillations damping and achieve uninterrupted power flow on long tie lines.

7.2 Future Work

There are several issues that are still to be addressed in the thesis subject:

- The successful implementation of the proposed approach is carried out on the test system. It is considered to be worth mentioning to implement this work on real-life systems e.g. Saudi grid and GCC grid to validate this research.
- FACTS installed on the substations are playing an important role in stability of power system. It is worth to investigate the PMUs integrated with FACTS devices to enhance the system stability.
- In this work latency of communication of PMU that can affect the efficiency of stabilizer that has been neglected. Therefore, communication time delay and data loss should be explored.
- We have developed supervisory control for high frequency oscillations, under low frequency conditions; priority load shedding should be investigated.

APPENDICES

Appendix A : GENERATOR DATA AND LINEARIZATION

A.1 3-Machine 9-Bus System Data

The generator and exciter data of the three-machine nine-bus power system is shown in Table A.1:

Table A. 1: 3-Machine 9-Bus System Generator and exciter data

Generator	**1**	**2**	**3**
H (sec)	23.64	6.40	3.01
D	0.0	0.0	0.0
x_d ***(pu)***	0.146	0.8958	1.3125
x'_d ***(pu)***	0.0608	0.1198	0.1813
x_q ***(pu)***	0.0969	0.1969	0.25
$T_{do}^{'}$ ***(sec)***	8.96	6.00	5.89
K_A	100	100	100
T_A ***(sec)***	0.05	0.05	0.05S

A.2 5-Machine 14-Bus System Data

The generator and exciter data of the five-machine fourteen-bus power system is shown in Table A.2:

Table A. 2: 5-Machine 14-Bus System Generator Data

Generator	**1**	**2,4**	**3,5**
MW	247.5	192	128
KV	16.5	18	13.8
H	23.64	6.4	3
D	0.25	0.12	0.23
x_d ***(pu)***	0.146	0.896	1.31
x'_d ***(pu)***	0.061	0.12	0.18
x_q ***(pu)***	0.097	0.197	1.26
$T_{do}^{'}$	8.96	6	5.89
K_A	200	200	200
T_A	0.02	0.05	0.02
xa(pu)	0.083	0.1	0.74
xq'(pu)	0.23	0.197	0.25
Ra(pu)	0.002	0.002	0
Tqo'	0.002	0.535	0.6

A.3 SMIB Initial Conditions Calculation

In SMIB the d-q axis voltages can be written as,

$$V_t = V_d + jV_q \tag{A. 1}$$

$$i = i_d + ji_q \tag{A. 2}$$

The torque angle δ is defined as shown in Phasor diagram. Hence,

$$V_\infty = V_{\infty d} + jV_{\infty q} = V_\infty(\sin\delta + j\cos\delta) \quad \text{(A. 3)}$$

$$\delta = \angle(e_q^{'}, V_\infty) \quad \text{(A. 4)}$$

For convenience, the following constants and parameters are introduced.

$$1 + ZY = C_1 + jC_2 \quad \text{(A. 5)}$$

$$C_1 = 1 + RG - XB \quad \text{(A. 6)}$$

$$C_2 = RB + XG \quad \text{(A. 7)}$$

$$R_1 = R - C_2 X'_d \quad \text{(A. 8)}$$

$$R_2 = R - C_2 X_q \quad \text{(A. 9)}$$

$$X_1 = X + C_1 X_q \quad \text{(A. 10)}$$

$$X_2 = X + C_1 X'_d \quad \text{(A. 11)}$$

$$Z_{eq}{}^2 = R_1 R_2 + X_1 X_2 \quad \text{(A. 12)}$$

$$Y_d = \frac{C_1 X_1 - C_2 R_2}{Z_{eq}{}^2} \quad \text{(A. 13)}$$

$$Y_q = \frac{C_1 R_1 + C_2 X_2}{Z_{eq}{}^2} \quad \text{(A. 14)}$$

From the system shown in the Fig. 3.3 ,

$$i = YV_t + \frac{V_t - V_\infty}{Z} \quad \text{(A. 15)}$$

$$Zi = (1 + ZY)V_t - V_\infty \quad \text{(A. 16)}$$

Separating the last equation into real and imaginary parts, the results can be written in

matrix form as

$$\begin{bmatrix} R & -X \\ X & R \end{bmatrix}\begin{bmatrix} i_d \\ i_q \end{bmatrix}=\begin{bmatrix} C_1 & -C_2 \\ C_2 & C_1 \end{bmatrix}\begin{bmatrix} V_d \\ V_q \end{bmatrix}-V_\infty \begin{bmatrix} \sin\delta \\ \cos\delta \end{bmatrix} \tag{A. 17}$$

A.4 Linearization of constants K_1 to K_6

$$P_e = V_d i_d + V_q i_q \tag{A. 18}$$

$$V_d = i_q X_q \tag{A. 19}$$

$$V_q = e'_q - X'_d\, i_d \tag{A. 20}$$

$$\begin{bmatrix} R & -X \\ X & R \end{bmatrix}\begin{bmatrix} i_d \\ i_q \end{bmatrix}=\begin{bmatrix} C_1 & -C_2 \\ C_2 & C_1 \end{bmatrix}\begin{bmatrix} V_d \\ V_q \end{bmatrix}-V_\infty \begin{bmatrix} \sin\delta \\ \cos\delta \end{bmatrix} \tag{A. 21}$$

$$\begin{bmatrix} V_d \\ V_q \end{bmatrix}=\begin{bmatrix} 0 & X_q \\ X'_d & 0 \end{bmatrix}\begin{bmatrix} i_d \\ i_q \end{bmatrix}+\begin{bmatrix} 0 \\ 1 \end{bmatrix} e'_q \tag{A. 22}$$

$$\begin{bmatrix} R & -X \\ X & R \end{bmatrix}\begin{bmatrix} i_d \\ i_q \end{bmatrix}=\begin{bmatrix} C_1 & -C_2 \\ C_2 & C_1 \end{bmatrix}\left\{\begin{bmatrix} 0 & X_q \\ X'_d & 0 \end{bmatrix}\begin{bmatrix} i_d \\ i_q \end{bmatrix}+\begin{bmatrix} 0 \\ 1 \end{bmatrix} e'_q\right\}-V_\infty \begin{bmatrix} \sin\delta \\ \cos\delta \end{bmatrix} \tag{A. 23}$$

Now,

$$\begin{bmatrix} R-C_2X'_d & -X-C_1X_q \\ X+C_1X'_d & R-C_2X_q \end{bmatrix}\begin{bmatrix} i_d \\ i_q \end{bmatrix}=\begin{bmatrix} -C_2 \\ C_1 \end{bmatrix} e'_q - V_\infty \begin{bmatrix} \sin\delta \\ \cos\delta \end{bmatrix} \tag{A. 24}$$

$$\begin{bmatrix} i_d \\ i_q \end{bmatrix}=\begin{bmatrix} Y_d \\ Y_q \end{bmatrix} e'_q - \frac{V_\infty}{Z^2_{eq}}\begin{bmatrix} R_2 & X_1 \\ -X_2 & R_1 \end{bmatrix}\begin{bmatrix} \sin\delta \\ \cos\delta \end{bmatrix} \tag{A. 25}$$

$$\begin{bmatrix} \Delta i_d \\ \Delta i_q \end{bmatrix}=\begin{bmatrix} Y_d \\ Y_q \end{bmatrix} \Delta e'_q - \frac{V_\infty}{Z^2_{eq}}\begin{bmatrix} R_2 & X_1 \\ -X_2 & R_1 \end{bmatrix}\begin{bmatrix} \sin(\delta+\Delta\delta) \\ \cos(\delta+\Delta\delta) \end{bmatrix} \tag{A. 26}$$

Linearize,

Since $\Delta\delta$ is very small

$$\begin{cases}\sin(\delta+\Delta\delta)=\sin\delta+\Delta\delta\cos\delta\\ \cos(\delta+\Delta\delta)=\cos\delta-\Delta\delta\sin\delta\end{cases} \tag{A. 27}$$

$$\begin{cases}\sin\Delta\delta\approx 0\approx\Delta\delta\\ \cos\Delta\delta\approx 1\end{cases} \tag{A. 28}$$

So,

$$\begin{bmatrix}\Delta i_d\\ \Delta i_q\end{bmatrix}=\begin{bmatrix}Y_d\\ Y_q\end{bmatrix}\Delta e'_q-\frac{V_\infty}{Z_{eq}}\begin{bmatrix}R_2 & X_1\\ -X_2 & R_1\end{bmatrix}\begin{bmatrix}\sin\delta+\Delta\delta\cos\delta\\ \cos\delta-\Delta\delta\sin\delta\end{bmatrix} \tag{A. 29}$$

$$\begin{bmatrix}\Delta i_d\\ \Delta i_q\end{bmatrix}=\begin{bmatrix}Y_d\\ Y_q\end{bmatrix}\Delta e'_q-\frac{V_\infty}{Z_{eq}}\begin{bmatrix}R_2(\sin\delta+\Delta\delta\cos\delta) & X_1(\cos\delta-\Delta\delta\sin\delta)\\ -X_2(\sin\delta+\Delta\delta\cos\delta) & R_1(\cos\delta-\Delta\delta\sin\delta)\end{bmatrix} \tag{A. 30}$$

$$\begin{bmatrix}\Delta i_d\\ \Delta i_q\end{bmatrix}=\begin{bmatrix}Y_d\\ Y_q\end{bmatrix}\Delta e'_q+\begin{bmatrix}F_d\\ F_q\end{bmatrix}\Delta\delta \tag{A. 31}$$

Where,

$$Y_d=\frac{C_1X_1-C_2R_2}{Z^2_{eq}} \tag{A. 32}$$

$$Y_q=\frac{C_1R_1+C_2X_2}{Z^2_{eq}} \tag{A. 33}$$

$$F_d=\frac{V_\infty}{Z^2_{eq}}(X_1\sin\delta_0-R_2\cos\delta_0) \tag{A. 34}$$

$$F_q=\frac{V_\infty}{Z^2_{eq}}(R_1\sin\delta_0+X_2\cos\delta_0) \tag{A. 35}$$

$$\begin{bmatrix}F_d\\ F_q\end{bmatrix}=\frac{V_\infty}{Z^2_{eq}}\begin{bmatrix}-R_2 & X_1\\ X_2 & R_1\end{bmatrix}\begin{bmatrix}\cos\delta_0\\ \sin\delta_0\end{bmatrix} \tag{A. 36}$$

Derivation of K_1 and K_2 (Electrical Torque)

$$P = VI \tag{A. 37}$$

$$T_e = P_e = V \cdot I = V_d i_d + V_q i_q \tag{A. 38}$$

$$\begin{cases} P_e = V_d i_d + V_q i_q \\ V_d = i_q X_q \\ V_q = e'_q - X'_d i_d \end{cases} \tag{A. 39}$$

$$T_e = (i_q X_q) i_d + (e'_q - X'_d i_d) i_q \tag{A. 40}$$

$$T_e = i_q X_q i_d + e'_q i_q - X'_d i_d i_q \tag{A. 41}$$

$$T_e = e'_q i_q + (X_q - X'_d) i_q i_d \tag{A. 42}$$

Linerizing,

$$\Delta T_e = \Delta e'_q i_q + e'_q \Delta i_q + (X_q - X'_d)\Delta i_q i_d + (X_q - X'_d) i_q \Delta i_d \tag{A. 43}$$

$$\begin{cases} \begin{bmatrix} \Delta i_d \\ \Delta i_q \end{bmatrix} = \begin{bmatrix} Y_d \\ Y_q \end{bmatrix} \Delta e'_q + \begin{bmatrix} F_d \\ F_q \end{bmatrix} \Delta\delta \end{cases} \rightarrow \begin{cases} \Delta i_d = Y_d \Delta e'_q + F_d \Delta\delta \\ \Delta i_q = Y_q \Delta e'_q + F_q \Delta\delta \end{cases} \tag{A. 44}$$

$$\begin{aligned} \Delta T_e = {} & \Delta e'_q i_q + e'_q (Y_d \Delta e'_q + F_q \Delta\delta) + (X_q - X'_d)(Y_q \Delta e'_q + F_q \Delta\delta) i_d \\ & + (X_q - X'_d) i_q (Y_d \Delta e'_q + F_d \Delta\delta) \end{aligned} \tag{A. 45}$$

$$\begin{aligned} \Delta T_e = {} & \Delta e'_q [i_q + e'_q Y_d + (X_q - X'_d) i_d Y_q + (X_q - X'_d) i_q Y_d] \\ & + \Delta\delta [e'_q F_q + (X_q - X'_d) i_d F_q + (X_q - X'_d) i_q F_d] \end{aligned} \tag{A. 46}$$

$$\begin{bmatrix} K_1 \\ K_2 \end{bmatrix} = \begin{bmatrix} 0 \\ i_q \end{bmatrix} e'_q + \begin{bmatrix} F_d & F_q \\ Y_d & Y_q \end{bmatrix} \begin{bmatrix} (X_q - X'_d) i_q \\ e'_q + (X_q - X'_d) i_d \end{bmatrix} \tag{A. 47}$$

Derivation of K_3 and K_4 (Electrical Torque)

The filed voltage equation is

$$\dot{e}'_q = \frac{1}{T'_{do}}[E_{FD} - e'_q - (X_d - X'_d)i_d] \quad \text{(A. 48)}$$

This equation can be rewritten as

$$T'_{do}\dot{e}'_q = [E_{FD} - e'_q - (X_d - X'_d)i_d] \quad \text{(A. 49)}$$

Linearize

$$T'_{do}\Delta\dot{e}'_q = [\Delta E_{FD} - \Delta e'_q - (X_d - X'_d)\Delta i_d] \quad \text{(A. 50)}$$

$$T'_{do}\Delta\dot{e}'_q = [\Delta E_{FD} - \Delta e'_q - (X_d - X'_d)\Delta i_d] \quad \text{(A. 51)}$$

$$T'_{do}\Delta s e'_q = [\Delta E_{FD} - \Delta e'_q - (X_d - X'_d)\Delta i_d] \quad \text{(A. 52)}$$

$$\therefore \Delta i_d = Y_d \Delta e'_q + F_d \Delta\delta \quad \text{(A. 53)}$$

$$T'_{do}\Delta s e'_q = \Delta E_{FD} - (X_d - X'_d)(Y_d \Delta e'_q + F_d \Delta\delta) \quad \text{(A. 54)}$$

$$\Delta e'_q + T'_d \Delta s e'_q + (X_d - X'_d)Y_d \Delta e'_q = \Delta E_{FD} - (X_d - X'_d)F_d \Delta\delta \quad \text{(A. 55)}$$

$$\Delta e'_q(1 + T'_d s + (X_d - X'_d)Y_d) = \Delta E_{FD} - (X_d - X'_d)F_d \Delta\delta \quad \text{(A. 56)}$$

$$\Delta e'_q\left[1 + (X_d - X'_d)Y_d\right]\left[1 + \frac{sT'_{do}}{1 + (X_d - X'_d)Y_d}\right] = \Delta E_{FD} - (X_d - X'_d)F_d \Delta\delta \quad \text{(A. 57)}$$

Let,

$$K_3 = \frac{1}{1+(X_d - X'_d)Y_d} \tag{A. 58}$$

$$K_4 = (X_d - X'_d)F_d \tag{A. 59}$$

So,

$$\Delta e'_q \frac{1}{K_3}\left[1+sT'_{do}K_3\right] = \Delta E_{FD} - K_4\Delta\delta \tag{A. 60}$$

$$\Delta e'_q \left[1+sT'_{do}K_3\right] = K_3\left[\Delta E_{FD} - K_4\Delta\delta\right] \tag{A. 61}$$

Derivation of K_5 and K_6 (Terminal Voltages)

$$V_t^2 = V_d^2 + V_q^2 \tag{A. 62}$$

Linearize,

$$2V_t \cdot \Delta V_t = 2V_d \cdot \Delta V_d + 2V_q \cdot \Delta V_q \tag{A. 63}$$

Then,

$$\Delta V_t = V_d \cdot \frac{\Delta V_d}{V_t} + V_q \cdot \frac{\Delta V_q}{V_t} \tag{A. 64}$$

Now,

$$V_d = i_q X_q \tag{A. 65}$$

$$V_d = i_q X_q \tag{A. 66}$$

Linearize,

$$\Delta V_d = X_q \Delta i_q \tag{A. 67}$$

$$V_q = \Delta e'_q - X'_d \Delta i_d \tag{A. 68}$$

Where,

$$\begin{cases} \Delta i_d = Y_d \Delta e'_q + F_d \Delta\delta \\ \Delta i_q = Y_q \Delta e'_q + F_q \Delta\delta \end{cases} \quad \text{(A. 69)}$$

So,

$$\Delta V_t = V_d \cdot \frac{X_q \Delta i_q}{V_t} + V_q \cdot \frac{\Delta e'_q - X'_d \Delta i_d}{V_t} \quad \text{(A. 70)}$$

$$\Delta V_t = V_d \cdot \frac{X_q (Y_q \Delta e'_q + F_q \Delta\delta)}{V_t} + V_q \cdot \frac{\Delta e'_q - X'_d (Y_d \Delta e'_q + F_d \Delta\delta)}{V_t} \quad \text{(A. 71)}$$

$$\Delta V_t = \Delta\delta \left[\frac{V_d}{V_t} X_q F_q - \frac{V_q}{V_t} X'_d F_d \right] + \Delta e'_q \left[\frac{V_d}{V_t} X_q Y_q + \frac{V_q}{V_t} - \frac{V_q}{V_t} X'_d Y_d \right] \quad \text{(A. 72)}$$

$$\Delta V_t = K_5 \Delta\delta + K_6 \Delta e'_q \quad \text{(A. 73)}$$

$$K_5 = \left[\frac{V_d}{V_t} X_q F_q - \frac{V_q}{V_t} X'_d F_d \right] \quad \text{(A. 74)}$$

$$K_6 = \left[\frac{V_d}{V_t} X_q Y_q + \frac{V_q}{V_t} - \frac{V_q}{V_t} X'_d Y_d \right] \quad \text{(A. 75)}$$

$$\begin{bmatrix} K_5 \\ K_6 \end{bmatrix} = \begin{bmatrix} 0 \\ \frac{V_q}{V_t} \end{bmatrix} + \begin{bmatrix} F_d & F_q \\ Y_d & Y_q \end{bmatrix} \begin{bmatrix} -\frac{V_q}{V_t} X'_d \\ \frac{V_d}{V_t} X_q \end{bmatrix} \quad \text{(A. 76)}$$

A.5 State Equations for Linearized SMIB model

From Philips Heffron block diagram Fig. 3.2,

$$\Delta\delta = \frac{\omega_b}{s} \Delta\omega \quad \text{(A. 77)}$$

$$s\Delta\delta = \omega_b \Delta\omega \quad \text{(A. 78)}$$

$$\Delta\dot{\delta} = \omega_b \Delta\omega \tag{A. 79}$$

$$\Delta\omega = \left[\frac{1}{D+sM}\right]\left[-K_1\Delta\delta - K_2\Delta e'_q\right] \tag{A. 80}$$

$$D\Delta\omega + sM\Delta\omega = \left[-K_1\Delta\delta - K_2\Delta e'_q\right] \tag{A. 81}$$

$$\Delta\dot{\omega} = -\frac{K_1}{M}\Delta\delta - \frac{D}{M}\Delta\omega - \frac{K_2}{M}\Delta e'_q \tag{A. 82}$$

$$\Delta E_{fd} = \left[\frac{K_A}{1+sT_A}\right]\left[U_{PSS} - K_5\Delta\delta - K_6\Delta e'_q\right] \tag{A. 83}$$

$$\Delta E_{fd} + s\Delta E_{fd}T_A = K_A\left[U_{PSS} - K_5\Delta\delta - K_6\Delta e'_q\right] \tag{A. 84}$$

$$\Delta\dot{E}_{fd} = -\frac{K_A K_5}{T_A}\Delta\delta - \frac{1}{T_A}\Delta E_{fd} - \frac{K_A K_6}{T_A}\Delta e'_q + \frac{K_A}{T_A}U_{PSS} \tag{A. 85}$$

$$\Delta e'_q = \left[\frac{K_3}{1+sT'_{do}K_3}\right]\left[-K_4\Delta\delta + \Delta E_{fd}\right] \tag{A. 86}$$

$$\Delta e'_q + T'_{do}K_3 s\Delta e'_q = -K_3K_4\Delta\delta + K_3\Delta E_{fd} \tag{A. 87}$$

$$\Delta\dot{e}'_q = -\frac{K_4}{T'_{do}}\Delta\delta + \frac{1}{T'_{do}}\Delta E_{fd} - \frac{1}{K_3T'_{do}}\Delta e'_q \tag{A. 88}$$

For the system with the supplementary excitation control UPSS, the system equations may be written as

$$\dot{X} = AX + BU_{PSS} \tag{A. 89}$$

We can write all these equations in a matrix form,

$$\begin{bmatrix} \Delta\dot{\delta} \\ \Delta\dot{\omega} \\ \Delta\dot{e}'_q \\ \Delta\dot{E}_{fd} \end{bmatrix} = \begin{bmatrix} 0 & \omega_b & 0 & 0 \\ -\frac{K_1}{M} & -\frac{D}{M} & -\frac{K_2}{M} & 0 \\ -\frac{K_4}{T'_{do}} & 0 & -\frac{1}{K_3 T'_{do}} & \frac{1}{T'_{do}} \\ -\frac{K_A K_5}{T_A} & 0 & -\frac{K_A K_6}{T_A} & -\frac{1}{T_A} \end{bmatrix} \begin{bmatrix} \Delta\delta \\ \Delta\omega \\ \Delta e'_q \\ \Delta E_{fd} \end{bmatrix} + \begin{bmatrix} 0 \\ 0 \\ 0 \\ \frac{K_A}{T_A} \end{bmatrix} U_{PSS} \qquad \text{(A. 90)}$$

A.6 Multimachine Power System Nonlinear Model

The multimachine nonlinear model can be described by the following set of differential equations[99], in all that follows i=1, 2, …, n:

$$\dot{\delta}_i = \omega_b(\omega_i - 1) \qquad \text{(A. 91)}$$

$$\dot{\omega}_i = (P_{mi} - P_{ei} - D_i(\omega_i - 1))/M_i \qquad \text{(A. 92)}$$

$$\dot{E}'_{qi} = (E_{fdi} - (x_{di} - x'_{di})i_{di} - E'_{qi})/T'_{doi} \qquad \text{(A. 93)}$$

$$\dot{E}_{fdi} = (K_{Ai}(V_{refi} - v_i + u_{PSSi}) - E_{fdi})/T_{Ai} \qquad \text{(A. 94)}$$

where,

$$P_{ei} = v_{di}i_{di} + v_{qi}i_{qi} \qquad \text{(A. 95)}$$

$$v_{di} = x_{qi}i_{qi},\ v_{qi} = E'_{qi} - x'_{di}i_{di} \qquad \text{(A. 96)}$$

$$v_i = (v_{di}^2 + v_{qi}^2)^{1/2} \qquad \text{(A. 97)}$$

Also,

$$I = YV \qquad \text{(A. 98)}$$

where,

$$I_i = (i_d + ji_q)e^{j(\delta_i - \frac{\pi}{2})} \quad \text{(A. 99)}$$

$$V_i = (v_d + jv_q)e^{j(\delta_i - \frac{\pi}{2})} \quad \text{(A. 100)}$$

$$Y_{ij} = y_{ij}e^{j\beta_{ij}} \quad \text{(A. 101)}$$

It is worth emphasizing that the capitalized variables I (n x 1), V (n x 1), and Y (n x n) represent complex quantities. Using (3.44)-(3.47) as well as (3.42) and (3.43), i_{di} and i_{qi} can be expressed as

$$i_{di} = \sum_{j=1}^{n} y_{ij}[x_{qj}i_{qj}C_{ij} - (E'_{qj} - x'_{dj}i_{dj})S_{ij}] \quad \text{(A. 102)}$$

$$i_{qi} = \sum_{j=1}^{n} y_{ij}[x_{qj}i_{qj}S_{ij} + (E'_{qj} - x'_{dj}i_{dj})C_{ij}] \quad \text{(A. 103)}$$

where

$$C_{ij} = \cos(\beta_{ij} + \delta_j - \delta_i) \quad \text{(A. 104)}$$

$$S_{ij} = \sin(\beta_{ij} + \delta_j - \delta_i) \quad \text{(A. 105)}$$

A.7 Multimachine System Linearized Model

Linearizing (3.48) yields

$$L_d\Delta i_d = P_d\Delta\delta + Q_d\Delta E'_q + M_d\Delta i_q \quad \text{(A. 106)}$$

Where

$$P_{dij} = -y_{ij}[x_{qj}i_{qj}S_{ij} + (E'_{qj} - x'_{dj}i_{dj})C_{ij}], \quad j \neq i \quad \text{(A. 107)}$$

$$P_{dii} = -\sum_{\substack{j=1 \\ j\neq i}}^{n} P_{dij} \quad \text{(A. 108)}$$

$$Q_{dij} = -y_{ij} S_{ij}, \quad j = 1, 2, ..., n \tag{A. 109}$$

$$M_{dij} = y_{ij} x_{qj} C_{ij}, \qquad j = 1, 2, ..., n \tag{A. 110}$$

$$L_{dij} = -y_{ij} x_{dj}^{'} S_{ij}, \qquad j \neq i \tag{A. 111}$$

$$L_{dij} = 1 - y_{ii} x_{di}^{'} S_{ii} \tag{A. 112}$$

Similarly, linearizing (3.49) yields

$$L_q \Delta i_q = P_q \Delta\delta + Q_q \Delta E_q^{'} + M_q \Delta i_d \tag{A. 113}$$

where,

$$P_{qij} = y_{ij}[x_{qj} i_{qj} C_{ij} - (E_{qj}^{'} - x_{dj}^{'} i_{dj}) S_{ij}], \qquad j \neq i \tag{A. 114}$$

$$P_{qii} = -\sum_{\substack{j=1 \\ j \neq i}}^{n} P_{qij} \tag{A. 115}$$

$$Q_{qij} = y_{ij} C_{ij}, \qquad j = 1, 2, ..., n \tag{A. 116}$$

$$M_{qij} = -y_{ij} x_{dj}^{'} C_{ij}, \qquad j = 1, 2, ..., n \tag{A. 117}$$

$$L_{qij} = -y_{ij} x_{qj} S_{ij}, \qquad j \neq i \tag{A. 118}$$

$$L_{qij} = 1 - y_{ii} x_{qi} S_{ii} \tag{A. 119}$$

Solving (3.52) and (3.59) simultaneously give

$$\Delta i_d = F_d \Delta\delta + Y_d \Delta E_q^{'} \tag{A. 120}$$

$$\Delta i_q = F_q \Delta\delta + Y_q \Delta E_q^{'} \tag{A. 121}$$

Where,

$$F_q = [L_q - M_q L_d^{-1} M_d]^{-1} . [P_q + M_q L_d^{-1} P_d] \tag{A. 122}$$

$$Y_q = [L_q - M_q L_d^{-1} M_d]^{-1} . [Q_q + M_q L_d^{-1} Q_d] \tag{A. 123}$$

$$F_d = L_d^{-1}[P_d + M_d F_q] \tag{A. 124}$$

$$Y_d = L_d^{-1}[Q_d + M_d Y_q] \tag{A. 125}$$

Solving (3.41)-(3.43), linearizing, and substituting for Δi_{di} and Δi_{qi} from (3.66) and (3.67) results in

$$\Delta P_e = K_1 \Delta\delta + K_2 \Delta E_q^{'} \tag{A. 126}$$

where,

$$K_1 = D_t F_d + Q_t F_q \tag{A. 127}$$

$$K_2 = I_q + D_t Y_d + Q_t Y_q \tag{A. 128}$$

$$K_1 = D_t F_d + Q_t F_q \tag{A. 129}$$

Also, linearizing (3.39) and substituting for Δi_{di} and Δi_{qi} from (3.41) and (3.43) yields

$$[I + sT_{d0}^{'} + (x_d - x_d^{'})Y_d]\Delta E_q^{'} = \Delta E_{fd} - (x_d - x_d^{'})F_d \Delta\delta \tag{A. 130}$$

For the ith machine, it can be written

$$[I + sT_{d0i}^{'} K_{3ii}]\Delta E_{qi}^{'} = K_{3ii}[\Delta E_{fdi} - \sum_{\substack{j=1 \\ j\neq i}}^{n} \frac{1}{K_{3ij}} \Delta E_{qj}^{'} - \sum_{j=1}^{n} K_{4ij} \Delta\delta_j] \tag{A. 131}$$

where,

$$K_{3ij} = [(x_{di} - x_{di}^{'})Y_{dij}]^{-1},\ j \neq i \tag{A. 132}$$

$$K_{3ii} = [1 + (x_{di} - x_{di}^{'})Y_{dii}]^{-1} \tag{A. 133}$$

$$K_{4ij} = (x_{di} - x_{di}^{'})F_{dij}, \quad j \neq i \tag{A. 134}$$

$$K_{4ii} = (x_{di} - x_{di}^{'})F_{dii} \tag{A. 135}$$

Moreover, linearizing (3.42) and (3.43) and solving for Δv

$$\Delta v = K_5 \Delta\delta + K_6 \Delta E_q^{'} \quad \text{(A. 136)}$$

where,

$$K_5 = D_v x_q F_q - Q_v x_d^{'} F_d \quad \text{(A. 137)}$$

$$K_6 = D_v x_q Y_q - Q_v x_d^{'} Y_d + Q_v \quad \text{(A. 138)}$$

$$D_v = v_0^{-1} v_{d0} \quad \text{(A. 139)}$$

$$Q_v = v_0^{-1} v_{q0} \quad \text{(A. 140)}$$

It should be noticed that v_0 and v_{d0} are diagonal matrices of the respective initial conditions.

Appendix B : STATE SPACE MODELING

B.1 State Space Model for SMIB model with Power System Stabilizers

From PSS block diagram Fig 3.we can write states equations of a controlled SMIB system.

$$x_5 = \Delta\omega \frac{sT_W}{1+sT_W} \tag{B. 1}$$

$$x_5 + T_W\, sx_5 = T_W\, s\Delta\omega \tag{B. 2}$$

$$\Delta\dot{x}_5 = \Delta\dot{\omega} - \frac{x_5}{T_W} \tag{B. 3}$$

$$\therefore \left\{ \Delta\dot{\omega} = -\frac{K_1\Delta\delta}{M} - \frac{K_2\Delta e'_q}{M} - \frac{D\Delta\omega}{M} \right. \tag{B. 4}$$

$$\Delta\dot{x}_5 = -\frac{K_1}{M}\Delta\delta - \frac{D}{M}\Delta\omega - \frac{K_2}{M}\Delta e'_q - \frac{1}{T_W}x_5 \tag{B. 5}$$

$$U_{PSS} = x_5 K_C \frac{(1+sT_1)}{(1+sT_2)} \tag{B. 6}$$

$$U_{PSS} + T_2 sU_{PSS} = x_5 K_C + K_C T_1 sx_5 \tag{B. 7}$$

$$\dot{U}_{PSS} = \frac{x_5 K_C}{T_2} - \frac{U_{PSS}}{T_2} + \frac{K_C T_1\, \Delta\dot{x}_5}{T_2} \tag{B. 8}$$

Put the value of $\Delta\dot{x}_5$

$$\dot{U}_{PSS} = \frac{x_5 K_C}{T_2} - \frac{U_{PSS}}{T_2} + \frac{K_C T_1}{T_2}\left[-\frac{K_1 \Delta\delta}{M} - \frac{K_2 \Delta e'_q}{M} - \frac{D\Delta\omega}{M} - \frac{x_5}{T_W} \right] \tag{B. 9}$$

$$\dot{U}_{PSS} = -\frac{K_1 K_C T_1}{T_2 M}\Delta\delta - \frac{D K_C T_1}{T_2 M}\Delta\omega - \frac{K_C K_2 T_1}{T_2 M}\Delta e'_q - \frac{K_C}{T_2}\left(1 - \frac{T_1}{T_W}\right)x_5 - \frac{1}{T_2}U_{PSS} \tag{B. 10}$$

The new state variable vector becomes,

$$\dot{W} = A_C W \tag{B. 11}$$

Where,

$$W = \left[\Delta\delta \;\; \Delta\omega \;\; \Delta e'_q \; \Delta E_{fd} \;\; x_5 \;\; U_{PSS}\right]^T \tag{B. 12}$$

and the controlled system matrix becomes

$$A_C = \begin{bmatrix} 0 & \omega_b & 0 & 0 & 0 & 0 \\ -\frac{K_1}{M} & -\frac{D}{M} & -\frac{K_2}{M} & 0 & 0 & 0 \\ -\frac{K_4}{T'_{do}} & 0 & -\frac{1}{K_3 T'_{do}} & \frac{1}{T'_{do}} & 0 & 0 \\ -\frac{K_A K_5}{T_A} & 0 & -\frac{K_A K_6}{T_A} & -\frac{1}{T_A} & 0 & \frac{K_A}{T_A} \\ -\frac{K_1}{M} & -\frac{D}{M} & -\frac{K_2}{M} & 0 & -\frac{1}{T_W} & 0 \\ -\frac{K_1 K_C T_1}{T_2 M} & -\frac{D K_C T_1}{T_2 M} & -\frac{K_C K_2 T_1}{T_2 M} & 0 & \frac{K_C}{T_2}\left(1 - \frac{T_1}{T_W}\right) & -\frac{1}{T_2} \end{bmatrix} \tag{B. 13}$$

B.2 State Space Model for IEEEST PSS Controller

From the IEEEST type PSS block diagram Fig. 3.6 we can write down the state space equations as follows

$$y_{16} = \frac{K_C s T_\omega}{1 + s T_\omega} \Delta\omega \tag{B. 14}$$

$$y_{16} + T_\omega \dot{y}_{16} = K_C T_\omega \dot{\Delta\omega} \tag{B. 15}$$

$$\dot{y}_{16} = K_C \dot{\Delta\omega} - \frac{y_{16}}{T_\omega} \tag{B. 16}$$

$$\therefore \left\{ \dot{\Delta\omega} = -\frac{K_1 \Delta\delta}{M} - \frac{K_2 \Delta e'_q}{M} - \frac{D\Delta\omega}{M} \right. \tag{B. 17}$$

$$\dot{y}_{16} = K_C \left(-\frac{K_1 \Delta\delta}{M} - \frac{K_2 \Delta e'_q}{M} - \frac{D\Delta\omega}{M} \right) - \frac{y_{16}}{T_\omega} \tag{B. 18}$$

$$\dot{y}_{16} = -\frac{K_C K_1}{M} \Delta\delta - \frac{K_C D}{M} \Delta\omega - \frac{K_C K_2}{M} \Delta e'_q - \frac{1}{T_\omega} y_{16} \tag{B. 19}$$

$$y_{17} = \frac{1 + s T_1}{1 + s T_2} y_{16} \tag{B. 20}$$

$$y_{17} + T_2 \dot{y}_{17} = y_{16} + T_1 \dot{y}_{16} \tag{B. 21}$$

$$\dot{y}_{17} = (y_{16} - y_{17} + T_1 \dot{y}_{16}) / T_2 \tag{B. 22}$$

$$\dot{y}_{17} = \left[y_{16} - y_{17} + T_1 \left(K_C \dot{\Delta\omega} - \frac{y_{16}}{T_\omega} \right) \right] / T_2 \tag{B. 23}$$

$$\dot{y}_{17} = -\frac{K_C K_1 T_1}{T_2 M}\Delta\delta - \frac{K_C D T_1}{T_2 M}\Delta\omega - \frac{K_C K_2 T_1}{T_2 M}\Delta e'_q + \left(\frac{1}{T_2} - \frac{T_1}{T_2 T_\omega}\right) y_{16} - \frac{1}{T_2} y_{17} \tag{B. 24}$$

$$U_{PSS} = \frac{1+sT_3}{1+sT_4} y_{17} \tag{B. 25}$$

$$U_{PSS} + T_4 \dot{U}_{PSS} = y_{17} + T_3 \dot{y}_{17} \tag{B. 26}$$

$$\dot{U}_{PSS} = \frac{y_{17}}{T_4} + \frac{T_3 \dot{y}_{17}}{T_4} - \frac{U_{PSS}}{T_4} \tag{B. 27}$$

$$\dot{U}_{PSS} = \frac{T_3}{T_4}\left[-\frac{K_C K_1 T_1 \Delta\delta}{T_2 M} - \frac{K_C D T_1 \Delta\omega}{T_2 M} - \frac{K_C K_2 T_1 \Delta e'_q}{T_2 M} + \left(\frac{1}{T_2} - \frac{T_1}{T_2 T_\omega}\right) y_{16} - \frac{y_{17}}{T_2}\right] + \frac{y_{17}}{T_4} - \frac{U_{PSS}}{T_4} \tag{B. 28}$$

$$\dot{U}_{PSS} = -\frac{K_C K_1 T_1 T_3 \Delta\delta}{T_2 T_4 M} - \frac{K_C D T_1 T_3 \Delta\omega}{T_2 T_4 M} - \frac{K_C K_2 T T_{31} \Delta e'_q}{T_2 T_4 M} - \frac{T_1 T_3 y_{1\_6}}{T_2 T_4 T_\omega} + \frac{T_3 y_{1\_6}}{T_2 T_4} + \frac{y_{17}}{T_4} - \frac{T_3 y_{17}}{T_2 T_4} - \frac{U_{PSS}}{T_4} \tag{B. 29}$$

$$\dot{U}_{PSS} = -\frac{K_C K_1 T_1 T_3}{T_2 T_4 M}\Delta\delta - \frac{K_C D T_1 T_3}{T_2 T_4 M}\Delta\omega - \frac{K_C K_2 T_1 T_3}{T_2 T_4 M}\Delta e'_q + \left(\frac{T_3}{T_2 T_4} - \frac{T_1 T_3}{T_2 T_4 T_\omega}\right) y_{16} + \left(\frac{1}{T_4} - \frac{T_3}{T_2 T_4}\right) y_{17} - \frac{1}{T_4} U_{PSS} \tag{B. 30}$$

The State space controlled matrix will become,

$$A_C = \begin{bmatrix} 0 & \omega_b & 0 & 0 & 0 & 0 & 0 \\ -\frac{K_1}{M} & -\frac{D}{M} & -\frac{K_2}{M} & 0 & 0 & 0 & 0 \\ -\frac{K_4}{T'_{do}} & 0 & -\frac{1}{K_3 T'_{do}} & \frac{1}{T'_{do}} & 0 & 0 & 0 \\ -\frac{K_A K_5}{T_A} & 0 & -\frac{K_A K_6}{T_A} & -\frac{1}{T_A} & 0 & 0 & \frac{K_A}{T_A} \\ -\frac{K_C K_1}{M} & -\frac{K_C D}{M} & -\frac{K_C K_2}{M} & 0 & -\frac{1}{T_\omega} & 0 & 0 \\ -\frac{K_C K_1 T_1}{T_2 M} & -\frac{K_C D T_1}{T_2 M} & -\frac{K_C K_2 T_1}{T_2 M} & 0 & \left(\frac{1}{T_2} - \frac{T_1}{T_2 T_\omega}\right) & -\frac{1}{T_2} & 0 \\ -\frac{K_C K_1 T_1 T_3}{T_2 T_4 M} & -\frac{K_C D T_1 T_3}{T_2 T_4 M} & -\frac{K_C K_2 T_1 T_3}{T_2 T_4 M} & 0 & \left(\frac{T_3}{T_2 T_4} - \frac{T_1 T_3}{T_2 T_4 T_\omega}\right) & \left(\frac{1}{T_4} - \frac{T_3}{T_2 T_4}\right) & -\frac{1}{T_4} \end{bmatrix} \quad \text{(B. 31)}$$

B.3 State Space Model of IEE2ST PSS Controller

From Fig. A.1 of IEE2ST type PSS model,

$$E_1 = \frac{\Delta\omega K_C}{1+sT_{\omega o}} \tag{B. 32}$$

$$E_1 + T_{\omega o}\dot{E}_1 = \Delta\omega K_C \tag{B. 33}$$

$$\dot{E}_1 = \frac{K_C}{T_{\omega o}}\Delta\omega - \frac{1}{T_{\omega o}}E_1 \tag{B. 34}$$

$$E_2 = \frac{\Delta P \cdot K_P}{1+sT_{Po}} \tag{B. 35}$$

$$\Delta P = K_1\Delta\delta + K_2\Delta e'_q \tag{B. 36}$$

$$E_2 + T_{PO}\dot{E}_2 = K_P \tag{B. 37}$$

$$\dot{E}_2 = \frac{K_P(K_1\Delta\delta + K_2\Delta e'_q)}{T_{PO}} - \frac{E_2}{T_{PO}} \tag{B. 38}$$

$$\dot{E}_2 = \frac{K_P K_1}{T_{PO}}\Delta\delta + \frac{K_P K_2}{T_{PO}}\Delta e'_q - \frac{1}{T_{PO}}E_2 \tag{B. 39}$$

$$E_3 = (E_1 + E_2)\frac{sT_\omega}{1+sT_\omega} \tag{B. 40}$$

$$E_3 + \dot{E}_3 T_W = T_W\dot{E}_1 + T_W\dot{E}_2 \tag{B. 41}$$

$$\dot{E}_3 = (\dot{E}_1 + \dot{E}_2) - \frac{E_3}{T_W} \tag{B. 42}$$

$$\dot{E}_3 = \left(\frac{K_C}{T_{\omega o}}\Delta\omega - \frac{E_1}{T_{\omega o}} + \frac{K_P(K_1\Delta\delta + K_2\Delta e'_q)}{T_{PO}} - \frac{E_2}{T_{PO}}\right) - \frac{E_3}{T_W} \tag{B. 43}$$

$$\dot{E}_3 = \left(\frac{K_C}{T_{\omega o}} \Delta\omega - \frac{1}{T_{\omega o}} E_1 + \frac{K_P K_1}{T_{PO}} \Delta\delta + \frac{K_P K_2}{T_{PO}} \Delta e'_q - \frac{1}{T_{PO}} E_2 \right) - \frac{1}{T_W} E_3 \tag{B. 44}$$

$$\dot{E}_3 = \frac{K_P K_1}{T_{PO}} \Delta\delta + \frac{K_C}{T_{\omega o}} \Delta\omega + \frac{K_P K_2}{T_{PO}} \Delta e'_q - \frac{1}{T_{\omega o}} E_1 - \frac{1}{T_{PO}} E_2 - \frac{1}{T_W} E_3 \tag{B. 45}$$

$$E_4 = \frac{1 + sT_1}{1 + sT_2} E_3 \tag{B. 46}$$

$$\dot{E}_4 = E_3 + T_1 \dot{E}_3 - E_4 \tag{B. 47}$$

$$\begin{aligned} \dot{E}_4 = {} & \frac{K_C T_1}{T_{\omega o}} \Delta\omega + \frac{K_P K_1 T_1}{T_{PO}} \Delta\delta + \frac{K_P K_2 T_1}{T_{PO}} \Delta e'_q - \frac{T_1}{T_{\omega o}} E_1 \\ & - \frac{T_1}{T_{PO}} E_2 - \frac{T_1}{T_W} E_3 + E_3 - E_4 \end{aligned} \tag{B. 48}$$

$$\begin{aligned} \dot{E}_4 = {} & \frac{K_P K_1 T_1}{T_{PO}} \Delta\delta + \frac{K_C T_1}{T_{\omega o}} \Delta\omega + \frac{K_P K_2 T_1}{T_{PO}} \Delta e'_q - \frac{T_1}{T_{\omega o}} E_1 - \frac{T_1}{T_{PO}} E_2 \\ & + \left(1 - \frac{T_1}{T_W} \right) E_3 - E_4 \end{aligned} \tag{B. 49}$$

$$U_{PSS} = \frac{1 + sT_3}{1 + sT_4} E_4 \tag{B. 50}$$

$$U_{PSS} + T_4 \dot{U}_{PSS} = E_4 + T_3 \dot{E}_4 \tag{B. 51}$$

$$\dot{U}_{PSS} = \frac{E_4}{T_4} + \frac{T_3}{T_4} \dot{E}_4 - \frac{U_{PSS}}{T_4} \tag{B. 52}$$

$$\begin{aligned} \dot{U}_{PSS} = {} & \frac{E_4}{T_4} + \frac{K_C T_1 T_3}{T_4 T_{\omega o}} \Delta\omega + \frac{K_P K_1 T_1 T_3}{T_4 T_{PO}} \Delta\delta + \frac{K_P K_2 T_1 T_3}{T_4 T_{PO}} \Delta e'_q - \frac{T_1 T_3}{T_4 T_{\omega o}} E_1 \\ & - \frac{T_1 T_3}{T_4 T_{PO}} E_2 + \left(\frac{T_3}{T_4} - \frac{T_1 T_3}{T_4 T_W} \right) E_3 - \frac{T_3 E_4}{T_4} - \frac{U_{PSS}}{T_4} \end{aligned} \tag{B. 53}$$

$$\dot{U}_{PSS} = \frac{K_C T_1 T_3}{T_4 T_{\omega o}} \Delta\omega + \frac{K_P K_1 T_1 T_3}{T_4 T_{PO}} \Delta\delta + \frac{K_P K_2 T_1 T_3}{T_4 T_{PO}} \Delta e'_q - \frac{T_1 T_3}{T_4 T_{\omega o}} E_1 - \frac{T_1 T_3}{T_4 T_{PO}} E_2 \tag{B. 54}$$

$$+\left(\frac{T_3}{T_4}-\frac{T_1T_3}{T_4T_W}\right)E_3+\frac{1}{T_4}E_4-\frac{T_3}{T_4}E_4-\frac{1}{T_4}U_{PSS}$$

$$\dot{U}_{PSS}=\frac{K_PK_1T_1T_3}{T_4T_{PO}}\Delta\delta+\frac{K_CT_1T_3}{T_4T_{\omega o}}\Delta\omega+\frac{K_PK_2T_1T_3}{T_4T_{PO}}\Delta e'_q-\frac{T_1T_3}{T_4T_{\omega o}}E_1-\frac{T_1T_3}{T_4T_{PO}}E_2$$
$$+\left(\frac{T_3}{T_4}-\frac{T_1T_3}{T_4T_W}\right)E_3+\left(\frac{1}{T_4}-\frac{T_3}{T_4}\right)E_4-\frac{1}{T_4}U_{PSS} \qquad \text{(B. 55)}$$

The Controlled AC Matrix will become

$$A_C = \begin{bmatrix} 0 & \omega_b & 0 & 0 & 0 & 0 & 0 & 0 & 0 \\ -\frac{K_1}{M} & -\frac{D}{M} & -\frac{K_2}{M} & 0 & 0 & 0 & 0 & 0 & 0 \\ -\frac{K_4}{T'_{do}} & 0 & -\frac{1}{K_3 T'_{do}} & \frac{1}{T'_{do}} & 0 & 0 & 0 & 0 & 0 \\ -\frac{K_A K_5}{T_A} & 0 & -\frac{K_A K_6}{T_A} & -\frac{1}{T_A} & 0 & 0 & 0 & 0 & \frac{K_A}{T_A} \\ 0 & \frac{K_C}{T_{\omega o}} & 0 & 0 & -\frac{1}{T_{\omega o}} & 0 & 0 & 0 & 0 \\ \frac{K_P K_1}{T_{PO}} & 0 & \frac{K_P K_2}{T_{PO}} & 0 & 0 & -\frac{1}{T_{PO}} & 0 & 0 & 0 \\ \frac{K_P K_1}{T_{PO}} & \frac{K_C}{T_{\omega o}} & \frac{K_P K_2}{T_{PO}} & 0 & -\frac{1}{T_{\omega o}} & -\frac{1}{T_{PO}} & -\frac{1}{T_W} & 0 & 0 \\ \frac{K_P K_1 T_1}{T_{PO}} & \frac{K_C T_1}{T_{\omega o}} & \frac{K_P K_2 T_1}{T_{PO}} & 0 & -\frac{T_1}{T_{\omega o}} & -\frac{T_1}{T_{PO}} & \left(1-\frac{T_1}{T_W}\right) & 1 & 0 \\ \frac{K_P K_1 T_1 T_3}{T_4 T_{PO}} & \frac{K_C T_1 T_3}{T_4 T_{\omega o}} & \frac{K_P K_2 T_1 T_3}{T_4 T_{PO}} & 0 & -\frac{T_1 T_3}{T_4 T_{\omega o}} & -\frac{T_1 T_3}{T_4 T_{PO}} & \left(\frac{T_3}{T_4}-\frac{T_1 T_3}{T_4 T_W}\right) & \left(\frac{1}{T_4}-\frac{T_3}{T_4}\right) & -\frac{1}{T_4} \end{bmatrix} \quad \text{(B. 56)}$$

REFERENCES

[1] M. Aghazadeh Tabrizi and G. Radman, “PMU-based multi-input SVC supplementary controller for damping inter-area oscillation,” *North American Power Symposium 2010*, IEEE, 2010, pp. 1–6.

[2] J. Lehner, M. Kaufhold, M. Treuer, and T. Weissbach, “Monitoring of inter-area oscillations within the european interconnected network based on a wide area measuring system,” *IEEE PES T&D 2010*, IEEE, 2010, pp. 1–8.

[3] I. Erlich, A. Hashmani, and F. Shewarega, “Selective damping of inter area oscillations using phasor measurement unit (PMU) signals,” *2011 IEEE Trondheim PowerTech*, IEEE, 2011, pp. 1–6.

[4] I. Voloh, J. Cardenas, I. Antiza, and F. Iliceto, “Inter-area oscillation detection by modern digital relays,” *2011 International Conference on Advanced Power System Automation and Protection*, IEEE, 2011, pp. 1396–1401.

[5] S.M. Bamasak and M.A. Abido, “Improving power oscillation damping via TCSC in interconnected power networks,” *2011 IEEE PES Conference on Innovative Smart Grid Technologies - Middle East*, IEEE, 2011, pp. 1–6.

[6] Q. Wang, “Study on relationship between inter-area oscillation damping and operating conditions in power systems,” *2010 International Conference on Power System Technology*, IEEE, 2010, pp. 1–6.

[7] P. Zhang, J.S. Thorp, X. Wang, and X. Wei, “The effect of electromechanical wave controllers on inter-area modes,” *2012 IEEE Power and Energy Society General Meeting*, IEEE, 2012, pp. 1–8.

[8] M. Klein, G.J. Rogers, and P. Kundur, “A fundamental study of inter-area oscillations in power systems,” *IEEE Transactions on Power Systems*, vol. 6, 1991, pp. 914–921.

[9] A.R. Messina, J.M. Ramirez, and J.M. Canedo C., “An investigation on the use of power system stabilizers for damping inter-area oscillations in longitudinal power systems,” *IEEE Transactions on Power Systems*, vol. 13, May. 1998, pp. 552–559.

[10] R. Majumder, B.C. Pal, C. Dufour, and P. Korba, “Design and Real-Time Implementation of Robust FACTS Controller for Damping Inter-Area Oscillation,” *IEEE Transactions on Power Systems*, vol. 21, May. 2006, pp. 809–816.

[11] G. Andersson, P. Donalek, R. Farmer, N. Hatziargyriou, I. Kamwa, P. Kundur, N.

Martins, J. Paserba, P. Pourbeik, J. Sanchez-Gasca, R. Schulz, A. Stankovic, C. Taylor, and V. Vittal, "Causes of the 2003 Major Grid Blackouts in North America and Europe, and Recommended Means to Improve System Dynamic Performance," *IEEE Transactions on Power Systems*, vol. 20, Nov. 2005, pp. 1922–1928.

[12] A.G. Phadke and B. Kasztenny, "Synchronized Phasor and Frequency Measurement Under Transient Conditions," *IEEE Transactions on Power Delivery*, vol. 24, Jan. 2009, pp. 89–95.

[13] A.G. Phadke and J.S. Thorp, *Synchronized Phasor Measurements and Their Applications*, Boston, MA: Springer US, 2008.

[14] J.S. Thorp, "New methods for computing power system dynamic response for real-time transient stability prediction," *IEEE Transactions on Circuits and Systems I: Fundamental Theory and Applications*, vol. 47, Mar. 2000, pp. 324–337.

[15] S. Rovnyak and J. Thorp, "Predicting future behavior of transient events rapidly enough to evaluate remedial control options in real-time," *IEEE Transactions on Power Systems*, vol. 10, 1995, pp. 1195–1203.

[16] X.A. L. Peng, W. Xiaochen, L. Chao, S. Jinghai, H. Jiong, H. Jingbo, Z. Yong, "Implementation of CSG's Wide-Area Damping Control System: Overview and experience," *2009 IEEE/PES Power Systems Conference and Exposition*, IEEE, 2009, pp. 1–9.

[17] A. Dysko, W.E. Leithead, and J. O'Reilly, "Enhanced Power System Stability by Coordinated PSS Design," *IEEE Transactions on Power Systems*, vol. 25, Feb. 2010, pp. 413–422.

[18] C.Y. Chung, C.T. Tse, K.W. Wang, and R. Niu, "PSS design for multi-area system based on combined sensitivity concept," *PowerCon 2000. 2000 International Conference on Power System Technology. Proceedings (Cat. No.00EX409)*, IEEE, , pp. 1197–1202.

[19] R. Lira, C. Mycock, D. Wilson, and H. Kang, "PMU performance requirements and validation for closed loop applications," *2011 2nd IEEE PES International Conference and Exhibition on Innovative Smart Grid Technologies*, IEEE, 2011, pp. 1–7.

[20] C. Li, Y. Sun, X. Chen, and Z. Ma, "Selection of Global Input Signals for Wide-area PSS to Damp Inter-area Oscillations in Multi-machine Power Systems," *2010 Asia-Pacific Power and Energy Engineering Conference*, IEEE, 2010, pp. 1–4.

[21] A.A. Hashmani and I. Erlich, "Mode selective damping of power system

electromechanical oscillations using supplementary remote signals," *IET Generation, Transmission & Distribution*, vol. 4, 2010, p. 1127.

[22] M.A. Abido, "Power system stabilizer tuning study of east-central power system in Saudi Arabia," *Computational Intelligence in Control and Automation (CICA)*, IEEE, 2011, pp. 60–66.

[23] M.A. Abido, "Optimal design of power-system stabilizers using particle swarm optimization," *IEEE Transactions on Energy Conversion*, vol. 17, Sep. 2002, pp. 406–413.

[24] Y. Chompoobutrgool, L. Vanfretti, and M. Ghandhari, "Survey on power system stabilizers control and their prospective applications for power system damping using Synchrophasor-based wide-area systems," *European Transactions on Electrical Power*, vol. 21, Nov. 2011, pp. 2098–2111.

[25] K.E. Martin, G. Benmouyal, M.G. Adamiak, M. Begovic, R.O. Burnett, K.R. Carr, A. Cobb, J.A. Kusters, S.H. Horowitz, G.R. Jensen, G.L. Michel, R.J. Murphy, A.G. Phadke, M.S. Sachdev, and J.S. Thorp, "IEEE Standard for Synchrophasors for Power Systems," *IEEE Transactions on Power Delivery*, vol. 13, 1998, pp. 73–77.

[26] "Phasor Technology Frequently Asked Questions" Available: www.phasor-rtdms.com.

[27] G. MISSOUT and P. Girard, "Measurement of Bus Voltage Angle Between Montreal and SEPT-ILES," *IEEE Transactions on Power Apparatus and Systems*, vol. PAS-99, Mar. 1980, pp. 536–539.

[28] G. Missout, J. Beland, G. Bedard, and Y. Lafleur, "Dynamic Measurement of the Absolute Voltage Angle on Long Transmission Lines," *IEEE Power Engineering Review*, vol. PER-1, Nov. 1981, pp. 23–24.

[29] P. Bonanomi, "Phase Angle Measurements with Synchronized Clocks-Principle and Applications," *IEEE Transactions on Power Apparatus and Systems*, vol. PAS-100, Dec. 1981, pp. 5036–5043.

[30] J.F. Hauer, N.B. Bhatt, K. Shah, and S. Kolluri, "Performance of 'WAMS East' in providing dynamic information for the North East blackout of August 14, 2003," *IEEE Power Engineering Society General Meeting, 2004.*, IEEE, , pp. 1685–1690.

[31] N. Grudinin and I. Roytelman, "Heading off emergencies in large electric grids," *IEEE Spectrum*, vol. 34, Apr. 1997, pp. 43–47.

[32] S. Corsi and C. Sabelli, "General blackout in Italy Sunday September 28, 2003, h.

03:28:00," *IEEE Power Engineering Society General Meeting, 2004.*, IEEE, , pp. 1691–1702.

[33] A.P. Sakis Meliopoulos, G.J. Cokkinides, F. Galvan, and B. Fardanesh, "GPS-Synchronized Data Acquisition: Technology Assessment and Research Issues," *Proceedings of the 39th Annual Hawaii International Conference on System Sciences (HICSS'06)*, IEEE, 2006, p. 244c–244c.

[34] A.G. Phadke and J.S. Thorp, *Synchronized Phasor Measurements and Their Applications*, Boston, MA: Springer US, 2008.

[35] I. Kamwa, R. Grondin, and Y. Hebert, "Wide-area measurement based stabilizing control of large power systems-a decentralized/hierarchical approach," *IEEE Transactions on Power Systems*, vol. 16, 2001, pp. 136–153.

[36] I. Kamwa and L. Gerin-Lajoie, "State-space system identification-toward MIMO models for modal analysis and optimization of bulk power systems," *IEEE Transactions on Power Systems*, vol. 15, 2000, pp. 326–335.

[37] C.W. Taylor, D.C. Erickson, K.E. Martin, R.E. Wilson, and V. Venkatasubramanian, "WACS-Wide-Area Stability and Voltage Control System: R&D and Online Demonstration," *Proceedings of the IEEE*, vol. 93, May. 2005, pp. 892–906.

[38] M.K. J. F. Hauer, W. A. Mittelstadt, R. Adapa, W. H. Litzenberger and Donnelly, *Chapter 11: Power System Dynamics and Stability. Section 8: Direct Analysis of Wide Area Dynamics*, CRC and IEEE press, 2001.

[39] N. Martins, A.A. Barbosa, J.C.R. Ferraz, M.G. dos Santos, A.L.B. Bergamo, C.S. Yung, V.R. Oliveira, and N.J.P. Macedo, "Retuning stabilizers for the north-south Brazilian interconnection," *199 IEEE Power Engineering Society Summer Meeting. Conference Proceedings (Cat. No.99CH36364)*, IEEE, , pp. 58–67.

[40] H.B. and E.G. and M.L. and R. Energie, "Analysis and Damping of Inter-Area Oscillations in the UCTE/CENTREL Power System," 2000, pp. 38–113.

[41] *U.S.- Canada Power System Outage Task Force, Final Report on the August 14, 2003 Blackout in the United States and Canada*.

[42] G. Rogers, "Demystifying power system oscillations," *IEEE Computer Applications in Power*, vol. 9, Jul. 1996, pp. 30–35.

[43] L. Vanfretti and J.H. Chow, "Analysis of power system oscillations for developing synchrophasor data applications," *2010 IREP Symposium Bulk Power System Dynamics and Control - VIII (IREP)*, IEEE, 2010, pp. 1–17.

[44] A.B. Khormizi and A.S. Nia, “Damping of power system oscillations in multi-machine power systems using coordinate design of PSS and TCSC,” *2011 10th International Conference on Environment and Electrical Engineering*, IEEE, 2011, pp. 1–4.

[45] A. Fischer and I. Erlich, “Impact of long-distance power transits on the dynamic security of large interconnected power systems,” *2001 IEEE Porto Power Tech Proceedings (Cat. No.01EX502)*, IEEE, , p. 6.

[46] A. Chakrabortty, “Wide-Area Monitoring & Control of Large Power Grids Using Synchrophasors Main trigger : 2003 Northeast Blackout,” *Main*, 2011.

[47] M. Zima, S. Member, M. Larsson, and P. Korba, “Design Aspects for Wide-Area Monitoring and,” vol. 93, 2005.

[48] A.G. Phadke, S. Shukla, J.S. Thorp, and L. Mili, “Communication network modeling and simulation for Wide Area Measurement applications,” *2012 IEEE PES Innovative Smart Grid Technologies (ISGT)*, IEEE, 2012, pp. 1–6.

[49] S.R. Samantaray, I. Kamwa, and G. Joos, “Ensemble decision trees for phasor measurement unit-based wide-area security assessment in the operations time frame,” *IET Generation, Transmission & Distribution*, vol. 4, 2010, p. 1334.

[50] D.R. W. Mittelstadt, P. Krause, P. Overholt, J. Hauer, R. Wilson, “The DOE Wide Area Measurement System (WAMS) Project - Demonstration of dynamic information technology for the future power system,” *in Proc. Fault and Disturbance Analysis/Precise Measurements in Power Syst. Conf*, 1995.

[51] J.F. Hauer, N.B. Bhatt, K. Shah, and S. Kolluri, “Performance of ‘WAMS East’ in providing dynamic information for the North East blackout of August 14, 2003,” *IEEE Power Engineering Society General Meeting, 2004.*, IEEE, , pp. 1685–1690.

[52] D.M. I. Kamwa, J. Beland, G. Trudel, R. Grondin, C. Lafond, “Wide-Area Monitoring and Control at Hydro-Québec: Past, present and future,” *IEEE Power Eng. Soc. General Meeting*, 2006.

[53] M. Balabin, K. Gorner, Y. Li, I. Naumkin, and C. Rehtanz, “Evaluation of PMU performance during transients,” *2010 International Conference on Power System Technology*, IEEE, 2010, pp. 1–8.

[54] Q.Y.T.B.J. Wu, “WAMS applications in Chinese power systems,” *IEEE Power and Energy Magazine*, vol. 4, Jan. 2006, pp. 54–63.

[55] Q. Yang, T. Bi, and J. Wu, “WAMS implementation in China and the challenges for bulk power system protection,” *Power Engineering Society General …*, 2007.

[56] I. Decker, D. Dotta, M. Agostini, S. Zimath, and A. Silva, "Performance of a Synchronized Phasor Measurements System in the Brazilian Power System," *2006 IEEE PES Power Systems Conference and Exposition*, IEEE, 2006, pp. 150–150.

[57] S. Bruno, M. Benedictis, and M. Scala, "'Taking the pulse' of Power Systems: Monitoring Oscillations by Wavelet Analysis and Wide Area Measurement System," *2006 IEEE PES Power Systems Conference and Exposition*, IEEE, 2006, pp. 436–443.

[58] Y. Narcisse and N. Tchokonte, *Real time identification and monitoring of the voltage stability margin in electric power transmission systems using synchronized phasor measurements*, Kassel university press GmbH, 2009.

[59] E.M. Martinez, "SIMEFAS: A phasor measurement system for the security and integrity of Mexico's electric power system," *2008 IEEE Power and Energy Society General Meeting - Conversion and Delivery of Electrical Energy in the 21st Century*, IEEE, 2008, pp. 1–7.

[60] A.B. Leirbukt, J.O. Gjerde, P. Korba, K. Uhlen, L.K. Vormedal, and L. Warland, "Wide Area Monitoring Experiences in Norway," *2006 IEEE PES Power Systems Conference and Exposition*, IEEE, 2006, pp. 353–360.

[61] A.G. Phadke, "The Wide World of Wide-area Measurement," *IEEE Power and Energy Magazine*, vol. 6, 2008, pp. 52–65.

[62] V. Madani, M. Parashar, J. Giri, S. Durbha, F. Rahmatian, D. Day, M. Adamiak, and G. Sheble, "PMU placement considerations — A roadmap for optimal PMU placement," *2011 IEEE/PES Power Systems Conference and Exposition*, IEEE, 2011, pp. 1–7.

[63] S. Azizi, A.S. Dobakhshari, S.A. Nezam Sarmadi, and A.M. Ranjbar, "Optimal PMU Placement by an Equivalent Linear Formulation for Exhaustive Search," *IEEE Transactions on Smart Grid*, vol. 3, Mar. 2012, pp. 174–182.

[64] F. Aminifar, A. Khodaei, M. Fotuhi-Firuzabad, and M. Shahidehpour, "Contingency-Constrained PMU Placement in Power Networks," *IEEE Transactions on Power Systems*, vol. 25, Feb. 2010, pp. 516–523.

[65] R.E.W.C. Taylor, "Using dynamic simulations to design the wide-area stability and voltage control," *IEEE/PES Power Systems Conference and Exposition*, vol. 1, 2004, pp. 100–107.

[66] A.F. Snyder, N. Hadjsaid, D. Georges, L. Mili, A.G. Phadke, O. Faucon, and S. Vitet, "Inter-area oscillation damping with power system stabilizers and synchronized phasor measurements," *POWERCON '98. 1998 International*

Conference on Power System Technology. Proceedings (Cat. No.98EX151), IEEE, , pp. 790–794.

[67] M. Chenine and L. Nordstrom, "Modeling and Simulation of Wide-Area Communication for Centralized PMU-Based Applications," *IEEE Transactions on Power Delivery*, vol. 26, Jul. 2011, pp. 1372–1380.

[68] M. Chenine, I. Al Khatib, J. Ivanovski, V. Maden, and L. Nordstrom, "PMU traffic shaping in IP-based Wide Area communication," *2010 5th International Conference on Critical Infrastructure (CRIS)*, IEEE, 2010, pp. 1–6.

[69] P. Kansal and A. Bose, "Bandwidth and Latency Requirements for Smart Transmission Grid Applications," *IEEE Transactions on Smart Grid*, vol. 3, Sep. 2012, pp. 1344–1352.

[70] Y. Chompoobutrgool and L. Vanfretti, "A fundamental study on damping control design using PMU signals from dominant inter-area oscillation paths," *2012 North American Power Symposium (NAPS)*, IEEE, 2012, pp. 1–6.

[71] T. Rauhala, K. Saarinen, P. Vuorenpaa, and P. Jarventausta, "Determining Subsynchronous Damping Based on PMU Measurements from Finnish 400 kV Transmission Network," *2007 IEEE Lausanne Power Tech*, IEEE, 2007, pp. 1700–1705.

[72] S.W. J. Chow, J. Sanchez-Gasca, H. Ren, "Power system damping controller design using multiple input signals," *IEEE Control Syst. Mag*, pp. 82–90.

[73] D.L. I. Kamwa, A. Heniche, G. Trudel, M. Dobrescu, R. Grondin, "Assessing the technical value of FACTS-based wide-area damping control loops," *IEEE Power Eng. Soc. General Meeting*, 2005.

[74] Y.H. I. Kamwa, R. Grondin, "Wide-Area Measurement based stabilizing control of large power systems - A decentralized/hierarchical approach," *IEEE Trans. Power Syst*, vol. 16, 2001, pp. 135–153.

[75] G.T. I. Kamwa, L. Gerin-Lajoie, "Multi-loop power system stabilizers using wide-area synchronous phasor measurements," *Proc. American Control Conference*, pp. 2963–2967.

[76] T. Rauhala, K. Saarinen, M. Latvala, M. Laasonen, and M. Uusitalo, "Applications of phasor measurement units and wide-area measurement system in Finland," *2011 IEEE Trondheim PowerTech*, IEEE, 2011, pp. 1–8.

[77] N.R. Chaudhuri, A. Domahidi, R. Majumder, B. Chaudhuri, P. Korba, S. Ray, and K. Uhlen, "Wide-area power oscillation damping control in Nordic equivalent

system," *IET Generation, Transmission & Distribution*, vol. 4, 2010, p. 1139.

[78] C. Lu, X. Wu, J. Wu, P. Li, Y. Han, and L. Li, "Implementations and experiences of wide-area HVDC damping control in China Southern Power Grid," *2012 IEEE Power and Energy Society General Meeting*, IEEE, 2012, pp. 1–7.

[79] X.A. L. Peng, W. Xiaochen, L. Chao, S. Jinghai, H. Jiong, H. Jingbo, Z. Yong, "Implementation of CSG's Wide-Area Damping Control System: Overview and experience," *2009 IEEE/PES Power Systems Conference and Exposition*, IEEE, 2009, pp. 1–9.

[80] D.S. E. Larsen, "Applying power system stabilizers: Parts I, II and III," *IEEE Trans. Power Syst.*, vol. PAS-100, 1981, pp. 3017–3046.

[81] A. Ragavendiran and R. Gnanadass, "Determination of location and performance analysis of power system stabilizer based on participation factor," *2012 IEEE Students' Conference on Electrical, Electronics and Computer Science*, IEEE, 2012, pp. 1–9.

[82] D.P. Parmar, V.M. Dholakiya, and S.C. Vora, "Optimal placement of power system stabilizers: Simulation studies on a test system," *2011 Nirma University International Conference on Engineering*, IEEE, 2011, pp. 1–6.

[83] P. Kundur, *Power System Stability and Control*, McGraw-Hill, 1993.

[84] E. Larsen and D. Swann, "Applying Power System Stabilizers Part I: General Concepts," *IEEE Transactions on Power Apparatus and Systems*, vol. PAS-100, Jun. 1981, pp. 3017–3024.

[85] E.V. Larsen and D.A. Swann, "Applying Power System Stabilizers Part III: Practical Considerations," *IEEE Transactions on Power Apparatus and Systems*, vol. PAS-100, Jun. 1981, pp. 3034–3046.

[86] A.B. Y. Zhang, "Design of Wide-Area damping controllers for interarea oscillations," *IEEE Trans. Power Syst*, vol. 23, pp. 1136–1145.

[87] L.P. Kunjumuhammed, R. Singh, and B.C. Pal, "Robust signal selection for damping of inter-area oscillations," *IET Generation, Transmission & Distribution*, vol. 6, 2012, p. 404.

[88] M.H. Nguyen, M. Eghbal, T.K. Saha, and N. Modi, "Investigation of Oscillation Damping for connecting remote generators to a large power system," *2011 IEEE PES Innovative Smart Grid Technologies*, IEEE, 2011, pp. 1–8.

[89] C.X.; M. Zhanjun, "Design a Wide-ara PSS for damping inter-area low-frequency

oscillation," *2010 5th IEEE Conference on Industrial Electronics and Applications*, IEEE, 2010, pp. 808–813.

[90] A. Heniche and I. Kamwa, "Assessment of Two Methods to Select Wide-Area Signals for Power System Damping Control," *IEEE Transactions on Power Systems*, vol. 23, May. 2008, pp. 572–581.

[91] E.V. Larsen, J.J. Sanchez-Gasca, and J.H. Chow, "Concepts for design of FACTS controllers to damp power swings," *IEEE Transactions on Power Systems*, vol. 10, May. 1995, pp. 948–956.

[92] A. Rahim and A. Al-Sammak, "Optimal switching of dynamic braking resistor, reactor or capacitor for transient stability of power systems," *Generation, Transmission and Distribution*, vol. 138, 1991.

[93] A.H.M.A. Rahim and D.A.H. Alamgir, "A closed-loop quasi-optical dynamic braking resistor and shunt reactor control strategy for transient stability (of synchronous generators)," *IEEE Transactions on Power Systems*, vol. 3, Aug. 1988, pp. 879–886.

[94] A. Sen and J. Meisel, "Transient stability augmentation with a braking resistor using optimal aiming strategies," *Proceedings of the Institution of Electrical Engineers*, vol. 125, 1978, p. 1249.

[95] F. Demello and C. Concordia, "Concepts of Synchronous Machine Stability as Affected by Excitation Control," *IEEE Transactions on Power Apparatus and Systems*, vol. PAS-88, Apr. 1969, pp. 316–329.

[96] Y. Yu and C. Siggers, "Stabilization and Optimal Control Signals for a Power System," *IEEE Transactions on Power Apparatus and Systems*, vol. PAS-90, Jul. 1971, pp. 1469–1481.

[97] Y. Yu and M. a. El-Sharkawi, "Estimation of External Dynamic Equivalents of a Thirteen-Machine System," *IEEE Transactions on Power Apparatus and Systems*, vol. PAS-100, Mar. 1981, pp. 1324–1332.

[98] Y. Yu and H. M. Moussa, "Optimal Stabilization of a Multi-Machine System," *IEEE Transactions on Power Apparatus and Systems*, vol. PAS-91, May. 1972, pp. 1174–1182.

[99] A.T. Al-Awami, M.A. Abido, and Y.L. Abdel-Magid, "Power system stability enhancement using unified power flow controllers," *2006 IEEE GCC Conference (GCC)*, IEEE, 2006, pp. 1–6.

[100] A.A. Ba-muqabel and M.A. Abido, "Review of conventional power system

stabilizer design methods," *2006 IEEE GCC Conference (GCC)*, IEEE, 2006, pp. 1–7.

[101] M.A. Abido and Y. Abdel-Magid, "Dynamic Stability Enhancement of East-Central System in Saudi Arabia via PSS Tuning," *Arabian Journal for Science*, vol. 32, 2007, pp. 85–99.

[102] M. Ishimaru, R. Yokoyama, O. Neto, and K. Lee, "Allocation and design of power system stabilizers for mitigating low-frequency oscillations in the eastern interconnected power system in Japan," *International Journal of Electrical Power & Energy Systems*, vol. 26, Oct. 2004, pp. 607–618.

[103] C.-L. Chen and Y.-Y. Hsu, "An efficient algorithm for the design of decentralized output feedback power system stabilizer," *IEEE Transactions on Power Systems*, vol. 3, 1988, pp. 999–1004.

[104] Y.-Y. Hsu and C.-L. Chen, "Identification of optimum location for stabiliser applications using participation factors," *IEE Proceedings C Generation, Transmission and Distribution*, vol. 134, 1987, p. 238.

[105] M.A. Abido, "Robust Design of Power System Stabilizers for Multimachine Power Systems Using Differential Evolution," *Computational Intelligence in Power Engineering*, 2010.

[106] S.R. Spea, A.A.A. El Ela, and M.A. Abido, "Multi-objective differential evolution algorithm for environmental-economic power dispatch problem," *2010 IEEE International Energy Conference*, IEEE, 2010, pp. 841–846.

[107] M.A. Abido and N.A. Al-Ali, "Multi-objective differential evolution for optimal power flow," *2009 International Conference on Power Engineering, Energy and Electrical Drives*, IEEE, 2009, pp. 101–106.

[108] F. Aboytes, F. Sanchez, A.I. Murcia Cabra, and J.E. Gomez Castro, "Dynamic stability analysis of the interconnected Colombia-Venezuela power system," *IEEE Transactions on Power Systems*, vol. 15, 2000, pp. 376–381.

[109] H. Ellis, J. Hardy, A. Blythe, and J. Skooglund, "Dynamic Stability of the Peace River Transmission System," *IEEE Transactions on Power Apparatus and Systems*, vol. PAS-85, Jun. 1966, pp. 586–600.

[110] M.L. Shelton, P.F. Winkelman, W.A. Mittelstadt, and W.J. Bellerby, "Bonneville power administration 1400-MW braking resistor," *IEEE Transactions on Power Apparatus and Systems*, vol. 94, Mar. 1975, pp. 602–611.

[111] P.M. ANDERSON and A.A. FOUAD, *Power-System -Control and Stability*, USA:

The Iowa State University Press, 1977.

[112] P. Kundu and A.K. Pradhan, “Stability assessment using synchrophasor data,” *2011 International Conference on Energy, Automation and Signal*, IEEE, 2011, pp. 1–6.

[113] P. Bera, D. Das, and T.K. Basu, “Coordinated Design of Excitation and TCSC - Based Stabilizers for Multimachine Power System,” 2010.

[114] A. Farah, T. Guesmi, H. Hadj Abdallah, and A. Ouali, “Optimal design of multimachine power system stabilizers using evolutionary algorithms,” *2012 First International Conference on Renewable Energies and Vehicular Technology*, IEEE, 2012, pp. 497–501.

Vitae

Name	Irfan Ahmed Khan
Nationality	Pakistani
Date of Birth	8th June, 1986
Email	iakhan@kfupm.edu.sa, irfan.kfupm@gmail.com
Address	P.O. Box 8638, KFUPM, 31261 Dhahran, KSA.
Academic Background	BS (Electronics)
	MS (Electrical)
Publications	→Irfan Ahmed Khan and M. A. Abido, *Power system stability enhancement through wide-area measurements*, Saudi Smart Grid 2012, In Process.
	→Irfan Ahmed Khan and M. A. Abido, *Optimal placement of wide area based power system*, 15th Saudi technical exchange meeting 2012, In Process.
Certifications	Certified in Microcontroller and Hardware Interfacing.
	Certified in Practical Robotics.